In Vitro Models of the Blood-Brain Barrier: Applications and Evaluation of a New Human Immortalized Brain Capillary Endothelial Cell Line

Inauguraldissertation

zur
Erlangung der Doktorwürde der Philosophie
vorgelegt der
Philosophisch-Naturwissenschaftlichen Fakultät
der Universität Basel

von

Manisha Kusch-Poddar
aus Baden (AG)

Basel, 2006

Genehmigt von der Philosophisch-Naturwissenschaftlichen Fakultät
auf Antrag von

Prof. Dr. Jürgen Drewe
PD Dr. Jörg Huwyler

Basel, den 6. Juni 2006

Prof. Dr. Hans-Jakob Wirz
Dekan

Für Dirk und meine Eltern

„Alles Wissen und alles Vermehren unseres Wissens endet nicht mit einem Schlusspunkt, sondern mit einem Fragezeichen.“

Hermann Hesse (1877-1962)

Acknowledgements

Die vorliegende Dissertation entstand am Universitätsspital Basel im Labor der Klinischen Pharmakologie und Toxikologie unter der Leitung von Prof. Dr. Jürgen Drewe. Mein allergrösster Dank gilt Prof. Dr. Jürgen Drewe für seinen grossen Einsatz als Doktorvater, sein Vertrauen und seine Grosszügigkeit. Er war mir mit seinen Anregungen und Ideen stets eine wertvolle Unterstützung und ist mir fachlich wie menschlich ein grosses Vorbild! Bei meinem Koreferenten PD Dr. Jörg Huwyler möchte ich mich herzlich für die hilfreichen Ratschläge bedanken. Prof. Dr. Matthias Hamburger danke ich für die Übernahme des Prüfungsvorsitzes.

Grosse Unterstützung erhielt ich auch von unserer ausgesprochen hilfsbereiten Laborchefin Dr. Heike Gutmann, welche jederzeit für alle grösseren und kleineren Laborsorgen ein offenes Ohr hatte.

Meine LaborkollegInnen haben einen riesigen Beitrag zum Gelingen dieser Arbeit geleistet. Von Ursula Behrens erhielt ich eine solide Einführung in die Zellkulturtechniken und eine zuverlässige Unterstützung bei der Zellisolierung. Zu Beginn meiner Arbeit fand ich in meinen VorgängerInnen Dr. Katrijn Bogman, Dr. Arabelle Pfrunder, Dr. Petr Hruz und Dr. Christian Zimmermann gute Vorbilder. Viel tatkräftige Unterstützung erfuhr ich auch von meinen nachfolgenden LaborkollegInnen Dr. Marco Netsch, Philipp Schlatter, Angelika Maier und Birk Poller und auch von meinen KollegInnen im Labor 410 und im Markgräflerhof. Eine Bereicherung war auch unserer Diplomand Shlomo Brill. Doch auch ausserhalb des Labors durfte ich mit meinen sympathischen KollegInnen unzählige schöne Erlebnisse teilen. Was für eine schöne Zeit es doch war...

Isabelle Fux danke ich für die wertvolle Vorarbeit, welche sie während ihrer Diplomarbeit geleistet hatte. Meine Arbeit baut teilweise auf ihren Erkenntnissen auf.

Prof. Dr. Christoph Hiemke danke ich für die Kooperation mit der Psychiatrischen Klinik der Universität Mainz. Bei Katrin Kirschbaum bedanke ich mich für die HPLC Messungen. Allen „Mainzern“ einen grossen Dank für die gute Zusammenarbeit.

In meiner Freizeit halfen mir meine Freundinnen und Freunde, mich von den Strapazen des Laboralltags zu erholen und neue Energie zu tanken. Ich möchte insbesondere Corinne für die wunderbare Freundschaft danken, die uns seit der Studienzeit verbindet.

Mein ganz besonderer Dank gilt meiner Familie. Ihr ist diese Arbeit gewidmet! Meinen Eltern danke ich, dass sie mich stets zu 100% bei der Verwirklichung all meiner Pläne und Ziele unterstützt haben. Meinem „besten Ehemann aller Zeiten“ Dirk danke ich für seine unermessliche Liebe, seine immense Unterstützung und sein Vertrauen, welche ich tagtäglich erleben darf.

Abbreviations

AhR	aryl hydrocarbon receptor
AJ	adherens junction
ABC	ATP binding cassette
ACM	astrocyte-conditioned medium
ANOVA	analysis of variance
AP	apical
ARI	aripiprazole
ATP	adenosine-5'-triphosphate
BBB	blood-brain barrier
BCE-A	brain capillary endothelial surface
BCEC	brain capillary endothelial cells
BCRP	breast cancer resistance protein
BCSFB	blood-cerebrospinal fluid barrier
BL	basolateral
bp	base pair
BSA	bovine serum albumin
BUI	brain uptake index
$[Ca^{2+}]_i$	intracellular calcium concentration
Caco-2	human Caucasian colon adenocarcinoma cell line
cAMP	cyclic adenosine monophosphate
CAR	constitutive androsane receptor
CCRF-CEM/MDR	human T-lymphocytic leukaemia cell line overexpressing MDR1
CCRF-CEM/Par	parental human T-lymphocytic leukaemia cell line
CLZ	clozapine
CPT-cAMP	chlorophenylthio-cAMP
CSF	cerebrospinal fluid
CYP	cytochrome P 450
DMSO	dimethyl sulfoxide
DNA	deoxyribonucleic acid
DOM	domperidone
FBS	fetal bovine serum

FGF	fibroblast growth factor
FITC	fluorescein isothiocyanate
GAPDH	glyceraldehyde-3-phosphate dehydrogenase
GLUT1	glucose transporter 1
HAL	haloperidol
HBSS	Hank's balanced salt solution
HBSS-P	HBSS supplemented with 1 mM sodium pyruvate, pH 7.4
HPLC	high performance liquid chromatography
HS	horse serum
IgG	immunglobulin class G
JAM	junctional adhesion molecules
kDa	kilodalton
LC-MS/MS	liquid chromatography with mass spectrometry
Mab	monoclonal antibodies
MCF-7/AdrVp	doxorubicin-resistant breast cancer cell line
MDCK	Madin-Darby canine kidney cells
MDR	multidrug resistance
mRNA	messenger ribonucleic acid
MRP	multidrug resistance associated protein
MW	molecular weight
NORCLZ	norclozapine
OHRIS	9-OH risperidone
OLZ	olanzapine
P388/mdr	murine monocytic leukaemia cell line overexpressing mdr1
P388/par	parental murine monocytic leukaemia cell line
p-AH	para-aminohippuric acid
PAH	polycyclic aromatic hydrocarbons
P_{app}	apparent permeability
P_e	permeability coefficient
PBS	phosphate buffered saline
PBS-T	PBS containing 0.05% Tween 20
PET	positron emission tomography
PETE	polyethylene terephthalate
P-gp	P-glycoprotein

PXR	pregnane X receptor
QUET	quetiapine
R123	rhodamine 123
RIS	risperidone
RT-PCR	reverse transcription polymerase chain reaction
RXR	retinoic X receptor
SDS	sodium dodecyl sulfate
SDS-PAGE	SDS polyacrylamide gel electrophoresis
SEM	standard error of the mean
SLC	superfamily of solute carriers
SRB	sulforhodamine B
SSeCKS	src-suppressed C-kinase substrate
StdD	standard dilution
TGF-β	transforming growth factor-β
TJ	tight junctions
TN	transcript number per µg RNA
TR^-	mrp2-deficient rat mutants
TRIS-HCl	tris(hydroxymethyl)aminomethane hydrochloride
ZIP	ziprasidone
ZO	zonula occludens

Summary

An optimal *in vitro* permeability screening model for the evaluation of BBB drug permeability accounts for active and passive transport processes, as well as for non-defined drug-cell interactions. In addition, it should be as little laborious as possible, and preferably from humans. Such an *in vitro* model would be an important tool for the evaluation of BBB permeability in drug development. However, most of the established *in vitro* models use cells of non-human origin, which is not optimal for the prediction of brain permeability in humans. Therefore, we evaluated the immortalized human brain capillary endothelial cell line BB19 as an *in vitro* model of the BBB. BB19 cells are derived from human brain endothelium and are immortalized with E6E7 genes of human papilloma virus. They express factor VIII-related antigen and von Willebrand's factor. Cells exhibit cobblestone-like morphology. However, tightness of the cell monolayer had not been investigated so far. Restrictive tight junctions are a prerequisite for drug transport studies. Therefore, the sucrose permeability of BB19 cells on different filters was tested and compared to porcine brain capillary endothelial cells. However, the tightness of BB19 cell monolayers was insufficient and still needs further optimization. Furthermore, the ability of BB19 cells to discriminate between the paracellular marker sucrose and the transcelluar marker propranolol was tested in a transport assay. However, hardly any discrimination between sucrose and propranolol (P_{app} = 1.30 x 10^{-5} vs. 2.18 x 10^{-5}) was seen. The effects of different supplements such as chlorophenylthio-cAMP with the phosphodiesterase inhibitor RO-20-1724, dexamethasone, 1,25 dihydroxyvitamin D_3, and C6-conditioned medium on cell morphology, ZO-1 expression, and tightness of the BB19 cell monolayers were investigated. Cells showed an improvement towards a more primary BCEC morphology with C6-conditioned medium, dexamethasone, and 1,25-dihydroxyvitamin D_3. In a next step, we studied the expression of important BBB transporters, such as P-gp, MRPs, SLCs, and BCRP. The presence of P-gp, MRP4, and BCRP has been shown on mRNA level, by immunostaining, and Western blot. MRP1, MRP2, MRP5, OAT3, and OAT4 were also detected by RT-PCR. Functional properties of the BBB were shown with uptake of propranolol, morphine, and sucrose. The uptake data was similar to the results gained from the established porcine brain capillary endothelial cell model. Uptake studies with daunomycin and

the P-gp inhibitor verapamil showed functional activity of P-gp. We conclude that BB19 cells might be feasible as a human *in vitro* model of the BBB for drug uptake studies. However, for the assessment of transport studies, further improvements of this model are necessary.

Furthermore, we assessed the expression and inducibility of CYPs, that may play a role in the metabolism of CNS-active drugs, in BB19 cells. So far, only little is known about the expression and functional role of CYPs at the BBB. The presence of CYP1A1, and to a lower extent, of CYP3A4 could be shown on RNA level. Treatment with benzo[a]pyrene induced the CYP1A1 transcript level approximately 11-fold, whereas the treatment with rifampicin did not significantly change the expression level of CYP3A4. CYP1A1 was also detected by immunostaining and Western blot. However, no inducibility of CYP1A1 could be observed on protein level. No functional activity could be shown in the P450-GLO^{TM} assay.

Only little is known about the impact of P-gp for the distribution of neuroleptic drugs into the brain. In collaboration with the Psychiatric Clinic of the University of Mainz, Germany, the potential of neuroleptic drugs and drug metabolites to modulate P-gp was studied in uptake and efflux assays in the P-gp overexpressing cell line P388/mdr1. Aripiprazole and quetiapine, and to a lower extend risperidone, the metabolite 9-OH risperidone, the metabolite norclozapine, and olanzapine could be identified as P-gp inhibitors. Clozapine was a weak inhibitor of P-gp, while haloperidol did not show any modulation of P-gp function.

In an industrial collaboration project, we evaluated the BBB permeability of different preclinical CNS active compounds in porcine BCECs, and aimed to develop a combined *in vitro* model, simultaneously studying BBB penetration and pharmacolological effect.
The investigated preclinical compounds could be ranked according to their BBB permeability in porcine BCEC.
Until now, drug candidates pass through a consecutive series of screening assays, where in a first screening procedure the antagonism or inhibition of a receptor or enzyme is tested *in vitro*. In a second step, the membrane permeability properties are assessed in cell-culture models (White, 2000). However, CNS-active compounds first

have to pass the BBB (which we assessed with the transport through porcine BCEC); only this fraction will contribute to the effects on the receptor (which we obtained in a target receptor screening assay). This situation was incorporated in our combined approach, improving the screening–criteria for the selection of potential drug candidates, by reason that a compound with a moderate pharmacological efficacy (which usually is excluded from further screens), but with high BBB permeability, might be a better drug candidate, than a compound with a high pharmacological efficacy but poor BBB permeability properties.

In addition, knowing the dose-response relationship of a test compound in the target receptor screening assay from a standard curve, we evaluated, whether it was possible to directly estimate the extent of BBB permeability of a test compound in this combined *in vitro* model, which could save elaborate analytical measurements.

In a first approach, we performed the transport of CNS active compounds from AP to BL in porcine BCEC. The collected samples from the BL compartment were applied in the target receptor screening assay. Our preliminary experimental results revealed that this combined *in vitro* assay might be a promising new approach for the identification of drug candidates. However, with the future goal of application in industrial drug screening, extensive further opimization is necessary.

Table of contents

1 Introduction

1.1 The blood-brain barrier

1.1.1 History

In the late 19th century, the German scientist Paul Ehrlich observed that systemic injection of water-soluble dyes stained all organs except the brain and spinal cord (Ehrlich, 1885). Subsequent experiments by his student Edwin Goldmann demonstrated that in opposite, dyes that were injected into the brain did not stain any of the peripheral organs. This provided the early evidence of a physical barrier between the CNS and the peripheral circulation (Goldmann, 1909). Lewandowsky (1900) was the first to use the term *Blut-Hirn Schranke*, while studying the limited permeation of potassium ferrocyanate into the brain (Hawkins and Davis, 2005). The current understanding of basic structures of the blood-brain barrier (BBB) is based upon the general work of Reese, Karnovsky, and Brightman in the late 1960s. In electron microscopy studies with mice, they demonstrated that the BBB exists as a selective diffusion barrier, built by the brain capillary endothelial cells (BCEC), and is characterized by the presence of tight cell-cell junctions (Reese and Karnovsky, 1967).

1.1.2 Anatomical description

The BBB is formed by brain capillary endothelial cells, which are surrounded and supported by astrocyt foot processes and pericytes. Figure 1.1 shows a cross-sectional representation of a brain capillary. The circumference of the capillary lumen is enclosed by a single endothelial cell. The endothelial cells of the BBB are distinguished from those in the periphery by increased mitochondrial content (Oldendorf et al., 1977), a lack of fenestrations (Fenstermacher et al., 1988), minimal pinocytotic activity (Sedlakova et al., 1999), and the presence of tight junctions (TJ), which limit paracellular transport (Rowland et al., 1991). Pericytes are cells of microvessels that wrap around endothelial cells, providing structural support. Pericytes and endothelial cells share a common basal lamina, a membrane of 30 to

40 nm thickness, composed of collagen type IV, heparin, sulphate proteoglycans, laminin, fibronectin, and other extracellular matrix proteins (Farkas and Luiten, 2001). Astrocytes are glial cells that wrap the cerebral capillaries continuously with their foot processes (Goldstein, 1988).

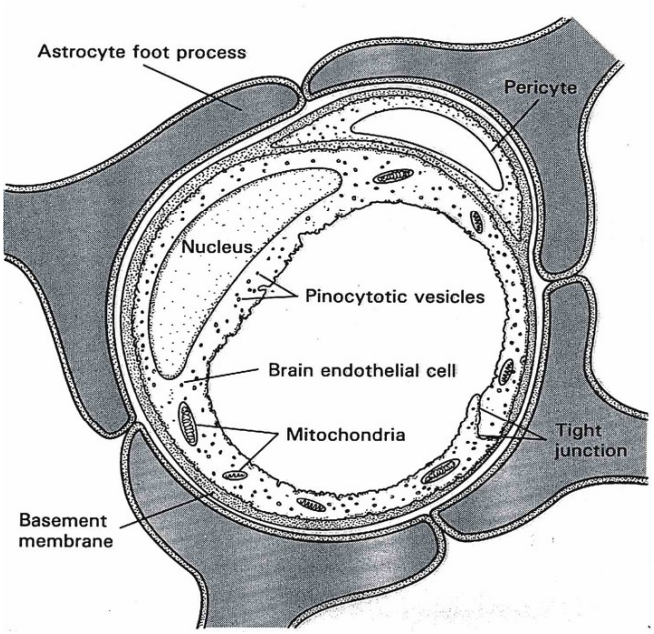

Figure 1.1 Schematic cross-sectional representation of a cerebral capillary. Astrocyte end-feet are closely applied to the endothelial cells and cover the entire basal surface area of the brain capillary endothelial cells. The basal lamina surrounds pericytes and endothelial cells. **From Rowland et al., 1991**

The BBB is present in all brain regions except for the circumventricular organs including area postrema, median eminence, neurohypophysis, pineal gland, subfornical organ, and lamina terminalis. (Ballabh et al., 2004).

1.1.3 Tight junctions

The junctional complex of the BBB comprises tight junctions (TJ) and adherens junctions (AJ). TJs interlink between the plasma membranes of adjacent endothelial

cells and limit the paracellular passage of molecules (Figure 1.2). In freeze-fracture replica electron micrographs TJs are depicted as a set of continuous intramembranous strands or fibrils. The TJ consists of three integral membrane proteins, namely claudin, occludin, and junctional adhesion molecules (JAM), and a number of cytoplasmic accessory proteins including the zonula occludens (ZO) proteins ZO-1, ZO-2, ZO-3, cingulin, and others. Cytoplasmic proteins link membrane proteins to actin, which is the primary cytoskeleton protein for the maintenance of structural and functional integrity of the endothelium.

Claudins are the major components of TJ. They are 22 kDa phosphoproteins and have four transmembrane domains. Claudins bind homotypically to claudins on adjacent cells to form the primary seal of the TJ. The COOH-terminus of claudins binds to cytoplasmic proteins, including ZO-1, ZO-2, and ZO-3 (Furuse et al., 1998, Furuse et al., 1999). The presence of claudin-1 and claudin-5 has been described in endothelial TJ forming the BBB (Liebner et al., 2000, Morita et al., 1999).

The integral TJ protein occludin is a 65 kDa phosphoprotein, which is significantly larger than claudin. Occludin has four transmembrane domains, a long cytoplasmic COOH-terminus, and a short cytoplasmic NH_2-terminus. The cytoplasmic domains of occludin are directly associated with ZO proteins (Hirase et al., 1997). The expression of occludin has been documented in adult human brain (Papadopoulos et al., 2001) but not in normal human newborn and fetal brain. Occludin appears to be a regulatory protein that can alter paracellular permeability (Hirase et al., 1997).

The junctional adhesion molecules (JAM, 40 kDa), belong to the immunoglobulin superfamily (Martin-Padura et al., 1998). They have a single transmembrane domain and an extracellular domain with two immunoglobulin-like loops formed by disulfide bonds. Three JAM proteins, JAM-1, JAM-2, and JAM-3 have been detected in rodent brain sections. JAM-1 and JAM-3, but not JAM-2 are expressed in brain blood vessels (Aurrand-Lions et al., 2001). The expression of JAM at the human BBB remains to be explored.

Cytoplasmic proteins involved in TJ formation include zonula occludens proteins (ZO-1, ZO-2, and ZO-3), cingulin, 7H6, and several others. They contain domains that function as protein binding molecules and thus play a role in organizing proteins at the plasma membrane, interacting directly with claudins, occludin, and JAM (Ebnet et al., 2000, Itoh et al., 1999, Mitic et al., 2000). Actin, the primary cytoskeleton protein, binds to the COOH-terminus of ZO-1 and ZO-2. This complex cross-links

transmembrane elements and thus provides structural support to the endothelial cells (Haskins et al., 1998).

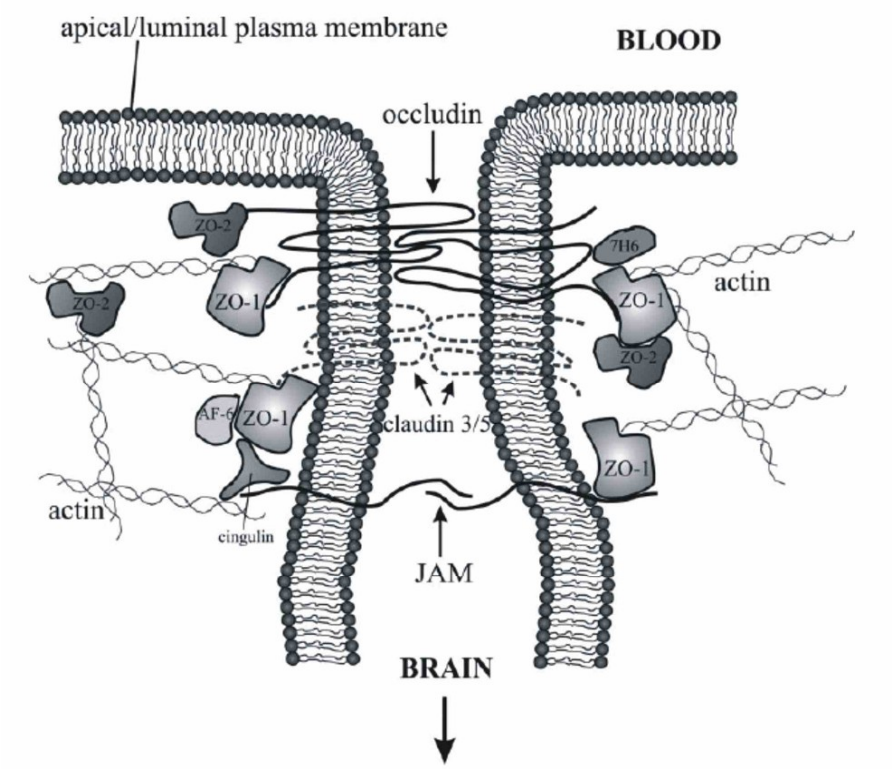

Figure 1.2 Basic molecular organization of BBB tight junctions. **From Hawkins and Davis, 2005**.

1.1.4 Adherens junctions

Adherens junctions (AJ) are composed of the membrane protein cadherin that joins the actin cytoskeleton via intermediary proteins, the catenins, to form adhesive contacts between cells. AJs assemble via homophilic interactions between the extracellular domains of calcium-dependent cadherin on the surface of adjacent cells. The cytoplasmic domains of cadherins bind to the submembranal plaque proteins ß- or γ-catenin, which are linked to the actin cytoskeleton via a-catenin. AJ components including cadherin, a-actinin, and vinculin have been shown in intact microvessels of the BBB in rat (Matter and Balda, 2003).

1.1.5 Astrocyte-endothelial interaction

It is generally assumed that astroglia induce and maintain the barrier properties of the brain capillary endothelium, improving BBB functions (Davson and Oldendorf, 1967), for a review see (Haseloff et al., 2005). The fact that astrocyte-conditioned medium (ACM) induces junction formation in cerebral capillary endothelial cells *in vitro* led to the search of one or more glia-derived soluble factors (Arthur et al., 1987, Rubin et al., 1991). The bovine fibroblast growth factor (FGF) has been found to increase the tightness of the BBB *in vitro* (el Hafny et al., 1996), which is consistent with the observation that mutant mice lacking FGF-2 and FGF-5 show decreased levels of tight junction proteins (occludin, ZO-1) and defects in the barrier function (Reuss et al., 2003). Furthermore, the transforming growth factor-β (TGF-β), released from astrocytes has been observed to mediate the regulation of certain EC proteins (Tran et al., 1999). In addition, factor src-suppressed C-kinase substrate (SSeCKS) has been shown to stimulate astrocytic expression of angiopoietin-1 and its secretion into the medium. Treatment of endothelial cells with SSeCKS-conditioned medium increases the expression of tight junctions and decreases the [^{3}H]-sucrose permeability (Lee et al., 2003).

Other authors claimed that the induction of BBB features depends on a close and long lasting contact between astrocytes and capillary endothelial cells (Risau et al., 1986, Stewart and Wiley, 1981), requiring their continuous presence in the medium. In addition, a direct contact between endothelial cells and astrocytes has been postulated to be essential (Tontsch and Bauer, 1991). Moreover, it has been reported that BBB-related marker enzymes were only induced in subconfluent endothelial cells (Meyer et al., 1991). However, the development of *in vitro* co-culture systems consisting of endothelial cells and astrocytes (Dehouck et al., 1990, Stanness et al., 1996), did not lead to unequivocal results. Cultured astrocytes were mainly derived from newborn animals (favourite origin rat or mouse) and mostly represented type I astrocytes in culture. Usually, these cells grow well under experimental conditions, proliferate and allow passaging several times without loosing expression of glial fibrillary acidic protein, a commonly monitored astrocytic marker. However, it is unknown at present whether the expression profiles of other glia-specific markers change during serial passaging of these cells, as it has been observed in cultured endothelial cells, which are known to exhibit decreased activities of BBB-associated

marker enzymes (such as γ-glutamyl transpeptidase) under culture conditions (Mischeck et al., 1989, Ballabh et al., 2004).

Most of the data concerning endothelial-glial interaction has been obtained with astrocytes and cerebral endothelial cells *in vitro*. However, in *in vivo* experiments, were astroglial cells were selectively injured following chronic systemic injections of the antimetabolite 6-aminonicotinamide in postnatal rats, no active role of astrocytes in BBB function could be seen. The postnatal microvasculature continued to express BBB markers robustly throughout the CNS without the influence of continuously secreted, astrocyte-derived substances (Krum, 1996). An alternative possibility would be that astrocytes mediate the removal of an internal blockade in the endothelium, which prevents the expression of BBB proteins.

1.1.6 Pericytes and the blood-brain barrier

Pericytes are cells of microvessels, such as capillaries, venules, and arterioles that wrap around the endothelial cells. They are thought to provide structural support and vasodynamic capacity to the microvasculature. Metabolic injury to pericytes in diabetes mellitus is inter alia associated with microaneurysm formation in the retina (Kern and Engerman, 1996), which supports the view that pericytes play an essential role in the structural integrity of microvessels. The role of pericytes in angiogenesis and differentiation of the BBB has been studied in an *in vitro* culture model (Ramsauer et al., 2002). This study suggests that pericytes stabilize capillary-like structures formed by endothelial cells in culture with astrocytes by preventing apoptosis of the endothelium. The fact that endothelial cells associated with pericytes are more resistant to apoptosis than isolated endothelial cells further supports the role of pericytes in structural integrity and genesis of the BBB. Other studies support the concept that pericytes regulate angiogenesis and may play a role in BBB differentiation (Balabanov and Dore-Duffy, 1998).

1.2 Other barriers in the brain

Besides the BBB, access to the brain is restricted by the blood-cerebrospinal fluid barrier (BCSFB). This is a composite barrier comprising the choroid plexus and the arachnoid epithelium, forming the middle layer of the meninges (Abbott, 2005, de

Lange, 2004). The choroid plexus has fenestrated and therefore highly permeable capillaries at the blood side, which are covered by a monolayer of epithelial cells that face the cerebrospinal fluid (CSF). These epithelial cells form the basis of the barrier function of the choroid plexus. The choroid plexus is present in the ventricles of the brain as leaf like floating structures. It is the main source for cerebrospinal fluid production (Cserr, 1971). The BCSFB resides between circulating blood and circulating CSF, and therefore, soluble factors in these fluids may regulate the function of this barrier. As well as the BCECs, the epithelial cells of the choroid plexus are connected by tight junctions, restricting paracellular transport. The organization of these tight junctions is parallel by sparsely interconnected strands, which makes them slightly more permeable that those between the BCECs. Furthermore both cell types express numerous transport systems for influx and/or efflux of nutrients, metabolic products, xenobiotics, and ions (de Lange, 2004).

1.3 Drug transporters at the BBB

The BBB comprises a multitude of transporters, which limit the passage of xenobiotics and endogenous substances, or allow the controlled passage of nutrients and other substances from and to the CNS (de Lange, 2004, Fricker and Miller, 2004, Loscher and Potschka, 2005). Figure 1.3 illustrates the cellular localization of selected drug transporters on brain capillary endothelial cells forming the blood-brain barrier.

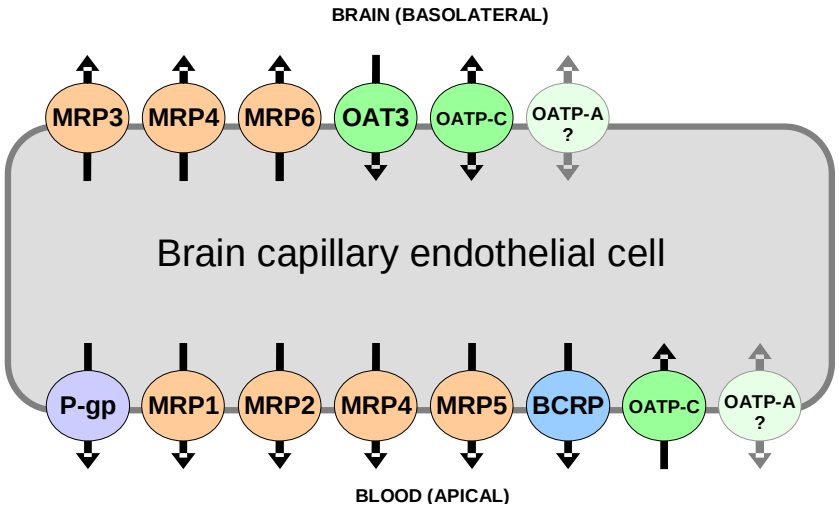

Figure 1.3 Schematic diagram of selected drug transporters on brain capillary endothelial cells forming the blood-brain barrier. The localization of OATP-A remains unclear.

1.3.1 ABC-Transporters

ATP-binding cassette (ABC) transporters play a major role for the distribution and elimination of drugs from and to the brain. This large superfamily consists of membrane proteins which are able to transport a wide variety of substrates across membranes against concentration gradients with ATP hydrolysis as a driving force. The human genome consists of 48 ABC genes, which can be classified into seven subfamilies based upon gene structure, amino acid alignment, and phylogenetic analysis (Dean, 2005, Loscher and Potschka, 2005). The following depiction focuses on those members of these subfamilies that are expressed at the BBB (ABCB, ABCC, and ABCG).

1.3.1.1 P-glycoprotein

The first identified and best studied ABC transporter is the MDR1 gene product P-glycoprotein (P-gp, ABCB1). P-gp is a 170-kDa phosphorylated glycoprotein, which acts as a multispecific, ATP-driven drug efflux pump (Sharma and Rose, 1995). Overexpression of P-gp in tumor cells causes multidrug resistance in these cells (Juliano and Ling, 1976). P-gp is expressed in endothelial cells of the blood-brain

barrier. Several studies, comprising isolated membranes, freshly isolated endothelial cells, isolated capillaries, and tissue slices, show a predominant distribution of P-gp at the apical membrane (Beaulieu et al., 1997, Fricker and Miller, 2004, Jette et al., 1993, Sugawara et al., 1990). Besides in humans, P-gp is expressed in BCECs of other species, such as fish, birds, monkeys, rats, mice, cattle and pigs, protecting the brain from lipophilic xenobiotics, which otherwise could penetrate the BBB by passive diffusion. In rodents, the MDR1 gene is encoded by two genes (mdr1a, mdr1b) with overlapping substrate specificity. While mdr1a is expressed in brain capillaries of mice and rats, mdr1b is only found in brain parenchyma (Cordon-Cardo et al., 1989, Thiebaut et al., 1989). In addition, P-gp is present in a variety of other tissues, including epithelial cells of the liver, kidney, choroid plexus, colon, small intestine, and adrenal gland (Chin and Liu, 1994).

P-gp has a broad substrate specificity including organic cations, weak organic bases, some organic anions and some uncharged compounds, such as polypeptides and polypeptide derivatives. Thus it appears that P-gp can handle various classes of drugs including chemotherapeutics, immunosuppressants, antibiotics, anti-HIV drugs, opioids, and calcium channel blockers (Fricker and Miller, 2004). Studies using mdr1a/b gene knockout mice, show that P-gp deficient mice exhibit significantly elevated drug levels, particularly in the brain (Schinkel et al., 1997, Schinkel et al., 1994). On the other hand, there is a loss of protection and subsequent neurotoxicity by the loss of P-gp function, which has been observed during the treatment of mdr1a gene knockout mice with the antihelminthic ivermectin. The enhanced uptake compared to ivermectin-treated control (wild type) mice, leads to significantly elevated drug concentrations in the brain, resulting in dramatic neurotoxicity (Kwei et al., 1999, Schinkel et al., 1994).

The first P-gp inhibitor described is the calcium channel blocker verapamil. It inhibits the efflux of drugs that are P-gp substrates and restores drug sensitivity in multidrug-resistant leukaemia cell lines (Tsuruo et al., 1981). Another first-generation inhibitor is the immunosuppressive drug cyclosporine A. Both drugs are substrates of P-gp as well, suggesting that they act as competitive inhibitors. However, due to low binding affinities of these inhibitors, high doses causing toxic effects would be required for the clinical use. Furthermore these first-generation compounds are unselective to P-gp and inhibit cytochrome P450 3A (CYP3A) as well (Benet et al., 2004). Many P-gp substrates are metabolized by CYP3A (e.g. cytostatic agents), where the

coadministration of the substrate together with the first-generation inhibitor leads to a decreased clearance, causing an additional degree of toxicity (Breedveld et al., 2006). Second-generation inhibitors, e.g. valspodar (PSC833), are analogs of the first generation of inhibitors, showing higher binding affinities and lower toxic effects. They were initially developed to reverse multidrug resistance. However, the second generation inhibits CYP3A as well, leading to a toxicity, that is unacceptable for clinical use (Fischer et al., 1998). The third generation of P-gp inhibitors, such as elacridar, zosuquidar, and tariquidar were developed with the goal to specifically interact with P-gp (Mistry et al., 2001, Slate et al., 1995, den Ouden et al., 1996, Martin et al., 1999). Preclinical studies have shown that their concomitant use with P-gp substrates, such as paclitaxel, docetaxel, and imatinib, can improve the distribution of these anticancer agents into the CNS (Kemper et al., 2003, Kemper et al., 2004, Kemper et al., 2004, Dai et al., 2003). However, no clinical studies with third generation inhibitors, investigating CNS penetration of drugs, have been published so far.

Several xenobiotics, such as rifampicin, phenobarbital, dexamethasone, clotrimazole, and reserpine are able to induce P-gp expression *in vitro* and *in vivo*, which can lead to drug-drug interactions. Some inducers affect both P-gp and cytochrome P450 enzymes, causing drug-drug interactions involving both of these systems (Westphal et al., 2000, Lin, 2003).

1.3.1.2 ABCC family (MRPs)

The multidrug resistance-associated proteins (MRPs, ABCC family) belong to the ABC superfamily of membrane transporters. Until now, 13 members of this family (including MRP1-9) have been identified (Conseil et al., 2005). However, compared to P-gp, the data on these ABC transporters in the BBB is much more limited (Loscher and Potschka, 2005). MRPs transport organic anions (e.g. methotrexate), glutathione, glucuronide-conjugated compounds, various nucleoside analogs, but also neutral drugs. Therefore P-gp and MRPs have an overlapping substrate specificity, so that several drugs are substrates for both families (Borst et al., 2000, Loscher and Potschka, 2005).

The first discovered member of the ABCC family is **MRP1** (ABCC1). It was identified in cancer cells in 1992, but has also been detected ubiquitously in normal human tissues (Zhang et al., 2004). MRP1 has been identified in bovine brain capillaries, and in porcine BCECs by RT-PCR. The extent of MRP expression is variable and depends on the culture conditions (Gutmann et al., 1999). Confocal laser scanning microscopy and Western blot analysis showed a predominant distribution of MRP1 in the apical membrane. In contrast, the localization of MRP1 in epithelial cells is basolateral, which has been demonstrated in numerous studies in various epithelial preparations (Zhang et al., 2004). However, the contribution of MRP1 to the BBB still is controversial at this time. Studies in mrp1 gene knockout mice do not show any differences in the transport kinetics for several MRP substrates compared to wild type (control) mice (Cisternino et al., 2003).

Immunostaining, RT-PCR, and functional experiments demonstrated the presence of **MRP2** (ABCC2) in fish, porcine, rat, and human brain, and showed a localization on the apical membrane of BCECs (Fricker et al., 2002, Miller et al., 2000, Miller et al., 2002, Potschka et al., 2003). Furthermore, MRP2 is found in epithelial cells of the liver, kidney and intestine of humans (Chu et al., 2006). Studies with mrp2-deficient rat mutants (TR^-) showed significantly enhanced phenytoin levels compared to normal rats, indicating that MRP2 limits the distribution of this compound into the CNS (Potschka et al., 2003).

Using primary cultured bovine brain microvessel endothelial cells and the capillary-enriched fraction from bovine brain homogenates, RT-PCR analysis only showed low levels of **MRP3** (ABCC3) (Zhang et al., 2000). It is predominantly found in liver, gut and kidney, where it is localized basolaterally (Kool et al., 1997), which has been proposed for BCECs as well (Potschka et al., 2003). However, little is known about the role of MRP3 at the BBB, so far.

MRP4 (ABCC4) has been detected in bovine brain capillaries by RT-PCR (Zhang et al., 2000). Besides the brain, MRP4 is expressed in many other tissues, such as lung, kidney, bladder, gallbladder, tonsil, skeletal muscle, pancreas, and prostate (Schinkel and Jonker, 2003). Confocal laser scanning microscopy and Western blot analysis showed an almost equal distribution of MRP4 on the apical and basolateral

membrane of bovine BCECs, suggesting that MRP4 may influence substrate transport both into and out of the brain (Zhang et al., 2004).

Using RT-PCR, **MRP5** (ABCC5) and **MRP6** (ABCC6) have been identified in cultured bovine brain capillaries as well (Zhang et al., 2000). Besides the brain, MRP5 is widely expressed throughout most tissues, whereas MRP6 is predominantly found in liver and kidney (Borst et al., 2000, Kool et al., 1997). While the apical localization of MRP5 has been clearly demonstrated in bovine BCECs by confocal laser scanning microscopy and by Western blot analysis (Zhang et al., 2004), the proposed basolateral localization of MRP6 (Loscher and Potschka, 2005) still needs to be confirmed by further investigations, as well as the potential role of MRP5 and MRP6 at the BBB, which still remains unclear.

1.3.1.3 BCRP (ABCG2)

ABCG2 was first identified in a highly doxorubicin-resistant breast cancer cell line (MCF-7/AdrVp), and was therefore named breast cancer resistance protein (BCRP) (Doyle et al., 1998). Like all members of the ABCG subfamily, it is a ABC half-transporter that forms a functional homodimer (Sugimoto et al., 2005). Besides the BBB, BCRP is expressed in placenta, bile canaliculi, colon, and small intestine (Doyle and Ross, 2003). The presence of BCRP at the BBB was first discovered in porcine BCECs (Eisenblatter and Galla, 2002). Using RT-PCR and Western blot analysis, the expression of BCRP was demonstrated in both normal and tumor human tissue as well. Like P-gp, BCRP is localized at the apical surface of the microvessel endothelium (Cooray et al., 2002). The substrate specificity of BCRP is broad, comprising a wide variety of drugs (e.g. mitoxantrone, topotecan, and prazosine), carcinogens and dietary toxins (van Herwaarden and Schinkel, 2006). BCRP has several substrates in common with P-gp, such as doxorubicine, daunorubicine, and rhodamine-123 (Doyle and Ross, 2003). Analysis of the total mRNA pool indicates that the expression of BCRP in the BBB is higher than P-gp and MRP1, therefore it was concluded that BCRP might play an important role in the exclusion of xenobiotics from the brain (Eisenblatter et al., 2003).

A small number of BCRP inhibitors has been discovered recently as well (Ahmed-Belkacem et al., 2006). The best studied so far is elacridar, which is an efficient

inhibitor of P-gp as well (Breedveld et al., 2006). *In vivo* studies in mdr1a/1b gene knockout mice with topotecan (which is a specific substrate of BCRP but not of P-gp) show a six-fold increase of the plasma concentration of topotecan when coadministered with elacridar. These observations may be a result from the inhibition of BCRP in these P-gp knockout mice (Jonker et al., 2000). A more specific BCRP inhibitor is fumitremorgin C, a fungal toxin derived from *aspergillus fumigatus*, which can be used for pharmacological studies *in vitro*. However, due to its neurotoxicity, no application in animals or humans is possible (Rabindran et al., 2000). Furthermore, the proton pump inhibitor pantoprazole has recently been identified as a specific BCRP inhibitor. Pantoprazole only has a minimal effect on CYP3A4 and has been safely used in patients with peptic ulcers so far, which is a promising prerequisite for its safe use in patients. A potential application may be the combined use with anticancer agents, which could lead to an enhanced CNS penetration of these drugs (Breedveld et al., 2006).

1.3.2 SLCs

The superfamily of solute carriers (SLC) includes ion coupled transporters, facilitated transporters, and exchangers. During the last decade, 298 transporter genes have been classified into 43 families of solute carriers (Hediger et al., 2004). The SLC membrane proteins use chemical and/or electrical gradients to move molecules across cell membranes. Na^+ is the favoured cation to move solutes into cells, whereas anion exchange moves solutes out of cells. Typical endogenous substrates comprise amino acids, glucose, bicarbonate, bile acids, ascorbic acid, urea or fatty acids. However, there is an involvement in drug transport and drug disposition as well. Besides the brain, SLC membrane proteins can be found in kidney, liver, and intestine. Here, we focus on solute carriers that have been identified at the BBB. These SLCs are members of the SLCO (also known as **OATP** or SLC21) and SLC22A (also known as **OAT**) family, and are characterized by their multispecificity.

Currently, the SLCO family includes fourteen members in rodents and human (Kusuhara and Sugiyama, 2005). Two members of this family, human **OATP-A** (alias, SLCO1A2, OATP1A2 or SLC21A3) and the rat Oatp2 (human homologue: SLCO1B1 alias OATP2, **OATP-C** or SLC21A6) have been detected in brain

capillaries by immunostaining (Gao et al., 1999, Gao et al., 2000). OATP-C is a bidirectional transport protein, which is localized both on the apical and the basolateral membrane of the endothelial cell. At present, neither the localization of OATP-A, nor the role of OATPs for the BBB function are clear (Fricker and Miller, 2004).

The SLC22A family includes organic cation transporters, organic cation/carnitine transporters and organic anion transporters. Among the SLC22A family, the organic anion transporter **OAT3** (SLC22A8) has been found at the BBB (Kusuhara and Sugiyama, 2005). Immunostaining reveals a basolateral localization of OAT3 in rat BCECs (Mori et al., 2003). OAT3 substrates include para-aminohippuric acid (p-AH), benzylpenicillin, indoxylsulfate, and homovanillic acid (Kusuhara and Sugiyama, 2005). *In vivo* transport studies with p-AH in rats suggest that Oat3 plays an important role in the elimination of this substrate from the cerebral cortex (Kakee et al., 1997). However, the elucidation of the function of OAT3 at the BBB is still ongoing.

1.4 Cytochrome P450 enzymes

Cytochrome P450 enzymes (CYP) are members of a superfamily of heme-containing monooxygenases. Currently, approximately 50 CYP enzymes can be divided into 17 gene families. The families CYP1, CYP2, and CYP3 contribute to hepatic drug metabolism, including many xenobiotics and endogenous, lipophilic substrates. Although CYPs are primarily located in the liver, CYPs can be found in many other organs, including lung, small intestine, and colon (Ding and Kaminsky, 2003). However, the amount of total CYPs in the brain is only about 0.5-2% of that in liver (Warner et al., 1988). Even though the actual role of brain CYPs remains to be elucidated, local cerebral drug metabolism is thought to be likely, as CYP enzymatic activity has been reported in human brain (Bhamre et al., 1993).

Typical CYP inducers, such as phenobarbital and phenytoin have been shown to increase the expression of certain CYP isoforms in the brain. Therefore, it has been suggested that the induction of brain CYPs has an impact on local drug metabolism (Gervasini et al., 2004, Schilter et al., 2000). However, little is known so far about the expression and functional role of CYPs at the BBB. Therefore in this thesis, we

studied the amount and inducibility of selected CYP isoforms that may play a role in the metabolism of CNS active drugs at the BBB with our human *in vitro* model, the BB19 cells.

1.4.1 CYP1A

Both **CYP1A1** and **CYP1A2** are involved in the oxidation of a wide spectrum of endogenous compounds and xenobiotics, and can be induced by polycyclic aromatic hydrocarbons. CYP1A2 is involved in the metabolism of psychotropic drugs, including amitriptyline, imipramine, fluvoxamine, clozapine, and olanzapine. The presence of CYP1A1 and CYP1A2 has been confirmed in brain tissue, repeatedly. However reports regarding their distribution in the brain are contradictory. Western blot analysis revealed, that CYP1A1, but not CYP1A2, can be induced in the arachnoid, dura mater, choroid plexus, pineal gland and pituitary, and might play a role in the protection of the brain from xenobiotics (Morse et al., 1998).

1.4.2 CYP2D6

CYP2D6 is involved in the metabolism of a large number of psychoactive drugs, including many antidepressants and neuroleptics, such as citaloprame, fluoxetine, nortryptiline, haloperidole, thioridazine, among many others (Dahl and Bertilsson, 1993, Gervasini et al., 2004). CYP2D6 is one of the most polymorphic isoforms of the cytochrome P450 enzymes in humans, resulting in poor, intermediate, efficient or ultrarapid metabolizers of CYP2D6 substrates (Casner, 2005, Ingelman-Sundberg, 2005). CYP2D6 is expressed in specific cerebral regions and cell types, such as the frontal cortex, putamen, hippocampus and Purkinje cells of the cerebellum (Siegle et al., 2001, Miksys et al., 2002). It has been suspected that the well established genetic variability of CYP2D6 in the liver may also exist in brain, leading to interindividual differences in the metabolism of drugs in the CNS. However, this presumption has not been proven yet, whereas conversely, quinidine, a specific CYP2D6 inhibitor that does not cross the BBB, is able to impair the biotransformation of codeine to morphine. (Gervasini et al., 2004, Kathiramalainathan et al., 2000). CYP2D6 activity can also be modulated by a number of endogenous compounds. Neurotransmitters and related substances, such as epinephrine, serotonin,

tryptamine, and tyrosine, have shown to be potent inhibitors of CYP2D6 (Gervasini et al., 2004). All these findings taken together indicate an important role of CYP2D6 in the human brain.

1.4.3 CYP3A

The human CYP3A subfamily plays the most important role in the metabolism of xenobiotics. The major isoform **CYP3A4** accounts for about 30% of the total hepatic CYPs. Other isoforms are CYP3A3, CYP3A5, and CYP3A7 (Gervasini et al., 2004). About 60% of all drugs are metabolized by CYP3A, including many CNS active drugs, such as antidepressants, antiepileptics, neuroleptics, and sedatives (Zhou et al., 2005).

Several potent inducers of CYP3A are known, including rifampicin, dexamethasone, and phenobarbital (Kato et al., 2005). CYP3A has been detected in human brain on mRNA level, with highest amounts in the pons region (Farin and Omiecinski, 1993). Furthermore, *in vitro* studies showed that CYP3A4 demethylates amitriptyline to nortriptyline in rat and human brain microsomes (Voirol et al., 2000). These findings may lead to the assumption that brain CYP3A may play a significant role in the metabolism of CNS active drugs. However, the functional relevance of these findings still needs to be proved.

1.4.4 Regulation of cytochrome P450 by nuclear receptors

The expression of CYPs is selectively regulated by ligand-activated nuclear receptors. The pregnane X receptor (PXR), an orphan nuclear receptor, has been shown to regulate the expression of CYP3A in mice, rats, and humans (Lehmann et al., 1998, Mikamo et al., 2003). PXR ligands comprise a wide range of compounds, including many steroids, antimycotics, and antibiotics (e.g. rifampicin). After activation by the ligand, PXR forms heterodimers with the retinoic X receptor (RXR), which is another nuclear receptor. This heterodimer binds to specific DNA sequences, and regulates the expression of its target genes. In addition to CYP3A, other targets of PXR are P-gp, other ABC transporters, and CYPs (Honkakoski and Negishi, 2000, Lehmann et al., 1998).

The constitutive androstane receptor (CAR) is another nuclear receptor. It plays an important role in the regulation of CYP2B, CYP2C, CYP3A, and MRPs, among other target genes. CAR is closely related to PXR. Besides showing a high sequence homology, CAR and PXR share a similar mechanism of action by forming heterodimers with RXR (Xiao et al., 2002, Tirona and Kim, 2005).
The expression of each member of the CYP1A family is inducible by the aryl hydrocarbon receptor (AhR). After activation by a ligand, such as polycyclic aromatic hydrocarbons (PAH), AhR heterodimerizes with the aryl hydrocarbon nuclear translocator and activates the transcription of its target gene (Denison and Whitlock, 1995).

1.5 Models for the prediction of BBB permeability

In drug discovery and development, the investigation of BBB permeability is demanded for CNS-active drug candidates, as well as for drug candidates with non-CNS indications. However, poor BBB permeability is recognized to be one of the leading causes of failure in the development of CNS-active drugs. This has led to the development of different *in vitro*, *in vivo*, and *in silico* methods for the assessment of BBB drug permeability.

1.5.1 *In vitro* models

Isolated brain capillaries were the first *in vitro* model of the BBB. Viable capillaries can be isolated from brain tissues of various species. The BBB-specific gene expression of endothelial receptors and carriers of these isolated brain capillaries remains close to the *in vivo* situation. They can be used for binding and uptake assays and to study BBB transport systems for nutrients and peptides at the mRNA and protein level (Pardridge, 1998). However, isolated brain capillaries are not metabolically viable and have very low levels of ATP (Pardridge, 1999, Lasbennes et al., 1983). Another disadvantage of isolated brain capillaries is a high potential of contamination of the preparation by other brain-derived cells (Takakura et al., 1991).

The successful isolation and culturing of brain capillary endothelial cells (BCEC) in the 1980s led to the development of **cell culture systems** for the assessment of

BBB drug permeability *in vitro* (Pardridge, 1998). Up to the present, a wide rage of *in vitro* models, including primary or immortalized brain capillary cells from different species have been established (Bickel, 2005, Gumbleton and Audus, 2001). Some groups even use cell lines of non-cerebral origin, such as the Madin-Darby canine kidney (MKCK) cells (Veronesi, 1996) or the human Caucasian colon adenocarcinoma (Caco-2) cell line (Lohmann et al., 2002). BCEC monolayers can be cultured on permeable filters, which allows the study of bidirectional substance transport from the apical to the basolateral side, and vice versa.

Primary cultures of BCECs can be obtained from many species, including rat, mouse, dog, or primate. However, cells of porcine and bovine origin are the most commonly used, as only these sources provide adequate quantities for a sufficient number of permeability experiments (Bickel, 2005). These cells maintain most of the *in vivo* BBB features, however some transporters are downregulated, as for example the glucose transporter 1 (GLUT1), which is suppressed 150-fold in bovine BCECs compared to the *in vivo* level (Boado and Pardridge, 1990). Some groups use co-cultures with astrocytes or glioma cell lines (Dehouck et al., 1990, Boveri et al., 2005) or add astrocyte conditioned medium to improve the tightness of the BBB (Shivers et al., 1988).

In this thesis, the porcine BCEC model was applied for the study of BBB permeability of different CNS active preclinical substances provided by an industrial collaboration partner. Therefore we investigated the bidirectional transport of these compounds in this *in vitro* model of the BBB.

A major drawback for the use of such systems as *in vitro* screening models for BBB permeability is that the preparation is time consuming and requires considerable technical resources. In addition, the function of primary cultures of BCECs may vary from batch to batch (Terasaki et al., 2003). Furthermore, due to ethical considerations, these cells cannot be obtained from humans.

Immortalized BCEC lines have the advantage that the generation of a sufficient amount of cells for high-throughput screening is less laborious compared to primary endothelial cells. However, the so far characterized immortalized cell lines fail to generate a sufficiently restrictive paracellular barrier for the use in transendothelial permeability investigations (Gumbleton and Audus, 2001). An efficient and predictive

in vitro permeability screening model, based on immortalized human BCECs, would be an important tool for the evaluation of BBB permeability in drug development. In this thesis, we evaluated the immortalized human brain capillary endothelial cell line BB19. This cell line has been used to study cytoadherence of *Plasmodium falciparum*-infected erythrocytes *in vitro* (Prudhomme et al., 1996). BB19 cells are derived from human brain endothelium and are immortalized with E6E7 genes of the human papilloma virus. They express factor VIII-related antigen and von Willebrand's factor. Cells exhibit a cobblestone like morphology. However tightness of BB19 monolayers had not been investigated so far.

1.5.2 *In vivo* models

A common method for the assessment of BBB permeability is the **intravenous administration** of a test substance into an animal. After a single bolus injection of a radiolabeled test compound, the animal is decapitated and the brain tissue is analyzed for radioactivity (Mater et al., 1959). Tissue uptake can also be measured over long periods using constant rate infusion. This method fully represents physiological conditions and offers simple technical handling. However, elaborate analytics are required, to exclude metabolite uptake (Bickel, 2005).

Metabolism in other organs is excluded with the **brain uptake index** (BUI) technique. In this method, a rapid bolus injection of radiolabeled test and reference substances is injected into the common carotid artery of anesthetized animals (Oldendorf et al., 1982, Oldendorf, 1970). The procedure is relatively fast and permits to analyze the effects of a wide range of modifications of the injectate composition, such as pH, osmotic pressure, or protein binding (Bickel, 2005).

A higher sensitivity compared to the BUI can be achieved with the **brain perfusion** method. This method uses a retrograde catherization of the carotid artery in the anesthetized animal, and ligation of all branches of the external and internal carotid artery. Subsequently, the perfusion with an oxygenated buffer, containing the test substance, is initiated. The cerebrovascular permeability can be estimated from the brain parenchymal uptake of the test substance (Takasato et al., 1984). However, this method is technically more difficult compared to the BUI technique.

In the last decade, the **microdialysis** technique has increasingly been applied. In this method, a microdialysis probe is implanted into the brain. After administration of the drug, the dialyzed drug from the extracellular fluid into the probe can be measured. This method allows repeated or continuous sampling in freely moving animals. However, major disadvantages of this technique are the variability of the results depending on the localization of the probe, and an invasive procedure causing traumatic injury (Aasmundstad et al., 1995, Westergren et al., 1995).

The latest method used to study transport across the BBB *in vivo* is **positron emission tomography** (PET). This non-invasive technique can be applied in humans. After intravenous injection of the radiotracer, the subject is positioned in a PET scanner, which can detect positrons emitted by the radiotracer. Additional to the assessment of BBB permeability, PET provides information about region-specific drug distribution in the brain (Webb et al., 1989). Limitations of this methods include a short half-life of the isotope, high cost of the instrumentation, and the lack of differentiation between parent drug and metabolites (Bonate, 1995).

1.5.3 *In silico* models

In silico models ought to predict BBB permeability from chemical structures. For the development of these computational models, experimental brain uptake data is correlated with molecular properties, such as lipophilicity and molecular weight (Goodwin and Clark, 2005, Clark, 2003). So far, only passive permeability at the BBB has been modelled, because the knowledge about the relationship between molecular structure and active or facilitated transport is still limited (Bickel, 2005). Thus, *in silico* models may be a useful tool for the initial screening of lead compounds to predict passive BBB permeability. However, up to the present, these models do not substitute *in vitro* or *in vivo* models of the BBB.

1.6 Models for the assessment of drug efflux transporter activity

Efflux transporters do not only influence the brain uptake of drugs, but also the absorption, elimination, and distribution into other tissues besides the brain. Therefore numerous *in vitro* and *in vivo* models have been developed for the identification of drugs that interact with drug efflux transporters, particularly for P-gp (Zhang et al., 2003) .

1.6.1 *In vitro* models

In general, three groups of *in vitro* systems for the assessment of P-gp drug efflux have been described, namely uptake/efflux, transport, and ATPase activity.

Uptake and Efflux studies can be performed with cell suspensions, cell monolayers, or membrane vesicle preparations. For uptake and efflux studies, the uptake or efflux of a fluorescent or radioactive P-gp substrate into cells or vesicles is monitored under control conditions and in the presence of P-gp inhibitors or test substances. In this thesis, we used a murine mdr1a/1b overexpressing monocytic leukaemia cell line (P388/mdr1) and the corresponding parental cell line (P388/par), and a human T-lymphocytic leukaemia cell line overexpressing MDR1 (CCRF-CEM/MDR1) and the corresponding parental cell line (CCRF-CEM/Par), which all are suspension cells (Pourtier-Manzanedo et al., 1992). This *in vitro* system was applied for the identification of P-gp inhibitors among selected neuroleptic drugs and drug metabolites. Therefore, we studied the influence of these compounds, on the uptake and efflux of the fluorescent P-gp substrate rhodamin123.

Transport assays for P-gp drug efflux can only be performed in P-gp expressing cells forming functionally polarized cell monolayers with highly restrictive tight junctions. Bidirectional transport of test substances from the apical to the basolateral side, and vice versa, can be studied under control conditions and in the presence of P-gp inhibitors (Drewe et al., 1999, Zhang et al., 2003, Schwab et al., 2003).
The transport assay with porcine BCEC was applied for the identification of P-gp substrates among selected neuroleptic compounds. Therefore, we studied the

influence of verapamil, a P-gp inhibitor, on the BBB permeability of neuroleptic compounds in porcine BCEC.

The **ATPase assay** is another *in vitro* assay to determine if a drug interacts with P-gp. During drug transport, ATP is hydrolyzed to ADP and inorganic phosphate, by the P-gp ATPase, which can be detected colorimetrically. Interacting test drugs modulate the activity of the P-gp, resulting in the modulation of the rate of ATP hydrolysis. This is a commercially available assay, which is performed with cell membrane preparations enriched with human P-gp. However, a high intra- and inter-assay variability has been reported for this assay (Orlowski et al., 1996, Zhang et al., 2003).

1.6.2 *In vivo* models

The influence of P-gp on drug disposition into the brain can be studied with P-gp gene knockout mice. As described earlier in chapter 1.3.1.1, in mice, P-gp is encoded by mdr1a and mdr1b. Only mdr1a is found at the BBB. There are single knockout mice, lacking mdr1a (Schinkel et al., 1994), as well as double knockout mice, lacking both mdr1a and mdr1b (Schinkel et al., 1997). Both types of knockout mice have been used extensively for the evaluation of brain accumulation of drugs. It has been shown in mdr1a and mdr1a/1b gene knockout mice that brain uptake of P-gp substrates can increase up to 100-fold compared to wild type mice (Schinkel and Jonker, 2003, Thompson et al., 2000). However, there are limitations of knockout mice. The absence of a gene may lead to a compensatory upregulation of other related genes, such as mrp1 and bcrp (Johnson et al., 2001, van der Deen et al., 2005). Furthermore, due to ubiquitous expression of P-gp, its removal will affect other tissues than the brain, which may lead to altered pharmacokonetics, lack of viability, or systemic toxicity (Zhang et al., 2003).

1.7 Applications of in vitro models

1.7.1 Neuroleptic drugs

Between 20-40% of schizophrenic patients are resistant to neuroleptic medication, even when these drugs are administered at maximum tolerated doses. Although the underlying causes of insufficient drug response are still unclear, there are numerous suspected assumptions, including neuropsychological impairment and abnormal brain morphology (Hellewell, 1999). Another possible explanation may be the modulation of brain uptake of neuroleptic drugs by P-gp. The modulation of P-gp activity may furthermore lead to pharmacokinetic drug-drug interactions, which could affect the safety and efficacy of neuroleptic drugs. Therefore, there is an increasing interest in the elucidation of the influence of P-gp on the distribution of neuroleptic compounds into the brain. There is increasing evidence from *in vitro* assays that neuroleptic drugs may modulate P-gp activity. Haloperidol and quetiapine, and to a low extend clozapine, and its metabolite norclozapine, have been identified as P-gp inhibitors in a radioligand displacement assay *in vitro* (El Ela et al., 2004). Quetiapine and risperidone, and to a lower extend olanzapine, were identified as P-gp substrates in an ATPase assay, whereas clozapine and haloperidol only showed very weak activity in this assay (Boulton et al., 2002). Other experiments using the ATPase assay with risperidone and its major metabolite 9-OH risperidone showed that risperidone is a better P-gp substrate than 9-OH risperidone, which was confirmed in experiments with mdr1a gene knockout mice (Ejsing et al., 2005). However, only little is known about the impact of P-gp for the distribution of neuroleptic drugs into the brain (El Ela et al., 2004).

In this thesis, we investigated the influence of the following neuroleptic compounds (provided by the Psychiatric Clinic of the University of Mainz, Germany) on uptake and efflux of rhodamin123 in P388/mdr1 cells (Figure 1.4): aripiprazole, clozapine and its metabolite norclozapine, haloperidol, quetiapine, ziprasidone, risperidone and its metabolite 9-OH risperidone, and olanzapine.

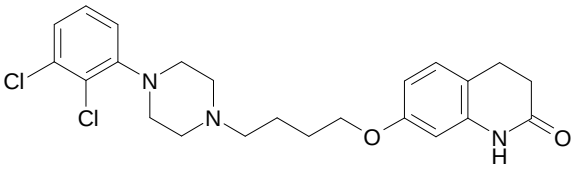

Aripiprazole

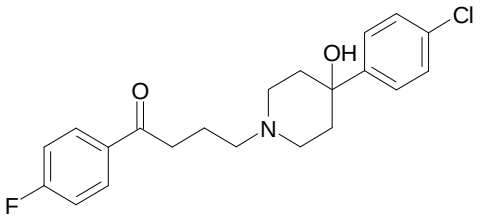

Haloperidol

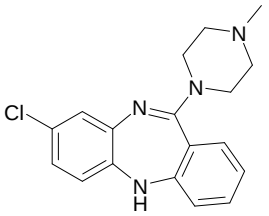

Clozapine

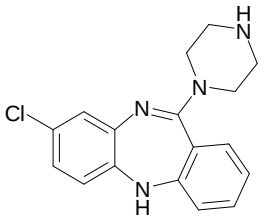

Norclozapine

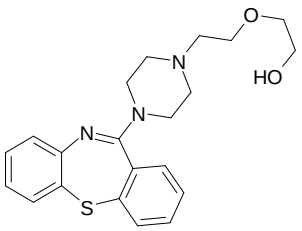

Quetiapine

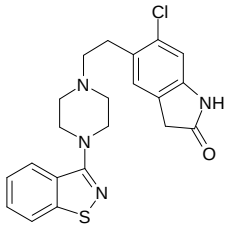

Ziprasidone

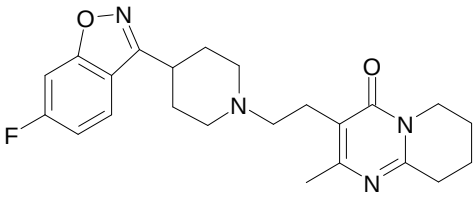

Risperidone

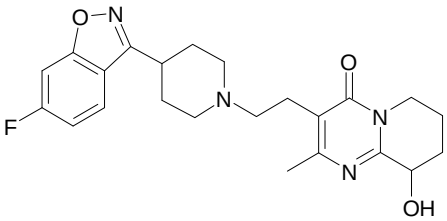

9-Hydroxyrisperidone

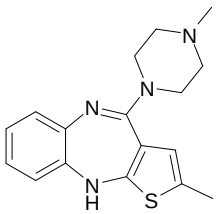

Olanzapine

Figure 1.4 Chemical structures of investigated neuroleptic compounds

2 Aim of the thesis

The major aim of this thesis was the evaluation of the immortalized human brain capillary endothelial cell line BB19 as an *in vitro* model of the BBB. An efficient and predictive *in vitro* permeability screening model, based on immortalized human BCECs, would be an important tool for the evaluation of BBB permeability in drug development.

Therefore, the following investigations were conducted during this project:

- The tightness of the cell monolayers and the ability of BB19 cells to discriminate between transcellular and paracellular markers were studied.
- The effects of specific cell culture supplements on cell morphology, ZO-1 expression, and tightness of the BB19 cell monolayers were investigated.
- The expression of important BBB transporters was studied.
- It was determined if the BB19 model exhibits functional properties of the BBB.
- Expression and inducibility of CYPs were assessed.

In addition, different *in vitro* models were applied for the assessment of BBB drug permeability in the following projects:

- In collaboration with the Psychiatric Clinic of the University of Mainz, Germany, the potential of neuroleptic drugs to modulate P-gp function was studied.
- The BBB permeability of different CNS active compounds was evaluated in an industrial collaboration project.

In a further industrial collaboration project we aimed to develop a combined *in vitro* model, simultaneously studying BBB penetration and pharmacological effect.

3 Materials and methods

3.1 Materials

RO-20-1724 and 1,25-dihydroxyvitamin D_3 were kindly provided by Roche Pharmaceuticals, Basel, Switzerland. All other chemicals were purchased from commercial sources at the highest purity available.

3.2 Evaluation of BB19 cells

3.2.1 BB19 cells

BB19 cells, human BCECs immortalized with the E6E7 genes of human papilloma virus, were kindly provided from Jacques G. Prudhomme, Department of Biology, University of California, Riverside, U.S.A. The cell line (passage 11-13) was cultured as monolayer culture (cell culture medium: MEM, 0.5 mM sodium pyruvate, MEM non essential amino acids, and 50 µg/ml gentamicin, containing 10% heat inactivated fetal bovine serum (FBS, Invitrogen, Basel, Switzerland)).

Cells were seeded onto culture surfaces precoated with 2 µg/cm^2 rat tail collagen at a density of 100,000 to 150,000 cells/cm^2 and were cultured in an incubator at 37°C with 5% CO_2, 95% fresh air and saturated humidity. Cell culture medium was changed every 2 to 3 days. Cells attached to the cell culture surfaces within one day, and started to grow after the second day in culture.

For transport assays, cells were seeded with a density of 100,000 cells/cm^2 onto BD Falcon^{TM} polyethylene terephthalate (PETE) culturing inserts (0.4 µm pore size, 0.9 cm^2 growth area) or on Transwell® polycarbonate filters (0.4 µm pore size, 1 cm^2 growth area), both precoated with 10 µg/cm^2 rat tail collagen, cultured under standard conditions. Transport assays were performed at confluency, after 5 days in culture. For immunostaining, BB19 cells were seeded onto chamber slides (Nunc, Naperville, IL, U.S.A.) precoated with rat tail collagen (20 µg/cm^2) and poly-D-lysine (10 µg/cm^2) at a density of 100,000-200,000 cells/cm^2.

3.2.2 Porcine BCEC

Primary cultures of porcine brain capillary endothelial cells were prepared as described (Audus and Borchardt, 1986) with the following modifications: Cortical grey matter from six freshly obtained porcine brains was minced and incubated in MEM (Invitrogen) containing 0.5% dispase (Roche Diagnostics AG, Rotkreuz, Switzerland) for 2 hours. Cerebral microvessels were obtained after centrifugation in MEM containing 1 mg/ml collagenase/dispase (Roche Diagnostics AG) for 4.25 hours. The resulting cell suspension was supplemented with 10% horse serum and filtered through a 150-µm nylon mesh. BCECs were isolated on a continuous 50% Percoll gradient (Pharmacia, Uppsala, Sweden) (centrifugation at 1000×g for 10 minutes). For transport assays, isolated endothelial cells were seeded onto BD Falcon™ PETE cell culture inserts with 0.4 µm pore size and 0.9 cm^2 growth area (BD Biosciences Discovery Labware, Le Pont de Claix, France) coated with 2 µg/cm^2 rat tail collagen (Roche Diagnostics), with a density of 100,000 cells/cm^2 or on Transwell® polycarbonate filters (Costar, Cambridge, MA, U.S.A) with 0.4 µm pore size and 1 cm^2 growth area coated with 2 µg/cm^2 rat tail collagen, in 12-well plates and cultured under standard cell culture conditions (Audus and Borchardt, 1986) (cell culture medium: 45% MEM, 45% Ham's F-12, and 20 mM HEPES and 100 µg/ml gentamicin containing 10% heat activated horse serum, (all Invitrogen)). Transport experiments were performed at confluency after 7 days in culture.

3.2.3 Conditioned medium

To test the influence of different supplements on the expression of tight junction proteins, BB19 cells were seeded onto chamber slides, and at the third day of culture, 10 µM dexamethasone, 0.5 µM 1,25-dihydroxyvitamin D3, 250 µM chlorophenylthio-cAMP (all Fluka Chemie GmbH, Buchs, Switzerland) with 35 µM RO-20-1724, or C6-conditioned medium taken from an astrocyte culture (mixed 1:1 with culture medium) were added to the culture medium. The influence on P-gp and BCRP expression was tested with 10 µM rifampicin. Cells were incubated with these factors for 72 hours.

3.2.4 RT-PCR

Total RNA was isolated from confluent monolayers of BB19 cells using the RNeasy Mini Kit (Qiagen, Hilden, Germany). After DNase I digestion the RNA was quantified with a GeneQuant photometer (Pharmacia). The purity of the RNA preparations was high, as demonstrated by the 260 nm/280 nm ratio (range 1.8-2.0). One µg of total RNA was reverse transcribed with Superscript II (Invitrogen) according to the manufacturer's protocol, using random hexamers as a primer. A total of 25 ng cDNA was used as a template for PCR with a set of primers. Primers (Table 3.1) were designed with the assistance of Primer Express software (Applied Biosystems, Rotkreuz, Switzerland). Primers were synthesized (Invitrogen) for the following genes: multidrug resistance-associated proteins (MRP1-5), organic anion transporting polypeptide (OATP-A) organic anion transporter (OAT1, OAT3, and OAT4) and breast cancer resistance protein (BCRP). Glyceraldehyde phosphate dehydrogenase primers (GAPDH) were used as an internal control.

The primers for RT-PCR of P-gp (MDR1) were synthesized according to the original sequence of Limtrakul and colleagues (Limtrakul et al., 2004) the primers for OATP-C were synthesized according to the original sequence of Briz and colleagues (Briz et al., 2003).

PCR was performed with a thermocycler (Biometra, Göttingen, Germany). Each sample was amplified for 40 cycles (94°C for 30s, 60°C for 40s, 72°C for 60s). The reaction mixture contained 2.5 µl of the cDNA template, 0.625 U AmpliTaq gold DNA polymerase (Applied Biosystems), 2.5 µl 10x PCR buffer (Mg^{2+} -free, Applied Biosystems), $MgCl_2$ at a final concentration of 3 mM, 2 µl of dNTP reaction mixture (2.5 mM each, Applied Biosystems), 7.5 pmol of each primer and water to a final volume of 25 µl. As negative control, not reverse transcribed RNA was used. The PCR products were separated by gel electrophoresis in 1.5% agarose and visualized by UV in the presence of ethidium bromide.

Primer	Access. no.	Sequence	Size (bp)
GAPDH	M17851	Forward: 5'-GGTGAAGGTCGGAGTCAACG-3'	577
		Reverse: 5'-ACCATGTAGTTGAGGTCAATGAAGG-3'	
MDR1	Limtrakul et al., 2004	Forward: 5'-GCCTGGCAGCTGGAAGACAAATACACAAAATT-3'	283
		Reverse: 5'-CAGACAGCAGCTGACAGTCCAAGAACAGGACT-3'	
MRP1	NM_004996	Forward: 5'-CACACTGAATGGCATCACCTTC-3'	317
		Reverse: 5'-CCTTCTCGCCAATCTCTGTCC-3'	
MRP2	NM_000392	Forward: 5'-CCAATCTACTCTCACTTCAGCGAGA-3'	473
		Reverse: 5'-AGATCCAGCTCAGGTCGGTACC-3'	
MRP3	AF085690	Forward: 5'-TCTATGCAGCCACATCACGG-3'	328
		Reverse: 5'-GTCACCTGCAAGGAGTAGGACAC-3'	
MRP4	AF071202	Forward: 5'-AAGTGAACAACCTCCAGTTCCA-3'	518
		Reverse: 5'-CCGGAGCTTTCAGAATTGAC-3'	
MRP5	NM_005688	Forward: 5'-CTAGAGAGACTGTGGCAAGAAGAGC-3'	333
		Reverse: 5'-AAATGCCATGGTTAGGATGGC-3'	
OATP-A	U21943	Forward: 5'-CTGTCAAACAAGCTGCCCACA-3'	497
		Reverse: 5'-GAATACAGCTGCAATTTTGGAACAC-3'	
OATP-C	Briz et al., 2003	Forward: 5'-TGTCTTTGCATGTGCTGGAAA-3'	604
		Reverse: 5'-TTGCCACTTGAAGATTTGCAAC-3'	
OAT1	AB009697 (004790)	Forward: 5'-GCCACTAGCTTTGCATACTATG-3'	636
		Reverse: 5'-CTCTTGTGCTGAGGCCTG-3'	
OAT3	AB042505	Forward: 5'-TCTTGGCTCTCACCTTTGTGC-3'	459
		Reverse: 5'-GATAGGCATCCCTTCCCAAAC-3'	
OAT4	AB026116	Forward: 5'-GCCTCGCCATTCTAGCCAA-3'	383
		Reverse: 5'-CAAAGACCACACGCAGGGT-3'	
BCRP	AY289766	Forward: 5'-TTTCAGCCGTGGAACTCTTT-3'	462
		Reverse: 5'-TGAGTCCTGGGCAGAAGTTT-3'	

Table 3.1 Primer sequences used for RT-PCR

3.2.5 Immunocytochemistry

For immunostaining, BB19 cells, grown in Chamber Slides® (Nunc, Wiesbaden, Germany), were used. Cells were washed twice with PBS and fixed for 20 minutes with 4% (w/v) paraformaldehyde in PBS. Subsequently, tissues were permeabilized for 5 minutes with 0.5% (v/v) Triton X-100 in PBS and washed twice again with PBS.

For immunostaining, cells were incubated for 2 hours at 37°C in a humid chamber with the primary antibody dissolved in PBS supplemented with 3% (w/v) FBS. After washing twice with PBS, the fluorochrome conjugated secondary antibody dissolved in PBS supplemented with 3% (w/v) BSA was added for 1 hour at room temperature, in a humid chamber and in the dark. Stained cells were then washed twice with PBS and mounted with FluorSave® (Calbiochem, San Diego, CA). Fluorescence stained

cells were examined on a confocal Zeiss LSM 150 inverted laser scanning microscope (Carl Zeiss, Oberkochen, Germany).

Primary antibodies used for these experiments were the murine monoclonal antibodies (Mab) JSB-1 (2.5 µg/ml; ALEXIS, Lausen, Switzerland), or C219 (5 µg/ml, ALEXIS) directed against P-gp, a murine Mab to MRP1 (MRPr1, 10 µg/ml; ALEXIS), a murine Mab to MRP2 (M_2I-4, 2.5 µg/ml, ALEXIS), a murine anti-MRP3 Mab (M_3 II-9, 5 µg/ml), a rat anti-MRP4 Mab (M4I-80, 4 µg/ml) a rat anti-MRP5 Mab (M_5 I-1, 10 µg/ml), a rabbit polyclonal anti-ZO-1 (2.5 µg/ml, Zymed Laboratories, San Francisco, CA), and the murine Mab BXP-21 directed against BCRP (5 µg/ml, ALEXIS). Cells were subsequently incubated for 1 hour at room temperature with a secondary antibody. Used antibodies were a Cy2™ conjugated rabbit anti-rat IgG (Dako Corp., Santa Barbara, CA) in PBS/3% rabbit serum, a Cy2™-conjugated anti-mouse (15 µg/ml, Jackson ImmunoResearch, Soham, UK), IgG, a Cy2™-conjugated goat anti-rabbit IgG (7 µg/ml, Jackson ImmunoResearch), and a Cy3™-conjugated goat anti-mouse IgG (15 µg/ml, Jackson ImmunoResearch). The cells were rinsed with PBS, mounted with FluoroSave®, and examined on a Zeiss Axiophot® fluorescence microscope equipped with a Zeiss Plan-Neofluar® objective.

3.2.6 Western blot

The presence of P-gp and BCRP was studied by Western blot analysis using the murine Mab C219 (ALEXIS) for P-gp and the murine Mab BXP-21 directed against BCRP (ALEXIS). SDS-polyacrylamide gel electrophoresis (SDS-PAGE) was performed with a Mini-Protean II apparatus (Bio-Rad, Zurich, Switzerland). To BB19 or porcine BCEC cell homogenates (2-4 mg/ml protein, obtained from cells either cultivated under standard conditions or supplemented with 10 µM rifampicin), the same amount of Lämmli buffer (Bio-Rad) was added. The samples were loaded onto a 4% acrylamide/bisacrylamide gel. After electrophoresis, the proteins were transferred electrophoretically (2 hours at a constant amperage of 250 mA) to a 0.45 µm pore size nitrocellulose membrane using a Mini Transblot cell (Bio-Rad). The transfer buffer contained 192 mM glycine, 25 mM Tris-HCl, and 20% methanol. The membrane was blocked overnight at 4°C with 5% powdered skimmed milk in PBS containing 0.05% Tween 20 (PBS-T). Washed membranes were incubated with Mab C219 (1 µg/ml) or Mab BXP-21 (1.25 µg/ml) in PBS-T and 1% powdered skimmed

milk for 2 hours at 37°C. Washed membranes were incubated for 1 hour at room temperature with horseradish peroxidase-conjugated rabbit anti-mouse IgG (1:500) (Dako) in PBS-T containing 1% milk powder. Membranes were washed in PBS-T and P-gp or BCRP were visualized using enhanced chemiluminescence detection (ECL-kit by Amersham, Buckinghamshire, UK).

3.2.7 Uptake assays

Uptake assays were performed at 20°C using confluent monolayers of BB19 cells, 5 days after seeding in 24-well cell culture plates with surface areas of 2 cm^2/well. Cells were washed using Hanks Balanced Salt Solution supplemented with 1 mM sodium pyruvate, pH 7.4 (HBSS-P) (both Invitrogen). Cells were incubated for 1, 2, 5, 10, 20, 30, 60 or 120 minutes with 0.3 µCi/well of the extracellular marker [^{14}C]-sucrose (Amersham) together with either 0.3 µCi/well of [^{3}H]-morphine (Du Pont, Boston, MA) or [^{3}H]-propranolol (Amersham). Then cells were washed with HBSS-P. The cell monolayers were solubilized in 0.8% triton-X for 20 minutes and the solutions were transferred to scintillation vials. Radioactivity was determined by liquid scintillation counting (Packard TriCarb 2000, Packard, Dreieich, Germany).

3.2.8 Daunomycin uptake – assay for P-gp functionality

The uptake assay was performed as described above, with the following modifications: After washing with HBSS-P, cells were preincubated for 15 minutes with HBSS-P with or without 100 µM verapamil. Cells were incubated for 30 minutes with 1 µM daunomycin (0.3 µCi/well [^{3}H]-daunomycin (Perkin Elmer, Boston, MA) and unlabelled daunomycin) with or without 100 µM verapamil. Then cells were washed with HBSS-P, and it was further proceeded as described above.

3.2.9 Transport assays

For the study of transendothelial transport, cells were used when they reached confluency. Cells were seeded onto BD Falcon™ PETE cell culture inserts, or on Transwell® polycarbonate filters, both in 12-well plates precoated with 10 µg/cm^2 rat tail collagen. Cell culture medium was removed from upper and lower compartment, and both compartments were washed with transport buffer (HBSS-P, pH 7.4). Both

sides of the compartments were filled with pre-warmed transport buffer. The transport assay was performed at constant temperature (37°C) on a rotary platform (50 RPM on an Orbital Shaker, Forma Scientific, Marietta, OH, U.S.A.). At time t=0, 0.3 µCi/well [^{14}C]-sucrose or [^{3}H]-propranolol was added to the upper compartment (donor chambers, apical side) or to the lower chamber (donor chambers, basolateral side) respectively. In defined time intervals, samples were drawn from the lower compartment (acceptor chamber, basolateral side) or from the upper compartment (acceptor chamber, apical side), respectively. Instagel® plus scintillation liquid was added (Canberra Packard S.A., Zurich, Switzerland), and samples were analyzed by scintillation counting (Packard TriCarb 2000, Canberra Packard S.A.). The acceptor volume was readjusted with assay buffer after each sample was taken, and counts from acceptor side samples were corrected for the amount of radioactivity removed by previous sampling. The compound apparent permeability $\mathbf{P_{app}}$ was calculated with equation 1:

$$P_{app} = \frac{dQ/dt}{A \times C_0} \qquad \text{(equation 1)}$$

where **dQ / dt** is the rate of translocation, **A** is the surface of the cell culture insert and $\mathbf{C_0}$ is the initial concentration of [^{3}H]-sucrose.

Permeability coefficients give a relation between the permeability of the monolayer and the permeability of empty filters (precoated with rat tail collagen, without cells). The slopes of the volume cleared vs. time represent the clearance for each condition. The clearance of each well was related to the clearance of empty wells and used to calculate the permeability coefficients ($\mathbf{P_e}$) of the endothelial monolayer, as shown in equations 2 and 3 according to (Rist et al., 1997):

$$\frac{1}{PS} = \frac{1}{m_e} - \frac{1}{m_f} \qquad \text{(equation 2)}$$

and

$$P_e = \frac{PS}{A} \qquad \text{(equation 3)}$$

where **PS** is the permeability-surface area product, **A** is the surface area of the filter and $\mathbf{m_e}$ and $\mathbf{m_f}$ are the volumes cleared vs. time, corresponding to endothelial cells on filters and to empty filters, respectively.

3.3 Expression and inducibility of CYPs in BB19 cells

3.3.1 Absolute quantification of mRNA expression of cytochrome P450 enzymes

3.3.1.1 Principle

Gene expression of different CYP isoforms in BB19 cells was studied with real time RT-PCR (TaqMan®). Before real-time PCR amplification could be performed, the isolated cellular mRNA had to be reverse transcribed into cDNA. The cDNA was subsequently quantified with TaqMan® analysis using the standard curve method. Therefore we used external standards, which comprised known amounts of specific cDNA fragments of the gene of interest. Consequently, the unknown amount of cDNA in the analyzed samples could be expressed as absolute transcript numbers of the corresponding gene.

3.3.1.2 Generation of cDNA standards for absolute mRNA quantification

In order to generate standard curves, we used gene-specific cDNA fragments with known concentrations as standards. These standards serve as a template during the real-time PCR, because they cover the TaqMan® primer/probe area and therefore they are amplified similar to the cellular reverse transcribed mRNA of the appropriate gene. Standards were obtained by classical PCR amplification using primers that anneal outside the area where the TaqMan® primers anneal on the template. Since CYPs are expressed in the liver, we used reverse transcribed RNA of human liver extract as a template for classical PCR amplification. For the gene-specific PCR, we used 25 ng cDNA per 25µl reaction volume including each primer at a concentration of 300 nM. The primers (Table 3.2) were designed using the primer express software 2.0 (Applied Biosystems) and were manufactured by Invitrogen. The components of the PCR reaction (AmpliTaq Gold, 10x PCR buffer, dNTPs, $MgCl_2$) were purchased from Applied Biosystems. Thermal cycling was conducted using a Mastercycler personal from Eppendorf (Hamburg, Germany), and an annealing temperature of 55°C was used. The PCR products were purified by running a 1.5% agarose gel (TAE buffer, 100 V, 50 minutes) and by a subsequent gel extraction (gel extraction kit, Qiagen). When cDNA yields were too low, the PCR amplification was repeated using the purified product of the first PCR as a template. The obtained standards

were quantified using the PicoGreen® dsDNA quantitation kit according to the manufacturer's protocol (Molecular Probes, Eugene, OR). The PicoGreen® reagent is an ultrasensitive fluorescent nucleic acid stain for quantitating double-stranded DNA using bacteriophage lambda DNA as a standard. The amount of cDNA in the sample was expressed as ng DNA per ml. In addition, the purified and quantified PCR products were analyzed by sequencing (Microsynth GmbH, Balgach, Switzerland). The received sequences were aligned to the genes of interest using the BLAST program (http://www.ncbi.nlm.nih.gov/BLAST), in order to confirm the identity of the PCR products. For further calculations, the molecular weights of the cDNA fragments were determined on the basis of the corresponding sequence with the help of a biopolymer calculator (http://paris.chem.yale.edu/extinct.frames.html).

Primer	Access. no.	Sequence	Size (bp)
CYP1A1	NM_000499	forward 5'-GAGGTCCTGATAAGCACGTTGC-3' reverse 5'-AGGTCCAAGACGATGTTAATGATCT-3'	439
CYP1A2	AF182274.1	forward 5'-ACTTTGACAAGAACAGTGTCCGG-3' reverse 5'-GCCAAACAGCATCATCTTCTCA-3'	536
CYP2C19	NM_000769	forward 5'-GATTGTAAGCACCCCCTGGA-3' reverse 5'-GGATGAGGTCGATGTATCTCTGG-3'	470
CYP2D6	NM_000106	forward 5'-CTTCTCCGTCTCCACCTTGC-3' reverse 5'-TCCCGGCAGAGAACAGGTC-3'	520
CYP3A4	AF182273	forward 5'-AGAAAGTCGCCTCGAAGATACAC-3' reverse 5'-TGCAGTTTCTGCTGGACATC-3'	613

Table 3.2 Sequences of primers that were used for the generation of gene-secific cDNA standards

3.3.1.3 Standard curve method

A standard curve for each gene on every plate is essential for the accurate quantification of mRNA transcript numbers. The standard curves were generated by a serial dilution of cDNA standard solutions with known amounts of PCR template. However, the starting amount for the PCR had to be evaluated in order to obtain curves that span the range above and below the amount of the unknown samples. Therefore, the quantified standard solutions were first analyzed in TaqMan® assays,

and were then adapted accordingly by further dilutions, receiving the standard dilution (**StdD**), in order to obtain adequate curves.

Linear standard curves were composed by plotting the Ct values of the standards against the log of their corresponding serial dilution factor. Slope and Y-intercept of the standard curve line were then calculated by linear regression. By measuring the Ct value of the unknown sample under the same conditions, its corresponding serial dilution factor **X** could then be determined.

Based on the serial dilution factor **X**, the number of cDNA molecules of the analyzed gene in the sample (transcript number) could be estimated. Therefore, the number of cDNA fragments in the applied standard solution was calculated and subsequently multiplied with the serial dilution factor (**X**) of the sample. Usually, the transcript number is normalized to 1 µg RNA. The transcript number per µg RNA (**TN**) was calculated as shown in equation 4:

$$TN = \frac{C \times V \times N \times X}{StdD \times MW} \qquad \text{(equation 4)}$$

where **C** is the concentration of the standard (determined with the PicoGreen® assay, **V** is the volume of sample cDNA that contains 1 µg of reverse transcribed RNA (this is 0.1 ml for the common cDNA concentration of 10 ng/µl. **N** is Avogadro's number (6.022×10^{23} molecules per mol), and **MW** is the molecular weight of the standard.

3.3.1.4 Incubation conditions of BB19 cells

To test the inducibility of different CYP isoforms in BB19 cells, they were seeded onto 6-well cell culture plates (9.2 cm^2/well) coated with 2 µg/cm^2 rat tail collagen and cultured under standard conditions. After 3 days, the cells had reached 70% of confluency, and were treated with 10 µM benzo[a]pyrene, 100 µM Aroclor 1254, or 10 µM rifampicin (all Fluka Chemie GmbH) for 72 h. The compounds were dissolved in dimethyl sulfoxide (DMSO). The final DMSO concentration did not exceed 1%.

3.3.1.5 Real-time PCR (TaqMan® assay)

The 5`nuclease assay or TaqMan® assay is a highly sensitive method to determine mRNA levels quantitatively. This method uses a target specific oligonucleotide, the TaqMan® probe, which anneals between the forward and reverse primer sites. The

probe carries a reporter dye on the 5`end (6-carboxy-fluorescein) and a quencher dye on the 3` end (6-carboxy-tetramethyl-rhodamine). As long as the probe is intact, the fluorescence of the reporter dye is suppressed by the quencher dye. However, during the PCR, the DNA polymerase (Taq polymerase) cleaves the probe due to its 5`-3` exonuclease activity. Now, a fluorescent signal is generated, because the reporter dye is separated from the quencher dye. Consequently, there is an increase of fluorescence after each PCR cycle. With the ability to measure the PCR products as they are accumulating, in "real time", it is possible to measure the amount of PCR product at a point in which the reaction is still in the exponential range. It is only during this exponential phase of the PCR reaction, where it is possible to extrapolate, to determine the starting amount of template. During the exponential phase in real-time PCR experiments, a fluorescence signal threshold is determined, at which point all samples can be compared. Therefore, the number of PCR cycles required to generate enough fluorescent signal to reach this threshold is defined as the cycle threshold, or Ct. These Ct values are directly proportionate to the amount of starting template and are the basis for calculating mRNA expression levels. The baseline is defined as the PCR cycles in which a signal is accumulating but is beneath the limits of detection of the instrument.

TaqMan® experiments were performed on a 7900HT Sequence Detection System using 384 well plates, with total reaction volumes of 10 µL (Applied Biosystems, Rotkreuz, Switzerland). PCR conditions were throughout 10 minutes 95°C followed by 40 cycles of 15 s 95°C and 1 minutes 60°C. TaqMan® Universal PCR Mastermix (Applied Biosystems) was used. Each reaction contained 1 ng/µL cDNA and the concentrations of primers and probes were 900 nM and 225 nM, respectively. Primers and probes (Table 3.3) were designed according to the guidelines of Applied Biosystems with help of the Primer Express 2.0 software. Primers were synthesized by Invitrogen (Basel, Switzerland), probes by Eurogentec (Seraing, Belgium).

Primer	Access. no.	Sequence	length (bp)
CYP1A1	NM_000499	probe 5`-CGCTATGACCACAACCACCAAGAACT-3`	26
		forward 5`-GTCATCTGTGCCATTTGCTTTG-3`	22
		reverse 5`-CAACCACCTCCCCGAAATTATT-3`	22
CYP1A2	AF182274.1	probe 5`-CACAGCCATCTCCTGGAGCCTCATGTA-3`	27
		forward 5`-CAATGACGTCTTTGGAGCAGGAT-3`	23
		reverse 5`-CAATCACAGTGTCCAGCTCCTTC-3`	23
CYP2C19	NM_000769	probe 5`-TAATCACTGCAGCTGACTTACTTGGAGCTGGG-3`	32
		forward 5`-GAACACCAAGAATCGATGGACA-3`	22
		reverse 5`-TCAGCAGGAGAAGGAGAGCATA-3`	22
CYP2D6	NM_000106	probe 5`-CAGCTGGATGAGCTGCTAACTGAGCACA-3`	28
		forward 5`-CCTACGCTTCCAAAAGGCTTT-3`	21
		reverse 5`-AGAGAACAGGTCAGCCACCACT-3`	22
CYP3A4	AF182273	probe 5`-TTCTCCTGGCTGTCAGCCTGGTGC-3`	24
		forward 5`-TCTCATCCCAGACTTGGCCA-3`	20
		reverse 5`-CATGTGAATGAGTTCCATATAGATAGA-3`	27

Table 3.3 Sequences of real-time PCR primers and specific probes

3.3.2 Immunocytochemistry of CYP1A1

BB19 cells were seeded onto chamber slides and at the third day of culture, 10 µM benzo[a]pyrene was added to the culture medium. After 72h incubation, the immunostaining was performed as previously described in chapter 3.2.5. Primary antibody used for this experiment was the rabbit polyclonal antibody to human CYP1A1 (1:50) (Abcam, Cambridge, UK). Secondary antibody used was a Cy2™-conjugated goat anti-rabbit antibody (7 µg/ml, Jackson ImmunoResearch, Soham, UK).

3.3.3 Western blot of CYP1A1

The presence of CYP1A1 was studied in BB19 cells and porcine BCEC, both cultured as described in chapter 3.2.10.4. Western blot analysis was performed as previously described in chapter 3.2.6, using the rabbit polyclonal antibody to human CYP1A1 (1:500) (Abcam).

3.3.4 Functional CYP1A1 activity with P450-GLO™ assay

3.3.4.1 Principle

The P450-GLO™ assay kit (Promega Corp., Madison, WI, USA) was used to measure CYP1A1 activity in intact cultured BB19 cells. Compounds that induce the CYP gene expression increase levels of CYP enzyme activity, which is assayed biochemically as an end point of gene induction. In P450-GLO™ assays, the luminogenic substrates used are cell permeable, as is D-luciferin, the P450-GLO™ reaction product. P450-GLO™ luminogenic substrates are added to the cell culture medium and are allowed to incubate for a predetermined period of time. Substrates enter cells, likely by passive diffusion, where CYPs convert them to D-luciferin that diffuses out of cells into medium. A sample of culture medium is then combined with P450-GLO™ luciferin detection reagent to initiate a luminescent reaction with firefly luciferase. The luminescence correlates directly to the level of CYP activity.

3.3.4.2 BB19 cell culture and CYP1A1 induction

BB19 cells were seeded on 24-well cell culture plates with a surface area of 2cm^2/well, coated with 2 µg/cm^2 rat tail collagen. Cells were cultured under standard culture conditions. After 2 days, cells were incubated with 10 µM benzo[a]pyrene or their vehicle controls for 72 h.

3.3.4.3 P450-GLO™ CYP1A1 assay

After termination of the incubation period, induction and vehicle control media were replaced with 0.3 ml fresh medium containing 0.1 mM D-luciferin-CEE, the luminogenic CYP1A1 substrate from the P450-GLO™ CYP1A1 assay kit. For basal CYP1A1 activity measurements, the luminogenic substrate was added to a set of vehicle control wells. For induced CYP1A1 activity measurements, the luminogenic substrate was added to the incubated wells. For background luminescence determinations, the luminogenic substrate was added to a set of empty coated wells without cells. The plate was incubated for 4 hours with the luminogenic substrate at 37°C. At the end of the incubation period, the luminescent assay was performed. 100 µl of medium was removed from each well to a 96-well opaque white luminometer plate, and 100 µl of reconstituted luciferin detection reagent from the P450-GLO™ kit

was added to initiate a luminescent reaction. After 20 minutes of incubation at room temperature, luminescence was read on a plate reading luminometer (Bio Assay Reader, HTS 7000 Plus, Perkin Elmer). Background luminescence values were subtracted from induced and uninduced (vehicle control) values.

3.4 Identification of P-glycoprotein substrates and inhibitors among neuroleptic compounds

3.4.1 Mouse monocytic leukaemia cell line (P388)

The murine monocytic leukaemia cell lines P388/par (parental cell line) and the doxorubicin-resistant subline P388/mdr (cell line overexpressing P-gp) were obtained from Dr. C. Geroni (Pharmacia & Upjohn, Centro Ricerche e Sviluppo, Milano, Italy). Both cell lines are growing in suspension and were cultured in RPMI glutamax 1640 medium supplemented with 10% heat-inactivated FBS, 1 mM sodium pyruvate, 10 mM HEPES buffer, 0.02 mg/ml asparagine, 1% 1x minimum essential medium with non-essential amino acids, 0.4% 1x minimum essential medium with vitamins, 0.05 mM mercapto-ethanol (all Invitrogen). The P388/mdr cells were continuously grown in the presence of 0.25 µg/ml doxorubicin. One day before each experiment, cells were grown in doxorubicin-free medium.

3.4.2 Human leukaemia cell lines (CCRF/CEM)

The human T-lymphocytic leukaemia cell line overexpressing MDR1 (CCRF-CEM/MDR), and its parental analogue CCRF-CEM/Par were a gift from Dr. A. Simon (Altana Pharma Ltd, Konstanz, Germany). Cells are growing in suspension and were cultured in RPMI 1640 medium with Glutamax-I, supplemented with 10% FBS. CCRF-CEM/MDR cells were continuously cultured in the presence of 1 µg/ml vincristine. One day before each experiment, cells were grown in vincristine-free medium.

3.4.3 Sulforhodamine B assay

The sulforhodamine B (SRB) cytotoxicity assay was performed to evaluate the toxicity of the solvent DMSO at various concentrations. In this assay, the total cell number was determined by measuring cellular protein. The protein binds to the dye, sulforhodamine B, and it is then extracted from the cells in a Tris base solution. The assay was carried out as follows: BB19 cells were seeded onto a 96-well plate. 24 hours later, when the confluency of the cell layer reached about 50%, the cells were treated with various DMSO concentrations (from 0 to 3%) for 45 minutes. Then the supernatant was removed and the cell layers were washed with medium. Then 200 µl medium and 20 µl fixative (trichloracetic acid 50%) were added to every well. The plates were incubated for 1 hour at 4 °C. The medium was aspirated and the plates were rinsed five times with ultrapure water. The plates were allowed to air-dry over night. 100 µl of the sulforhodamine B solution (0.4% SRB in 1% acetic acid) was added to the cells. The plates were stained for 30 minutes. Subsequently, the stain was removed, and the cells were rinsed five times with 1% acetic acid. Again, the plates were allowed to air-dry. 200 µl of the solubilisation solution (100 mM Tris, pH 10.5) was added to the plates, and incubated on a shaker at room temperature for 5 minutes. The samples were analyzed at λ=540 nm on a Spectra MAX 250 microplate spectrophotometer (Molecular Devices Corporation, California, USA).

3.4.4 Microtiter plate based rhodamine 123 uptake and efflux assay

To load P388 or CCRF-CEM cells with rhodamine 123 (R123) prior to efflux, cells were incubated with 1 µM (P388) or 5 µM (CCRF-CEM) of R123 in the presence of 100 µM verapamil in order to block P-gp. After 10 minutes, incubation was stopped by transferring the samples on ice. Cells were dispersed onto a 96-well microtiter plate and washed twice with or without the neuroleptic drugs at 4°C. Efflux was initiated by resuspending the cell pellet in R123-free HBSS-P with or without test drug (efflux buffer) at room temperature. After 6 minutes (P388) or 12 minutes (CCRF-CEM) of efflux, 180 µl of the efflux buffer was removed from each well, and added to a 96-well opaque white plate for analysis. For the uptake studies, cells were washed twice with HBSS-P. Then, the cells were lysed with 0.8% triton X for at least 20 minutes. 180 µl of the lysed cell suspension was removed from each well, and added to another 96-well opaque white plate. Samples were analyzed for R123

fluorescence in a plate reader (Bio Assay Reader, HTS 7000 Plus) with 485 nm excitation and 535 nm emission filters.

3.4.5 Transport studies with neuroleptic compounds

For the preliminary study of transendothelial transport, porcine BCEC were used when they reached confluency. Cells were seeded onto 12-well Transwell® polycarbonate filter plates, precoated with 10 µg/cm^2 rat tail collagen. Cell culture medium was removed from upper and lower compartment. After washing with HBSS-P, cells were preincubated for 15 minutes with HBSS-P, with or without 100 µM verapamil at the upper compartment. The incubation buffer consisted of the test compounds in a solution containing 250 µg/ml of the paracellular marker fluorescein isothiocyanate dextran (FITC-dextran, MW=4000) in HBSS-P with or without 100 µM verapamil. Cells were incubated with the incubation buffer either at the upper or at the lower compartment. After 45 minutes at constant temperature (37°C) on a rotary platform (50 RPM on an Orbital Shaker), samples were drawn from the upper and lower compartment. Samples were analyzed by the Psychiatric Clinic of the University of Mainz, (Mainz, Germany) by quantitative HPLC. The preliminary results of these experiments are shown in the appendix.

3.4.6 Estimation of kinetic parameters

ED$_{50}$, which is the concentration of test compound, that exerts a half-maximal efflux or uptake inhibition of the marker, was estimated from a saturable relationship using non-linear regression analysis using Microcal Origin, version 6.1 (Northampton, MA, USA). The data points obtained with the R123 uptake and efflux assay were fitted with the sigmoidal E_{max} model (equation 5):

$$E = E_0 - \frac{E_{\max} \times C^n}{ED_{50}{}^n + C^n} \qquad \text{(equation 5)}$$

where **E$_{max}$** is the maximal response (fluorescence of marker substrate when maximal P-gp inhibition is achieved), **E$_0$** is the baseline response (fluorescence of marker substrate when P-gp is not inhibited), **C** is the concentration of inhibitor, and **n** is the Hill sigmoidicity coefficient (the slope factor, which quantifies the steepness).

The inhibitory capacity of a test compound ($\mathbf{I_{compound}}$) at concentration x µM, to inhibit the R123 uptake or efflux is described by equation 6:

$$I_{compound} = \frac{\Delta F_{compound.at.conc.x}}{F_{HBSS-P}} \qquad \text{(equation 6)}$$

where **x** is the concentration at which maximal inhibition is achieved, ∆**F** is the difference in R123 assay buffer in absence and in presence of test compound, and $\mathbf{F_{HBSS-P}}$ represents the R123 fluorescence in assay buffer in absence of test compound. The inhibitory capacity of the test compounds is systematically related to the inhibitory capacity of 100 µM verapamil in the same experiment where verapamil has the function of an internal standard. The resulting $\mathbf{I_{rel}}$ is described by equation 7:

$$I_{rel} = \frac{\Delta F_{compound.at.conc.x}}{\Delta F_{verapamil}} \qquad \text{(equation 7)}$$

3.5 Evaluation of BBB permeability of different CNS active compounds

3.5.1 Transport studies

For the study of transendothelial transport, porcine BCEC cells were used when they reached confluency. Cells were seeded onto 12-well Transwell® PETE filters with 0.4 µm pore size, precoated with 20 µg/cm^2 collagen S, type I from calf skin (Roche Diagnostics). Cell culture medium was removed from upper and lower compartment and both compartments were washed with transport buffer (HBSS-P, pH 7.4). Both sides of the compartments were filled with pre-warmed transport buffer. The transport assay was performed at constant temperature (37°C) on a rotary platform (50 RPM on an Orbital Shaker. At time t=0, different concentrations of the test compounds, in HBSS-P containing 250 µg/ml FITC-dextran, were added to the upper compartment (donor chambers, apical side) or to the lower chamber (donor chambers, basolateral side) respectively. In defined time intervals, samples were drawn from the lower compartment (acceptor chamber, basolateral side) or from the upper compartment (acceptor chamber, apical side), respectively. The acceptor volume was readjusted

with assay buffer after each sample was taken, and amounts from acceptor side samples were corrected for the amount of removed compound by previous sampling. Samples were analyzed by liquid chromatography with mass spectrometry (LC-MS/MS) by the industrial collaboration partner. Calculation of P_{app} values were done as described in chapter 3.2.9.

3.5.2 Assay for the screening of target receptor antagonists

The assay was performed by the industrial collaboration partner. The binding of an agonist to its receptor is associated with an increase in intracellular calcium concentrations ($[Ca^{2+}]_i$). This can be monitored in cells, stably expressing the target receptor using a fluorescent calcium indicator. The fluorescence increases after binding to intracellular free calcium, which can be measured. The response can be abolished by antagonists.

3.5.3 Combined study of BBB permeability and target receptor effect

Porcine BCEC were seeded onto 12-well Transwell® PETE filters with 0.4 µm pore size, precoated with 20 µg/cm^2 collagen S, type I from calf skin (Roche Diagnostics) and cultured until cells reached confluency. Cell culture medium was removed from upper and lower compartment and both compartments were washed with transport buffer (HBSS-P, pH 7.4). The transport assay was performed at constant temperature (37°C) on a rotary platform (50 RPM on an Orbital Shaker. At time t=0, different concentrations of the test compounds in HBSS-P, were added to the upper compartment. After 45 minutes, samples were drawn from the lower compartment. In order to test these samples in the target receptor screening assay, samples were added to 96-well-plates and it was further proceeded as described in chapter 3.5.2. Samples were also analyzed by LC-MS/MS by the industrial collaboration partner.

3.6 Statistics

Data are given as mean ± standard error of the mean (SEM). For statistical comparison, groups of data were compared by analysis of variance (one-way ANOVA). Mean values were considered to be statistically different at a value of

P<0.05. Pair wise comparisons were performed by two-tailed unpaired t-test. The P-values were adjusted by Bonferroni's correction for multiple comparisons. All statistical calculations were done using SPSS for Windows software (version 11.0).

4 Results

4.1 Evaluation of BB19 cells as an in vitro model of the BBB

Since it was our principal goal to develop a human *in vitro* model for the BBB, in a first step, the genetic karyotype of BB19 cells was determined to ensure that the cells are of human origin (data not shown), which BB19 cells proved to be.

4.1.1 Tightness of BB19 cells compared to porcine BCEC

Transport of the extracellular marker [^{14}C]-sucrose across confluent cells cultured on cell culture inserts was investigated. Transport of sucrose across monolayers of BB19 was compared with the transport across our established system of primary porcine BCEC (Table 4.1). Transwell® polycarbonate filters were the optimal insert to obtain highly resistant porcine BCEC monolayers (P_{app}=1.19 x 10^{-5} cm/sec, empty filters P_{app}= 7.55 x 10^{-5} cm/sec, P_e=1.45 x 10^{-5} cm/sec), whereas tightness of BB19 cells was not reached with these inserts (P_{app}=5.44 x 10^{-5} cm/sec). BB19 cells grown on these filters were more than 4.5-fold leakier than the primary porcine BCECs. Other cell culture inserts (such as Transwell® clear) were investigated to evaluate if tightness of BB19 cell could be improved. However, these filter inserts failed to improve cellular tightness. Only cultivation of BB19 cells on BD Falcon™ PETE culturing inserts lead to a higher tightness of BB19 monolayers (P_{app}=1.30 x 10^{-5} cm/sec, empty filters P_{app}= 3.17 x 10^{-5} cm/sec, P_e=2.25 x 10^{-5} cm/sec). When BB19 cells were cultivated on BD Falcon™ PETE inserts, the tightness of these monolayers was in the same range as the primary porcine cell culture system (P_{app}=1.51 x 10^{-5} cm/sec, empty filters P_{app}= 3.17 x 10^{-5} cm/sec P_e=2.66x10^{-5}cm/sec). However, hardly any discrimination between the paracellular marker sucrose and the transcellular marker propranolol (P_{app}= 1.30x 10^{-5} vs. 2.18 x 10^{-5} cm/sec) was seen.

	$P_{(app)}$ (x 10^{-5} cm/sec)	$P_{(app)}$ empty filter (x 10^{-5} cm/sec)	P_e (x 10^{-5} cm/sec)
BB19 on BD Falcon™ PETE inserts	1.30±0.12	3.17±0.22	2.25±0.34
BB19 on Transwell® polycarbonate filters	5.44±0.02	7.55±0.17	19.5±0.2
pBCEC on BD Falcon™ PETE inserts	1.51±0.05	3.17±0.22	2.66±0.16
pBCEC on Transwell® polycarbonate filters	1.19±0.26	7.55±0.17	1.45±0.39

Table 4.1 Sucrose permeability across BB19 and porcine BCEC monolayers on different filters. Values are mean ±SEM, n=3.

4.1.2 Influence of cell culture conditions on staining of ZO-1

Immunostaining of ZO-1 was performed in cells cultured under previously described conditions after 15 days in culture (Figure 4.1). A high staining of ZO-1 was observed in control cells, as well as in all the other cells cultured with different cell culture conditions.

A change towards a more spindle-like shape, closer to primary BCEC appearance, was most pronounced with C6-conditioned medium, and was observed with dexamethasone and 1,25-dihydroxyvitamin D_3 as well. No morphological difference in BB19 cells cultured in chlorophenylthio-cAMP combined with RO-20-1724 compared to control cells, and no change towards a more spatial ZO-1 expression was observed. However, none of the cell culture conditions could improve the tightness (i.e. sucrose permeability) of the BB19 monolayers (data not shown).

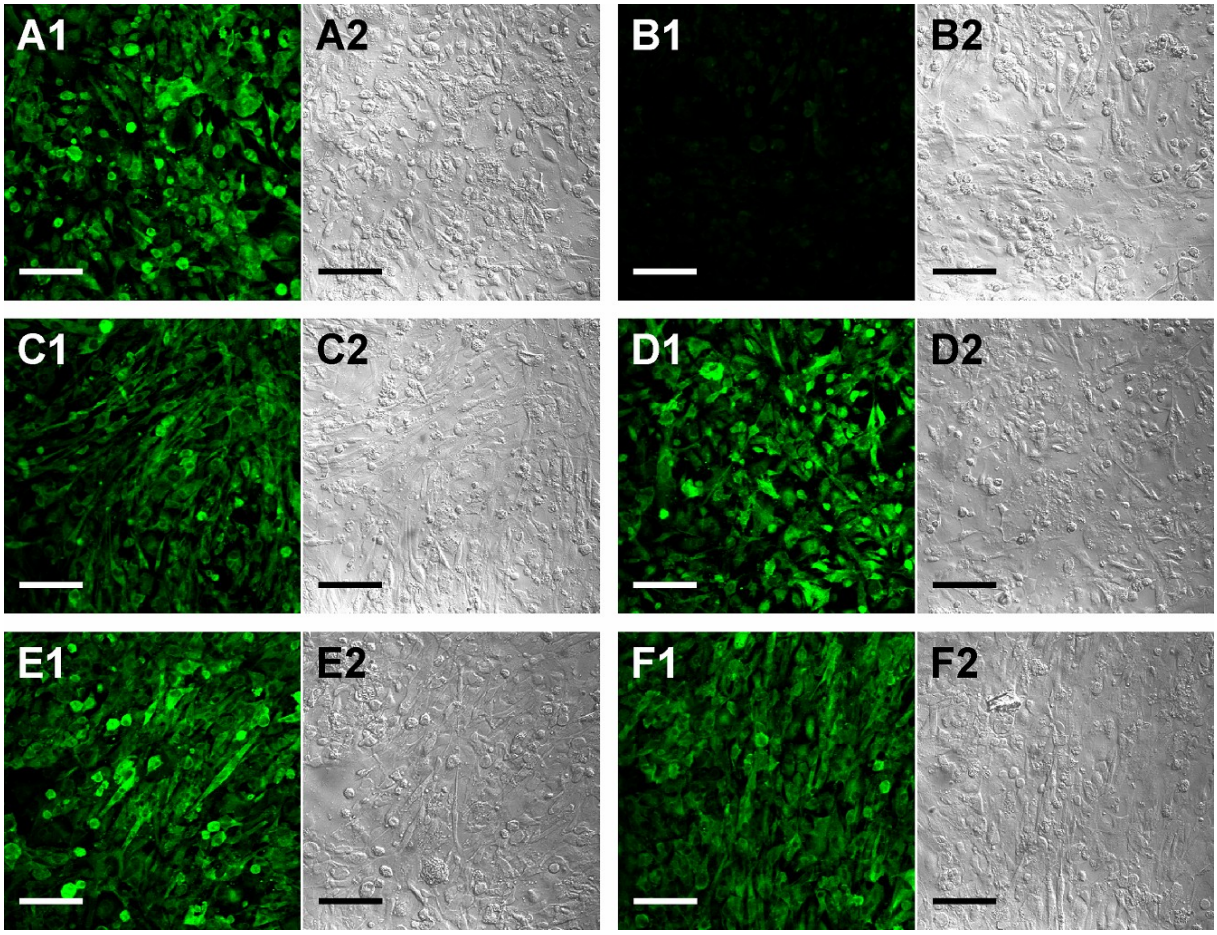

Figure 4.1 Immunocytochemical staining of the tight junction associated protein ZO-1 in confluent BB19 cells, grown under different culture conditions (200x magnification), bar is 100 µm, 1 is Z0-1 staining, 2 is the corresponding transmission image: (A) standard medium, (B) negative control (C) with C6-conditioned medium (D) with 250 µM chlorophenylthio-cAMP (CPT-cAMP) combined with 35 µM RO-20-1724, (E) with 10 µM dexamethasone, (F) 1,25-dihydroxyvitamin D_3

4.1.3 Expression of ABC-transporters

The expression of MDR1, MRP1, MRP2, MRP3, MRP4, MRP5, OATP-A, OATP-C, OAT1, OAT3, OAT4, and BCRP was investigated in our BBB model BB19 on mRNA level. The presence of MDR1, MRP1, MRP2, MRP4, MRP5, OAT3, OAT4, and BCRP mRNA in BB19 cells could be shown by conventional RT-PCR (Figure 4.2).

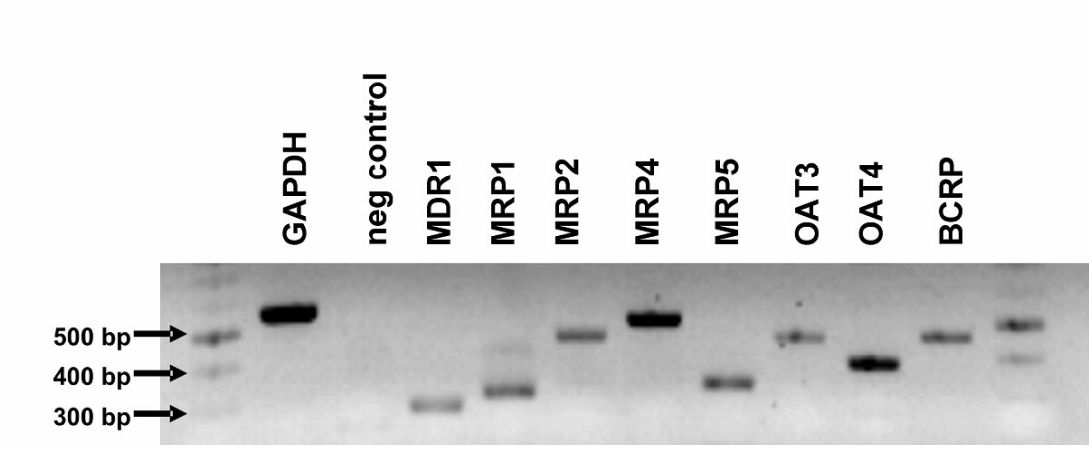

Figure 4.2 RT-PCR of BBB transporters MDR1, MRP1, MRP2, MRP4, MRP5, OAT3, OAT4, and BCRP in BB19 cells

To evaluate the expression of some of these ABC transporters on protein level, we performed immunocytochemistry. As shown in Figure 4.3, P-gp, MRP4, and BCRP were detected on protein level as well. However, MRP5 staining was not significantly different from the negative control, no MRP3, and only very low amounts of MRP1, and MRP2 could be detected by immunocytochemistry (data not shown).

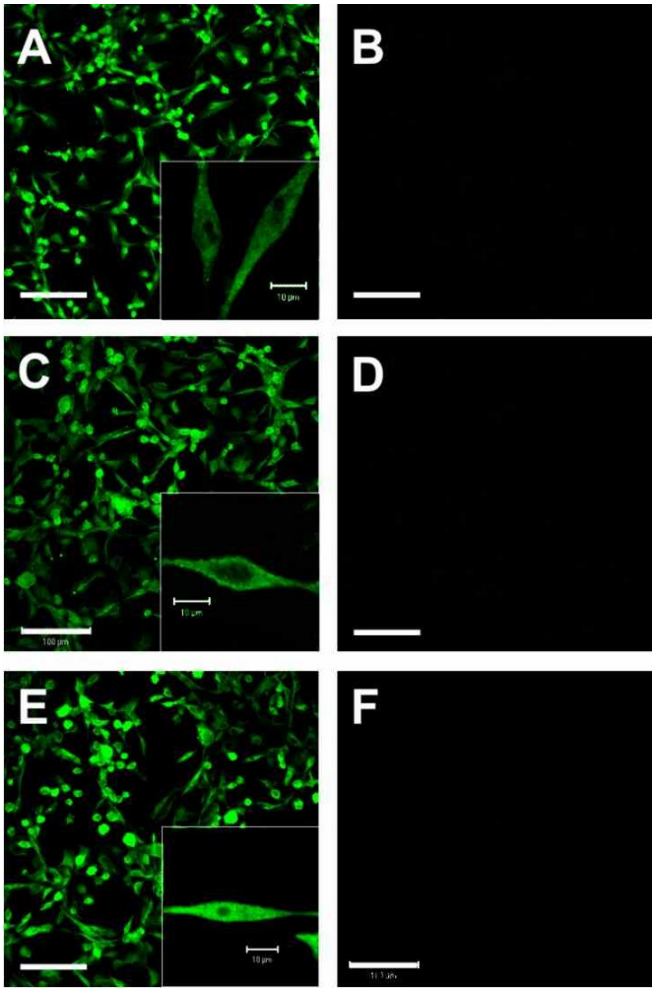

Figure 4.3 Immunocytochemical staining of BBB transporters in confluent BB19 cells: (A) BCRP (bar is 100 µm), insert shows enlarged cell (bar is 10 µm) (B) negative control for BCRP (bar is 100 µm), (C) MDR1 (bar is 100 µm), insert shows enlarged cell (bar is 10 µm) (D) negative control for MDR1 (bar is 100 µm) E) MRP4 (bar is 100 µm), insert shows enlarged cell (bar is 10 µm) (F) negative control for MRP4 (bar is 100 µm)

The presence of P-gp and BCRP in BB19 cells and porcine BCEC was studied by Western blot analysis (Figure 4.4). P-gp over-expressing P388 cells were used as a positive control for P-gp. BB19 cells as well as the porcine BCEC showed an immunoreaction with the Mab C219 in the molecular weight range of 170 kDa, which was present in P388-cells as well, indicating the presence of P-gp in both BB19 cells and porcine BCEC. Porcine BCEC, but not BB19 cells treated with rifampicin, showed a broader band than cells cultivated in regular medium, indicating a higher amount of P-gp. Western blot analysis with the Mab BXP-21 showed a distinct immunoreaction in the molecular weight range of 70 kDa in BB19 cells. A lower, but also distinct staining was seen in porcine BCEC. This is indicative for the expression of BCRP in both BBB cell culture models. The BCRP staining was not influenced by rifampicin, neither in BB19 cells nor in porcine BCEC.

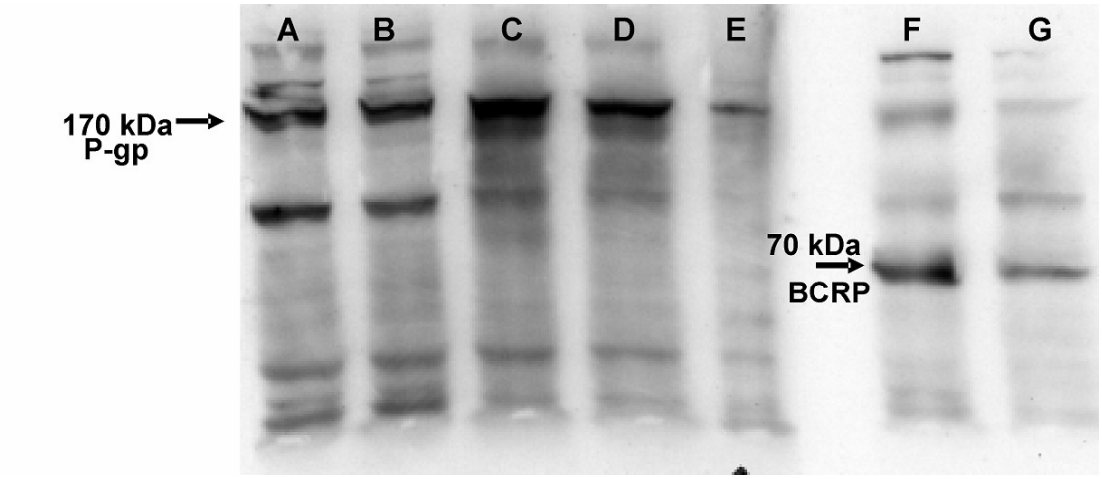

Figure 4.4 Western blot analysis (A) P-gp in BB19 cells treated with 10 µM rifampicin, (B) P-gp in BB19 cells (standard medium), (C) P-gp in porcine BCEC treated with 10 µM rifampicin, (D) P-gp in porcine BCEC in standard medium, (E) P-gp positive control, MDR1 transfected P388 cells 1:5 diluted, (F) BCRP in BB19 cells, (G) BCRP in porcine BCEC

4.1.4 Uptake assays

Uptake of the reference substances propranolol, morphine and sucrose into BB19 cells was measured at various time points up to 120 minutes (Figure 4.5). As expected, from uptake data gained from the established porcine BCEC model (Huwyler et al., 1996), morphine penetrated into BCECs to a lower degree than propranolol, and diffusion of sucrose into the cells was minimal. Uptake of the extracellular marker sucrose was followed over a time period of 120 minutes; 0.06% of the applied dose of sucrose was recovered. This value did not increase with incubation time.

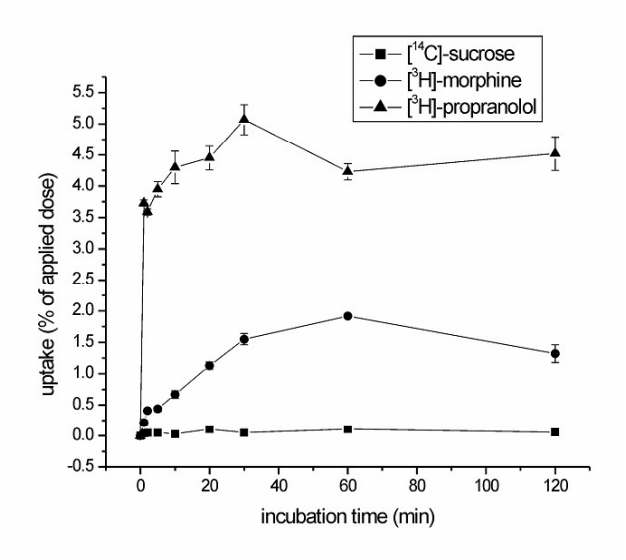

Figure 4.5 Uptake of [^{14}C]-sucrose, [^{3}H]-morphine, and [^{3}H]-propranolol into BB19 cells. Symbols represent means ± SEM. (vertical lines) for 3 data points

In a next step, the influence of the P-gp inhibitor verapamil on the uptake of the P-gp substrate daunomycin into BB19 cells was investigated. Figure 4.6 shows that the inhibition of P-gp by verapamil led to a significantly (P<0.01) increased (1.45-fold) uptake of daunomycin.

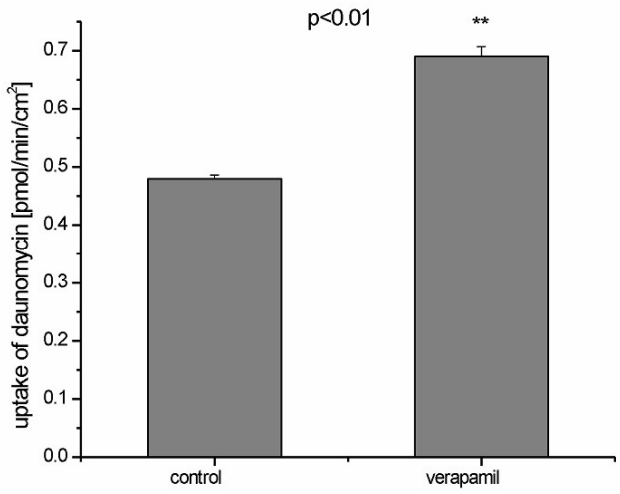

Figure 4.6 Uptake of [^{3}H]-daunomycin with or without verapamil. Columns represent means ± SEM. (vertical lines) for 3 data points. An asterisk indicates statistical significance by Student's t-test

4.1.5 Expression and inducibility of CYPs in BB19 cells

To investigate the presence and inducibility of selected CYPs, which are known to play a role in the metabolism of CNS active drugs, in BB19 cells, cells were incubated either with or without known inducers of CYPs for 72 hours, as previously described in chapter 3.3.1.4: CYP1A1 and CYP1A2 with 10 µM benzo[a]pyrene (Krishnan and Maru, 2005), CYP2C19 with 100 µM Aroclor 1254 (Borlak and Zwadlo, 2003), and CYP3A4 with 10 µM rifampicin (Goodwin et al., 1999). The expression of CYP2D6 was investigated without any treatment, as CYP2D6 is not inducible (Anzenbacher and Anzenbacherova, 2001). After RNA extraction, DNase I digestion and reverse transcription, real time PCR (TaqMan® assay) was performed to investigate the expression of CYP1A1, CYP1A2, CYP2D6, CYP2C19, and CYP3A4, determined as the number of transcripts per µg total RNA.

The presence of CYP1A1 and, to a lower extent, of CYP3A4 in BB19 cells could be shown, whereas CYP1A2, CYP2D6, and CYP2C19 were not detected by the TaqMan® assay. The transcript level of CYP3A4 was about 33-fold lower than the transcript level of CYP1A1. As seen in Figure 4.7, the treatment with benzo[a]pyrene induced the CYP1A1 transcript level approximately 11-fold, whereas the treatment with rifampicin did not significantly change the expression level of CYP3A4.

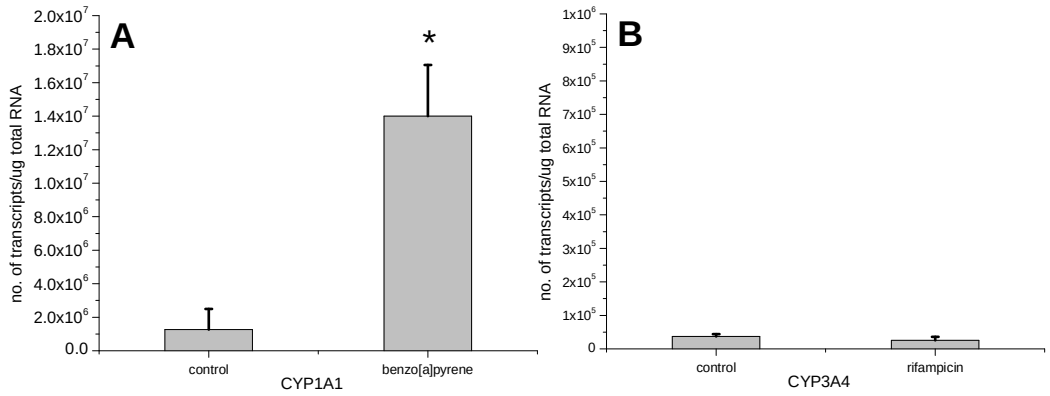

Figure 4.7 Absolute mRNA expression of CYPs in BB19 cells, treated with medium only or with a common inducer for 72hours: (A) CYP1A1 ± benzo[a]pyrene, (B) CYP3A4 ± rifampicin. Data represent mean ± SEM, n=3. *P< 0.05.

Only CYP1A1 was found to be inducible in BB19 cells. Therefore, we performed immunocytochemistry, to determine the CYP1A1 expression and inducibility on protein level. Cells were either cultivated in their standard culture medium or with 10 µM benzo[a]pyrene for 72 hours. As shown in Figure 4.8, CYP1A1 was detected in BB19 cells on protein level as well. However, CYP1A1 staining was not significantly changed after treatment with benzo[a]pyrene. Notably, the treated BB19 cells appear to be larger than the untreated cells.

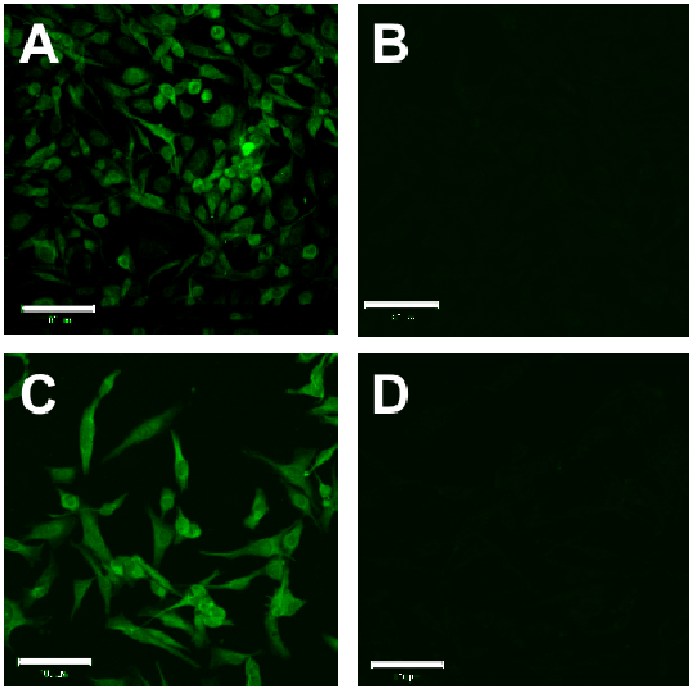

Figure 4.8 Immunocytochemical staining of CYP1A1 in BB19 cells, grown under different culture conditions (200x magnification), bar is 100 µm. (A) standard medium, (B) negative control (C) with 10 µM benzo[a]pyrene (D) negative control with 10 µM benzo[a]pyrene.

The presence of CYP1A1 in BB19 cells was also studied by Western blot analysis and compared with the expression in porcine BCEC (Figure 4.9). BB19 cells, as well as the porcine BCEC, showed an immunoreaction with the CYP1A1 antibody in the expected molecular weight range of approximately 54 kDa, indicating the presence of CYP1A1 in both BB19 cells and porcine BCEC. Neither the porcine BCEC, nor the BB19 cells treated with benzo[a]pyrene, showed a modified band compared to cells cultivated in regular medium.

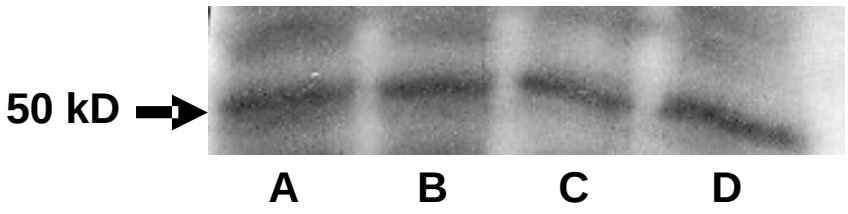

Figure 4.9 Western blot analysis (A) CYP1A1 in BB19 cells treated with 10 µM benzo[a]pyrene, (B) CYP1A1 in BB19 cells (standard medium), (C) CYP1A1 in porcine BCEC treated with 10 µM benzo[a]pyrene, (D) CYP1A1 in porcine BCEC in standard medium.

4.1.6 Functional investigation of CYP1A1 activity

To investigate, whether the expression of CYP1A1 in BB19 cells and can also be observed at a functional level, the P450-GLO^{TM} assay was performed as previously described in chapter 3.3.4. Cells incubated with benzo[a]pyrene for 72 hours were compared with cells cultivated under standard culture conditions, whereas the background luminescence was determined with empty coated wells without cells. The incubated BB19 cells, as well as the cells under standard culture conditions, only evolved luminescence in the range of the background luminescence, indicating that neither of the BB19 cells show any functional CYP1A1 activity (data not shown).

4.2 Identification of P-glycoprotein substrates and inhibitors among neuroleptic compounds

4.2.1 Preliminary investigations

Prior to the functional experiments, we investigated the maximal final dimethyl sulfoxide (DMSO) concentration that could be used to dissolve our test compounds without any toxic effects in the utilized cells. Furthermore, the influence of test compounds on the fluorescence of R123 (quenching) was investigated.

4.2.1.1 Toxicity of DMSO

The sulforhodamine B assay was performed with P388/mdr1, P388/par, CCRF/mdr1, and CCRF/par cells to assess the maximal DMSO concentration that could be used to dissolve our test compounds. In the investigated DMSO concentration range (0.01-3%), no toxicity could be seen (data not shown).

Other solvents used to dissolve the test compounds were ethanol and methanol (no toxicity assay was performed for these solvents). Table 4.2 shows the final solvent concentrations of each test compound. The final solvent concentration did not exceed 2%.

4.2.1.2 Quenching

In order to avoid false interpretations, we checked if the spectral behaviour of R123 is changed in the presence of our test compounds (so-called quenching). Therefore, we investigated the influence of the highest applied test compound concentration on R123 fluorescence intensity without cells. None of the applied test compounds showed any influence on the intensity of R123 fluorescence (data not shown).

4.2.2 Inhibition of P-gp mediated R123 uptake in P388 cells

Inhibition of P-gp mediated R123 uptake was measured in a microtiter plate based uptake assay using mdr1 overexpressing mouse lymphocytes (P388/mdr1). The corresponding parental cell line P388/par was used to account for effects that are not related to P-gp. The neuroleptic compounds haloperidol, clozapine, norclozapine,

olanzapine, quetiapine, and risperidone were investigated up to a maximal concentration of 200 µM, whereas due to solubility limitations, the highest applied concentrations were 100 µM for aripiprazole and 9-OH risperidone, and 10 µM for ziprasidone. Domperidone, a known P-gp inhibitor (Schinkel et al., 1996) and a peripherally acting dopamine antagonist without CNS effects, was used up to a concentration of 200 µM. In every experiment, 100 µM verapamil (a known P-gp inhibitor) was used as internal standard. None of the applied compounds modulated the uptake of R123 into P388/par cells (Figure 4.10A and B).

The assay discriminates between effective and noneffective inhibitors of R123 uptake, as shown in Figure 4.10C and D). Ziprasidone did not exert any influence on the uptake of R123. However, because of its poor solubility, the maximal concentration applied was too low for an accurate experimental determination of the ED_{50}. Therefore, a possible affinity of ziprasidone to P-gp could not be determined. No affinity of haloperidole to P-gp could be shown, as no modulation of the R123 uptake was observed. All other studied compounds showed an affinity to P-gp, as demonstrated by inhibition of R123 uptake. The ED_{50} values of uptake inhibition are summarized in Table 4.2. The metabolite 9-OH risperidone showed the highest affinity to P-gp with an estimated ED_{50} value of 0.09. High affinities were also observed for aripiprazole and to a lower extent for quetiapine. Norclozapine, risperidone, olanzapine, and domperidone showed intermediate affinites with estimated ED_{50} values between 40.2 and 86.5 µM. Clozapine displayed the lowest P-gp affinity of all compounds tested in the uptake assay, with an ED_{50} value of 178.2 µM.

The observed P-gp inhibition was concentration-dependent. Regarding the relative inhibitory capacity (I_{rel}), diplayed in Table 4.2, olanzapine, 9-OH risperidone, and quetiapine showed the highest inhibiton, with an inhibitory capacity above verapamil. Inhibitiory capacity of risperidone was equal to verapamil, while all other compounds displayed intermediate inhibitory capacities I_{rel} between 0.45 (norclozapine) and 0.74 (aripiprazole).

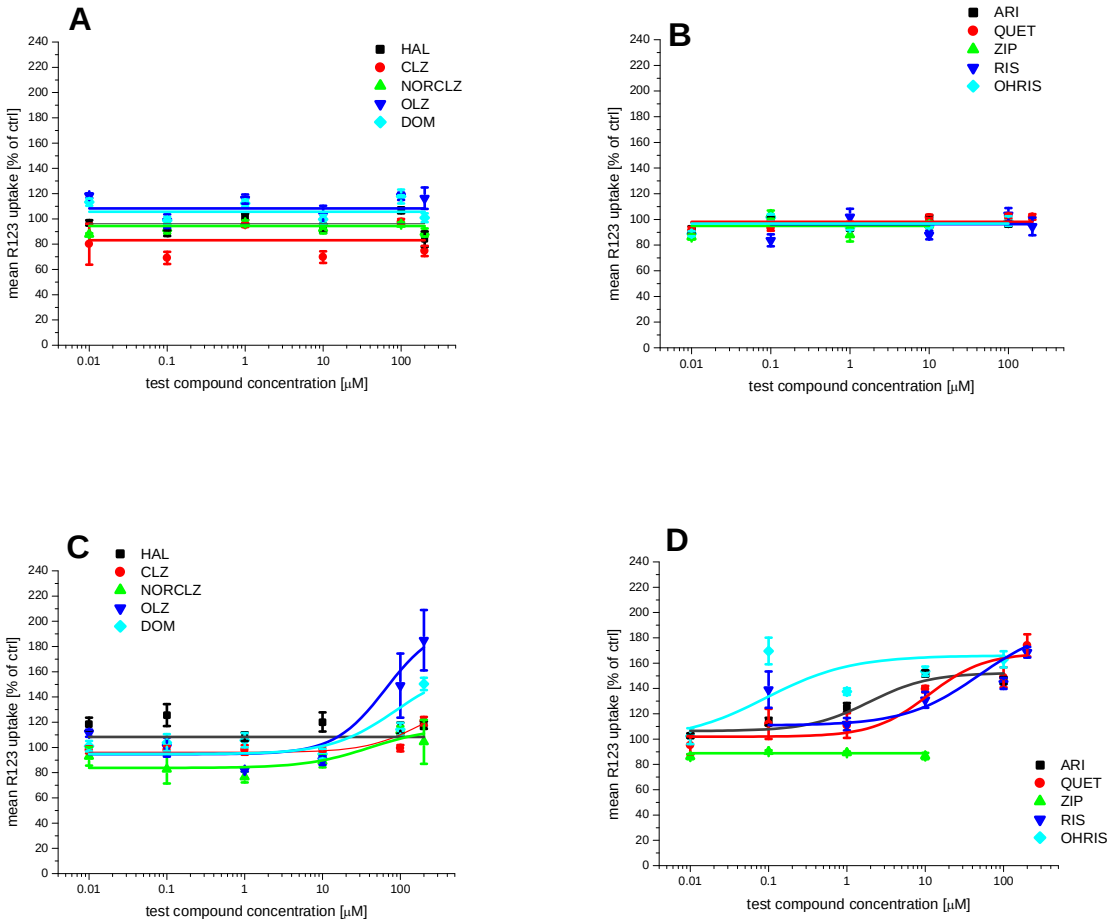

Figure 4.10 Effect of the neuroleptic test compounds haloperidol (HAL), clozapine (CLZ), norclozapine (NORCLZ), olanzapine (OLZ), aripiprazole (ARI), quetiapine (QUET), ziprasidone (ZIP), risperidone (RIS) and 9-OH risperidone (OHRIS) and domperidone (DOM), a known P-gp inhibitor on R123 uptake into P388/par cells (**A** and **B**) and P388/mdr cells (**C** and **D**). The extent of R123 uptake in buffer, only containing the equivalent concentration of solvent, was used as control and set to 100%. Values represent mean ±SEM for n=3-6. Data points were fitted with regression analysis using equation 5 as described in the methods section (chapter 3.4.6).

4.2.3 Inhbibition of P-gp mediated R123 efflux in P388 cells

Inhibition of P-gp mediated R123 efflux of all compounds was measured in the same microtiter plate based assay with P388/mdr1 and P388/par cells, which was used for uptake studies, as described in the methods section (chapter 3.4.4). In every experiment, 100 µM verapamil (a known P-gp inhibitor) was used as internal standard. None of the applied compounds modulated the efflux of R123 into P388/par cells (Figure 4.11A and B).

The assay discriminates between effective and noneffective inhibitors of R123 efflux, as shown in Figure 4.11C and D). Again, because of the poor solubility of ziprasidone, the maximal concentration applied (10 µM) was too low for an accurate experimental determination of the ED_{50} value. Therefore, a possible affinity of ziprasidone to P-gp could not be determined. In agreement with the uptake assay, no affinity of haloperidole to P-gp could be shown, as no modulation of the R123 efflux was observed either. All other studied compounds demonstrated an inhibition of R123 efflux as well. The ED_{50} values of efflux inhibition are summarized in Table 4.2. Risperidone and aripiprazole showed the highest affinity to P-gp with an estimated ED_{50} value of 1.

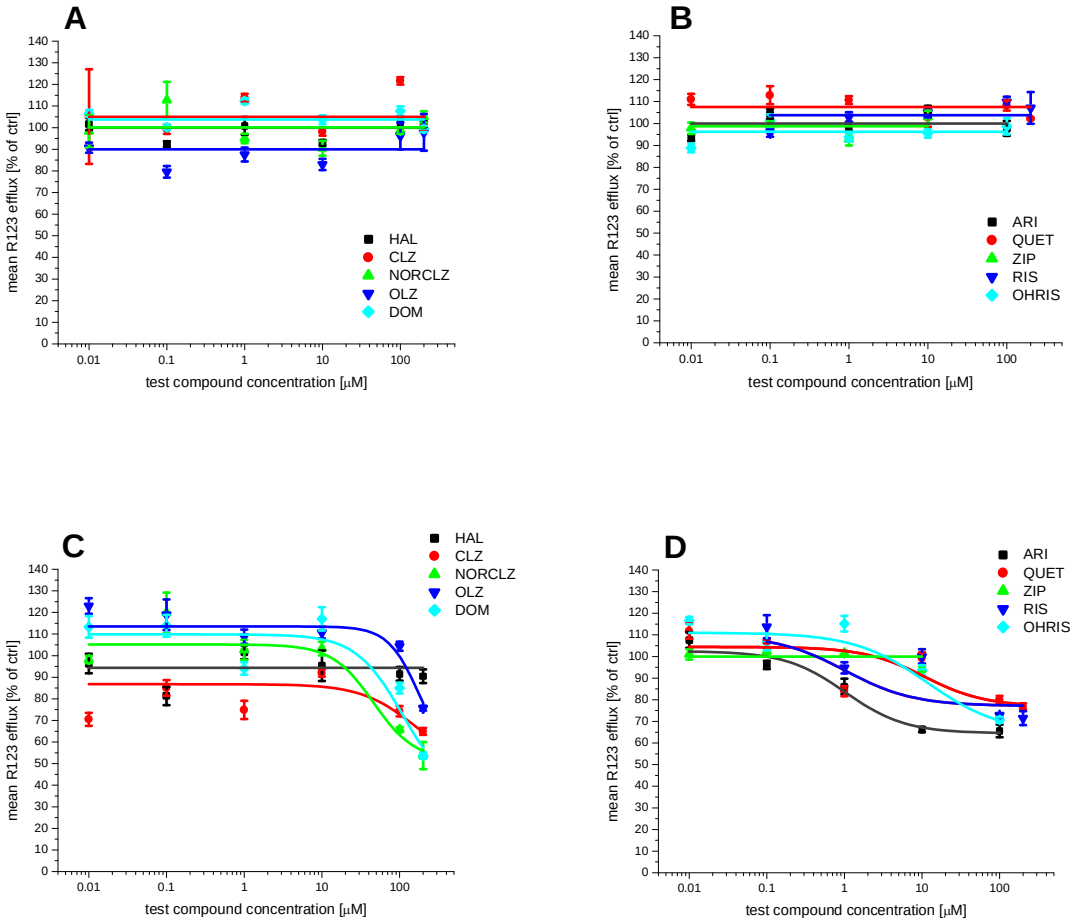

Figure 4.11 Effect of the neuroleptic test compounds haloperidol (HAL), clozapine (CLZ), norclozapine (NORCLZ), olanzapine (OLZ), aripiprazole (ARI), quetiapine (QUET), ziprasidone (ZIP), risperidone (RIS) and 9-OH risperidone (OHRIS) and domperidone (DOM), on R123 efflux from P388/par cells (**A** and **B**) and P388/mdr cells (**C** and **D**). The extent of R123 efflux in buffer, only containing the equivalent concentration of solvent, was used as control and set to 100%. Values represent mean ±SEM for n=3-6. Data points were fitted with regression analysis using equation 5 as described in the methods section (chapter 3.4.6).

High affinities were also observed for 9-OH riperidone and quetiapine. Norclozapine comparatively showed an intermediate affinity, whereas the lowest affinities were determined for domperidone, clozapine, and olanzapine, with estimated ED_{50} values between 109.8 and 151.9 µM.

Regarding the relative inhibitory capacity (I_{rel}), diplayed in Table 4.2, norclozapine showed the highest inhibiton, with an inhibitory capacity equal to verapamil. Inhibitiory capacity of olanzapine was slightly lower compared to verapamil, while all other compounds displayed intermediate inhibitory capacities, with I_{rel} between 0.44 (olanzapine) and 0.82 (domperidone).

		uptake assay		**efflux assay**	
test compound	**Used solvents [% v/v]**	**ED_{50} P388/mdr1 [µM]**	**max I_{rel}[c]**	**ED_{50} P388/mdr1 [µM]**	**max I_{rel}[c]**
haloperidol	1% DMSO	nil[a]	nil[a]	nil[a]	nil[a]
clozapine	1% DMSO	178.2	0.65	151.9	0.68
norclozapine	1% DMSO	40.2	0.45	45.8	1.05
olanzapine	1% DMSO	64.8	1.81	179.1	0.44
domperidone	1% methanol/DMSO in HBSS-P pH 6.9	86.5	0.52	109.8	0.82
aripiprazole	1 % DMSO in HBSS-P pH 6.8	1.9	0.74	1.0	0.9
quetiapine	1% DMSO	11.1	1.35	10.7	0.67
ziprasidone	1% DMSO	nil[b]	nil[b]	nil[b]	nil[b]
risperidone	1% DMSO/ethanol	48.6	1.00	1.0	0.79
9-OH risperidone	2% DMSO/ethanol	0.09	1.5	11.8	0.62

Table 4.2 Used solvent concentrations (in HBSS-P, pH 7.4, unless otherwise noted) and biological effects of tested neuroleptic compounds. All ED_{50} values were estimated from a regression analysis, using equation 5, as described in the methods section.

[a]Parameter could not be estimated. Most likely mdr1 is not inhibited.

[b]Due to solubility limitations, the highest concentration applied was 10 µM. Up to this concentration, no manifestation of the described parameters was seen.

[c]relative inhibitory capacity (I_{rel}), calculated with equation 7, is the capacity of a test compound (at the concentration where maximal inhibition was reached) to inhibit the R123 uptake or efflux relative to the inhibitory capacity of 100 µM verapamil, inhibitory capacity of verapamil was set to 1.

4.2.4 Uptake and efflux experiments with CCRF-CEM cells

Inhibition of P-gp mediated R123 uptake and efflux was investigated in CCRF-CEM cells as well. However, for unknown reasons, the data gained from these assays were highly divergent in both parental and MDR1 overexpressing cells. Therefore, the obtained results could not be interpreted (data not shown).

4.3 Evaluation of BBB permeability of different CNS active compounds

4.3.1 Transport studies

The blood-brain barrier permeability of nine different CNS active compounds, preclinical substances provided by an industrial collaboration partner, was studied in bi-directional transport studies in porcine BCEC. The paracellular marker FITC-dextran, which was used to monitor the integrity of the cell monolayer, showed permeabilities of P_{app}= 2-4 x 10^{-6} cm/sec, empty filters P_{app}= 6.18 x 10^{-6} cm/sec. Transport was investigated with 2.5, 5, 10, 20, and 40 µM of test compound either applied to the apical (AP) or the basolateral (BL) side.

The following Figures 4.12-4.20 depict the results of the transport experiments with these different preclinical substances: (A) shows the time dependent transport (up to 60 minutes) of the test compound at all the investigated concentrations from AP to BL, (B) shows the time dependent transport (up to 60 minutes) of the test compound at all the investigated concentrations from BL to AP, whereas (C) depicts the dose dependent transport (up to 40 µM) from AP to BL and from BL to AP.

The involvement of active transport can be concluded, when the transport from AP to BL differed from BL to AP. A higher transport from BL to AP than from AP to BL indicates efflux by a transporter localized on the AP (luminal) side of the BCEC, restricting the brain uptake.

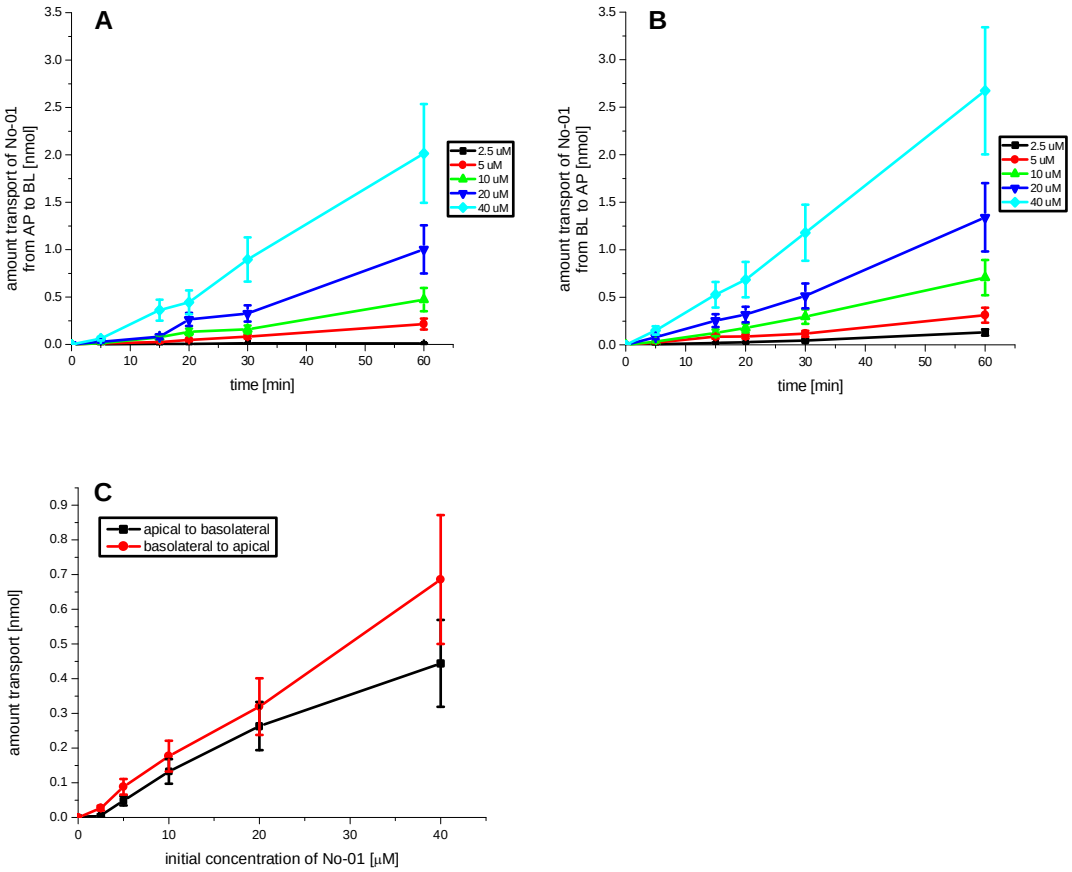

Figure 4.12 Transport of No-01 through porcine BCEC from AP to BL (**A**) and from BL to AP (**B**), and dose dependent transport after 20 minutes from AP to BL and BL to AP (**C**). Values are mean ±SEM, n=3.

Time dependent transport of No-01 (Fig. 4.12) from AP to BL was not significantly lower than transport from BL to AP at all time points and concentrations investigated. Overall high transport (up to 2.3 nmol/60 min/cm^2, which corresponds to 230 µmol/60 min/total brain capillary endothelial surface (BCE-A) [approx. 10 m^2]) was observed in both directions (Table 4.3). The linear dose dependent transport in both directions indicated passive diffusion.

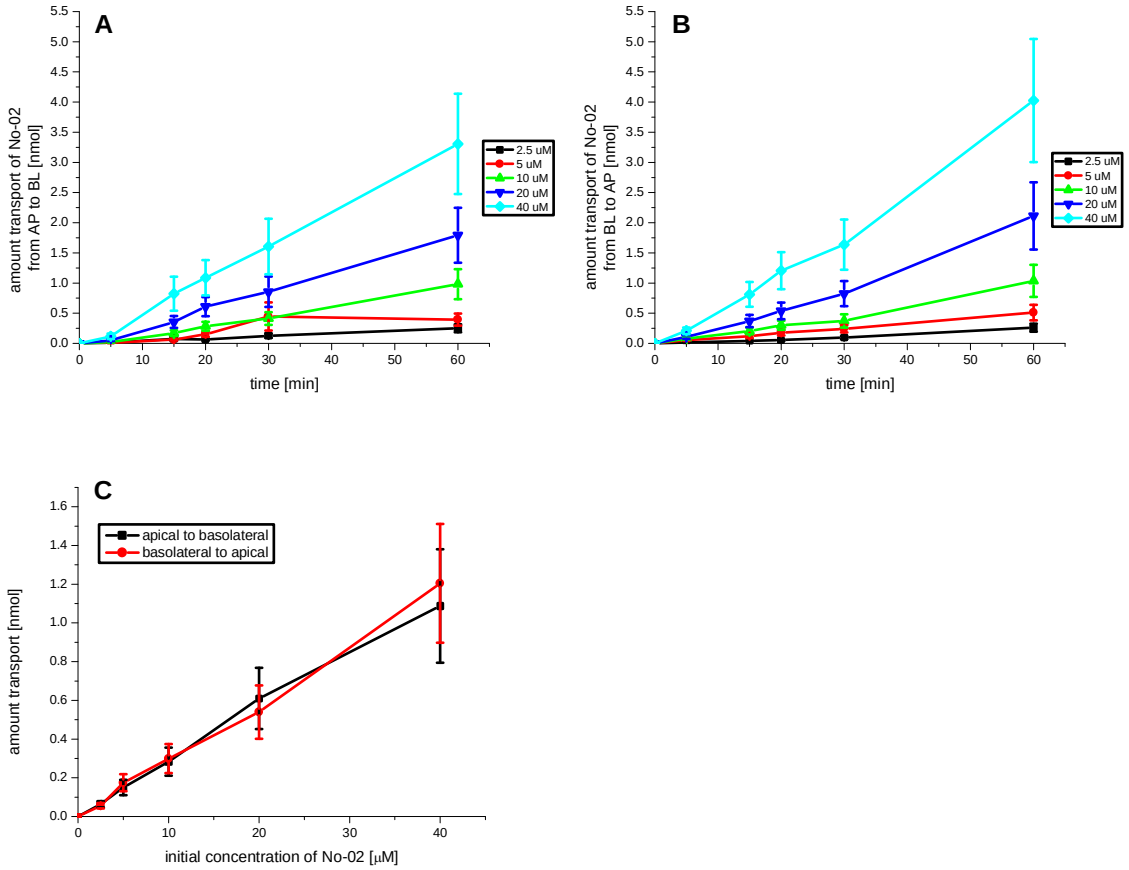

Figure 4.13 Transport of No-02 through porcine BCEC from AP to BL (**A**) and from BL to AP (**B**), and dose dependent transport after 20 minutes from AP to BL and BL to AP (**C**). Values are mean ±SEM, n=3.

Time dependent transport of No-02 (Figure 4.13) from AP to BL was equal to transport from BL to AP at all time points and concentrations investigated. Overall high transport (up to 3.5 nmol/60 min/cm^2, which corresponds to 350 µmol/60 min/total BCE-A in both directions, as well as linear dose dependent transport in both directions indicated passive diffusion.

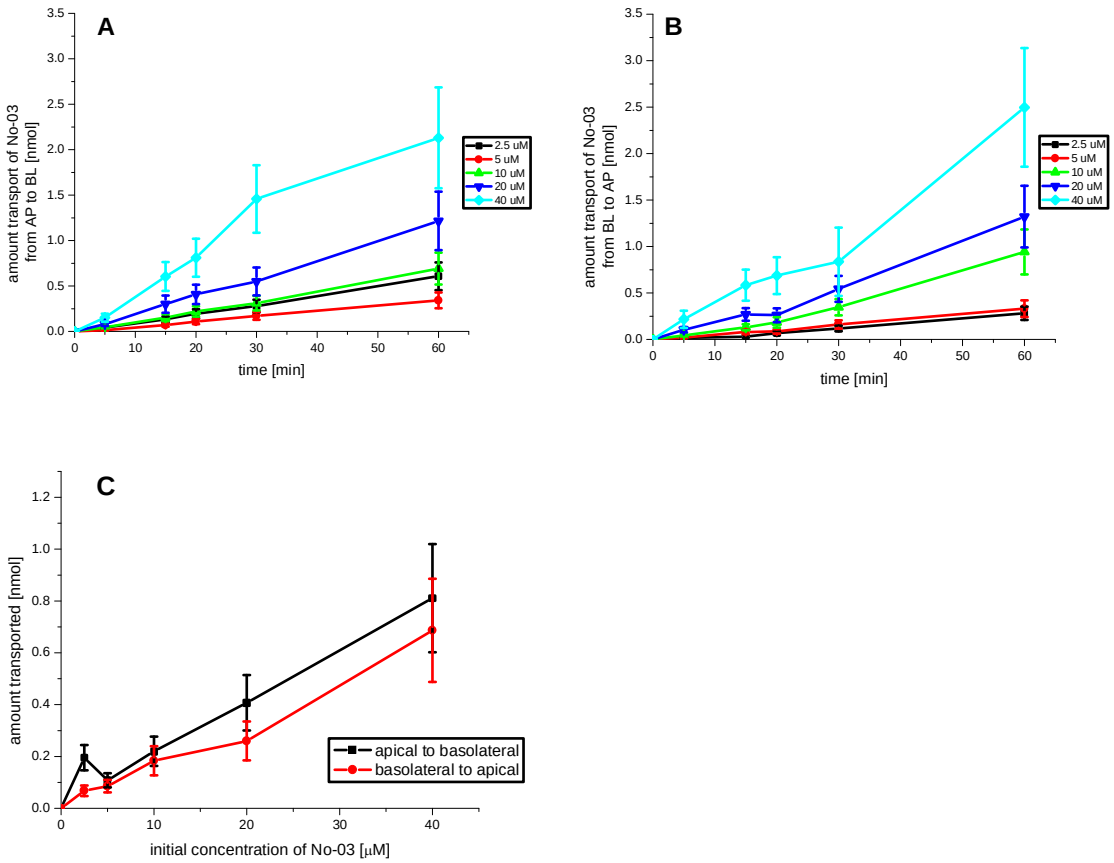

Figure 4.14 Transport of No-03 through porcine BCEC from AP to BL (**A**) and from BL to AP (**B**), and dose dependent transport after 20 minutes from AP to BL and BL to AP (**C**). Values are mean ±SEM, n=3.

Time dependent transport of No-03 (Figure 4.14) from AP to BL was equal to transport from BL to AP at all time points and concentrations investigated. Overall high transport (up to 2.2 nmol/60 min/cm^2, which corresponds to 220 µmol/60 min/total BCE-A in both directions, as well as linear dose dependent transport in both directions indicated passive diffusion.

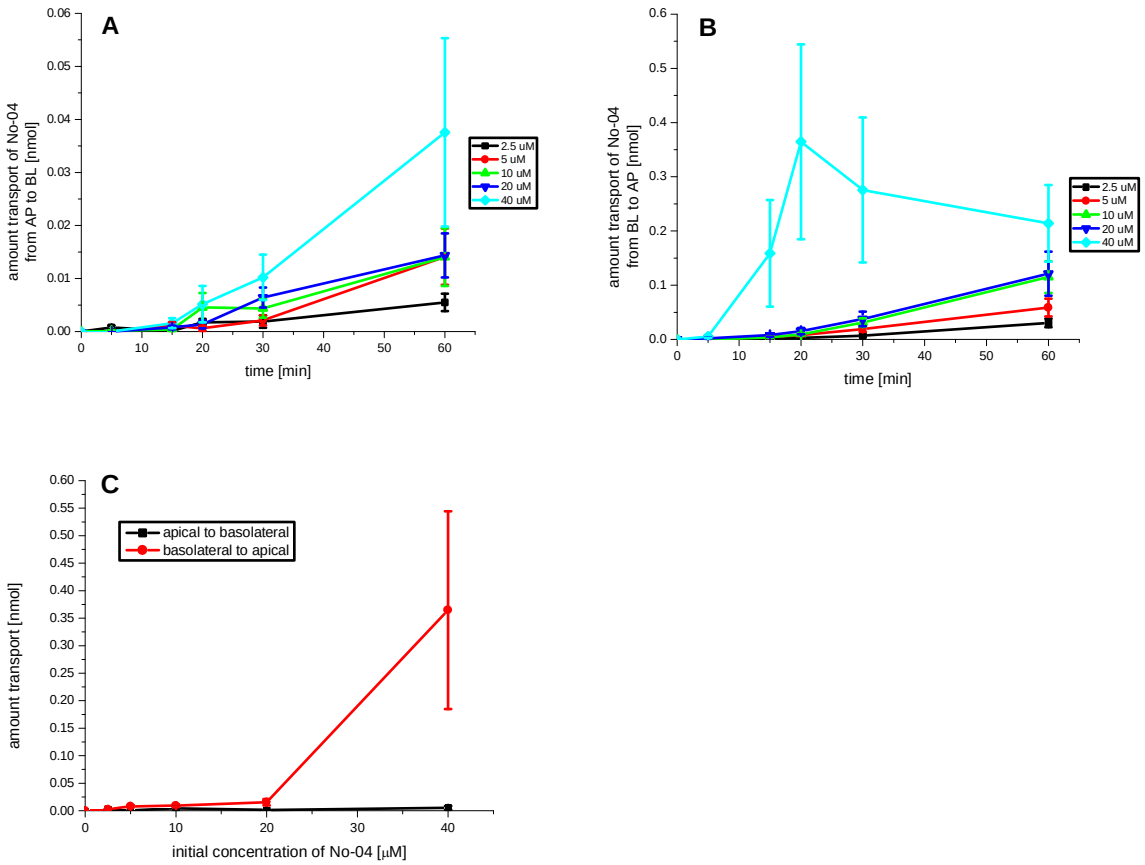

Figure 4.15 Transport of No-04 through porcine BCEC from AP to BL (**A**) and from BL to AP (**B**), and dose dependent transport after 20 minutes from AP to BL and BL to AP (**C**). Values are mean ±SEM, n=3.

The difference in time dependent transport of No-04 from AP to BL and from BL to AP (Figure 4.15) is not statistically significant at any time point or concentration. Overall very low transport (up to 0.04 nmol/60 min/cm^2, which corresponds to 4 µmol/60 min/total BCE-A from AP to BL, and up to 0.2 nmol/60 min/cm^2, which corresponds to 20 µmol/60 min/total BCE-A from BL to AP) was observed. Dose dependent transport from AP to BL was not significantly lower than transport from BL to AP. The high standard deviation indicated divergent data.

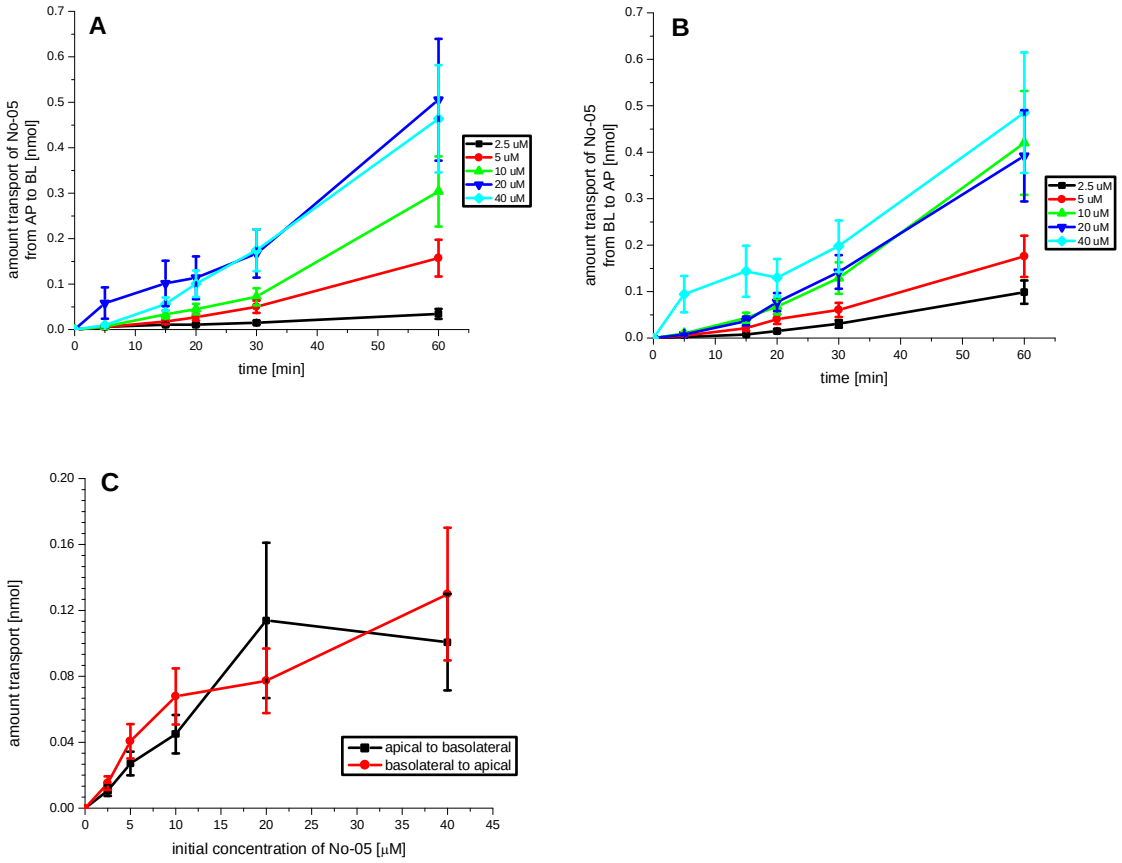

Figure 4.16 Transport of No-05 through porcine BCEC from AP to BL (**A**) and from BL to AP (**B**), and dose dependent transport after 20 minutes from AP to BL and BL to AP (**C**). Values are mean ±SEM, n=3.

Time dependent transport of No-05 (Figure 4.16) from AP to BL was equal to transport from BL to AP at all time points and concentrations investigated. Overall low transport (up to 0.5 nmol/60 min/cm^2, which corresponds to 50 µmol/60 min/total BCE-A) was observed in both directions. A saturation curve was observed in both directions of dose dependent transport, which indicated that the involvement of efflux transporters was possible.

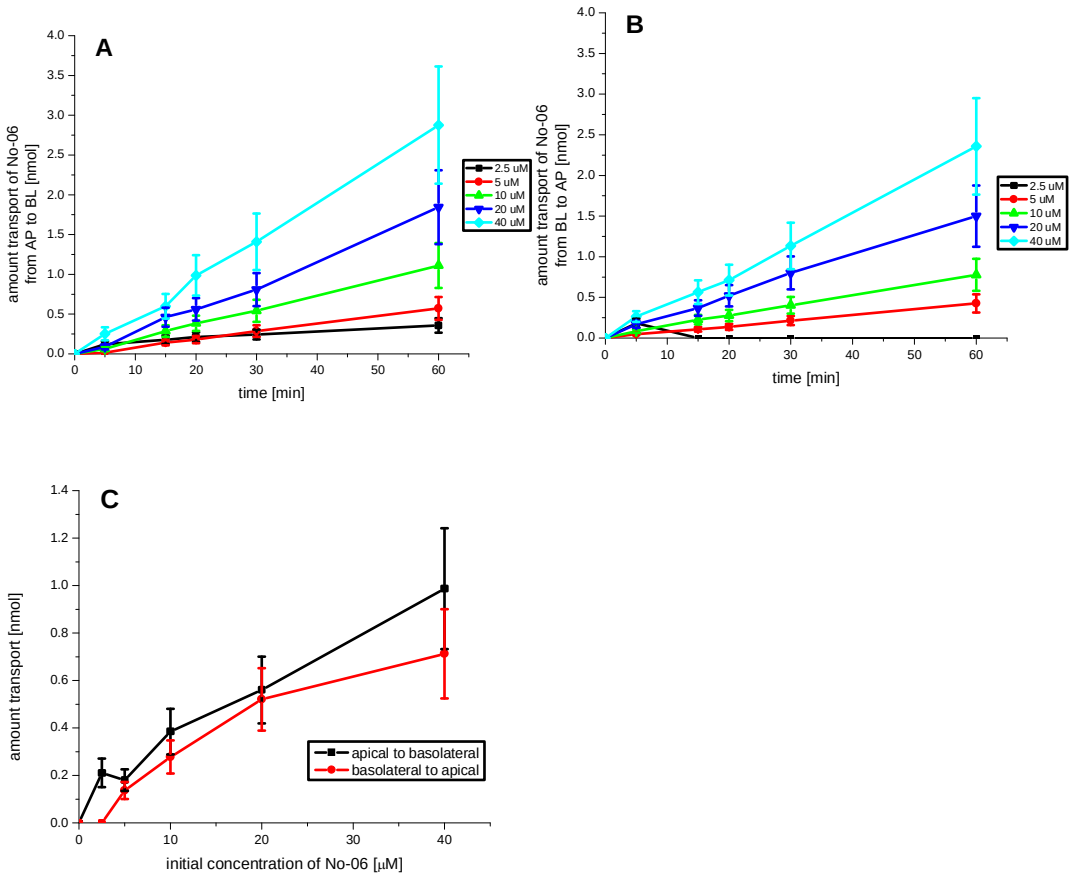

Figure 4.17 Transport of No-06 through porcine BCEC from AP to BL (**A**) and from BL to AP (**B**), and dose dependent transport after 20 minutes from AP to BL and BL to AP (**C**). Values are mean ±SEM, n=3.

Time dependent transport of No-06 (Figure 4.17) from AP to BL was not significantly higher than transport from BL to AP at any time point or concentration investigated. Overall high transport (up to 2.9 and 2.3 nmol/60 min/cm^2 from AP to BL and from BL to AP respectively, which corresponds to 290 and 230 µmol/60 min/total BCE-A from AP to BL and from BL to AP respectively) was observed in both directions. There was a tendency to a saturation curve in both directions of dose dependent transport, which indicated that the involvement of transporters and facilitated transport was possible. However, as this observation was small and considering the high standard deviation, simply passive diffusion cannot be ruled out.

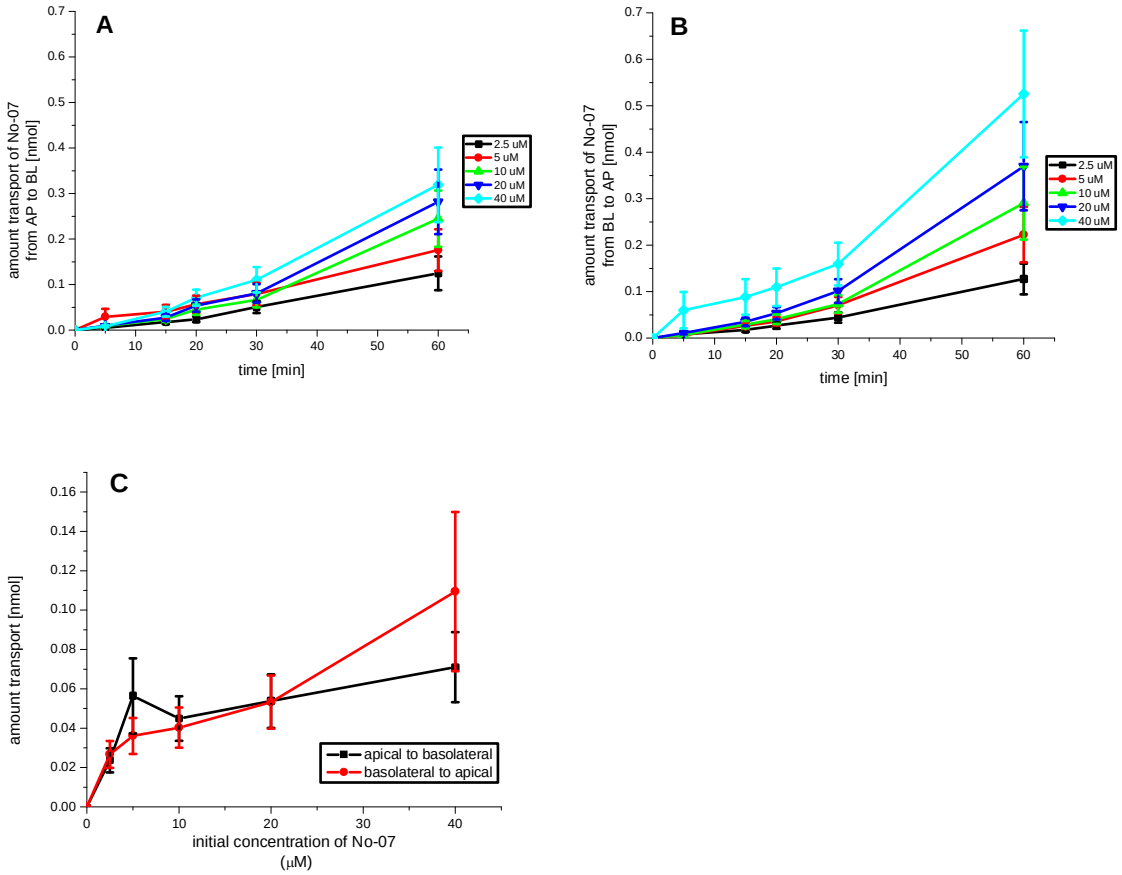

Figure 4.18 Transport of No-07 through porcine BCEC from AP to BL (**A**) and from BL to AP (**B**), and dose dependent transport after 20 min. from AP to BL and BL to AP (**C**). Values are mean ±SEM, n=3.

Time dependent transport of No-07 (Figure 4.18) from AP to BL was not significantly lower than transport from BL to AP at any time point or concentration investigated. Overall low transport (up to 0.3 nmol/60 min/cm^2, which corresponds to 30 µmol/60 min/total BCE-A) was observed in both directions. Dose dependent transport showed clear saturation curves in both directions, which indicated that the involvement of transporters was possible.

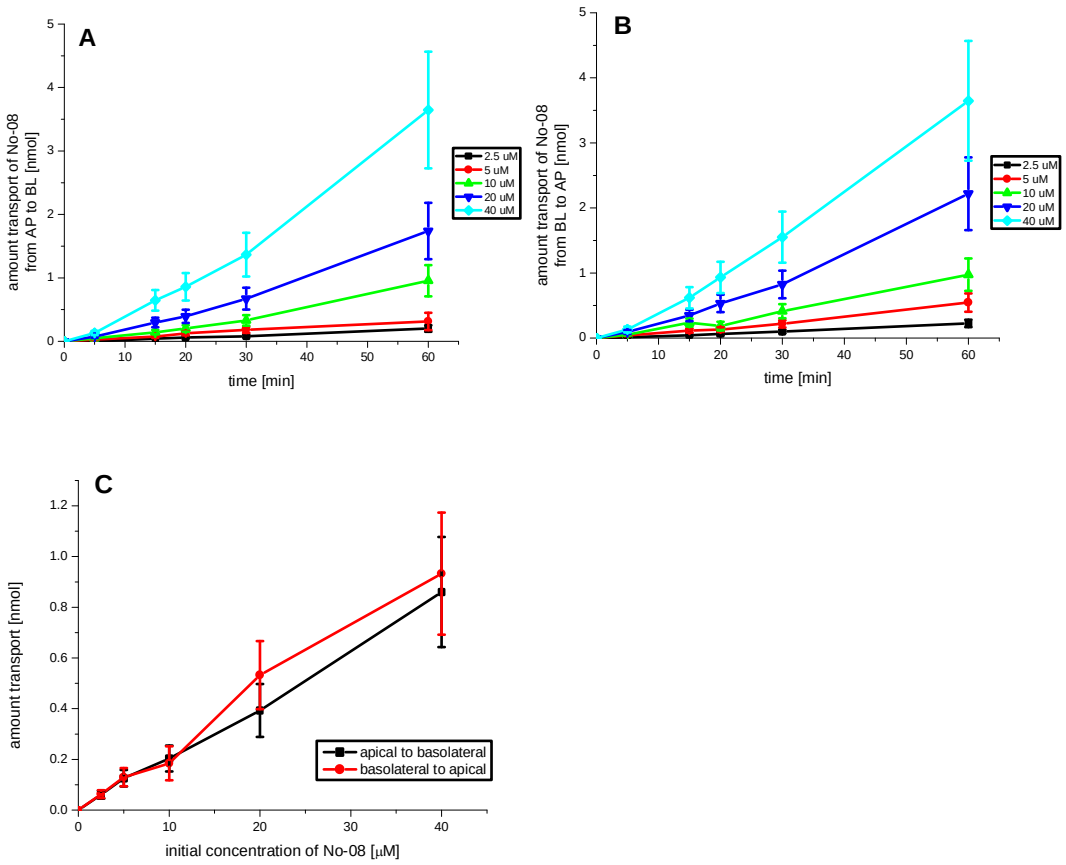

Figure 4.19 Transport of No-08 through porcine BCEC from AP to BL (**A**) and from BL to AP (**B**), and dose dependent transport after 20 min. from AP to BL and BL to AP (**C**). Values are mean ±SEM, n=3.

Time dependent transport of No-08 (Fig. 4.19) was equal in both directions at all time points and concentrations. Overall high transport (up to 3.5 nmol/60 min/cm^2, which corresponds to 350 µmol/60 min/total BCE-A) in both directions, as well as linear dose dependent transport in both directions indicated passive diffusion.

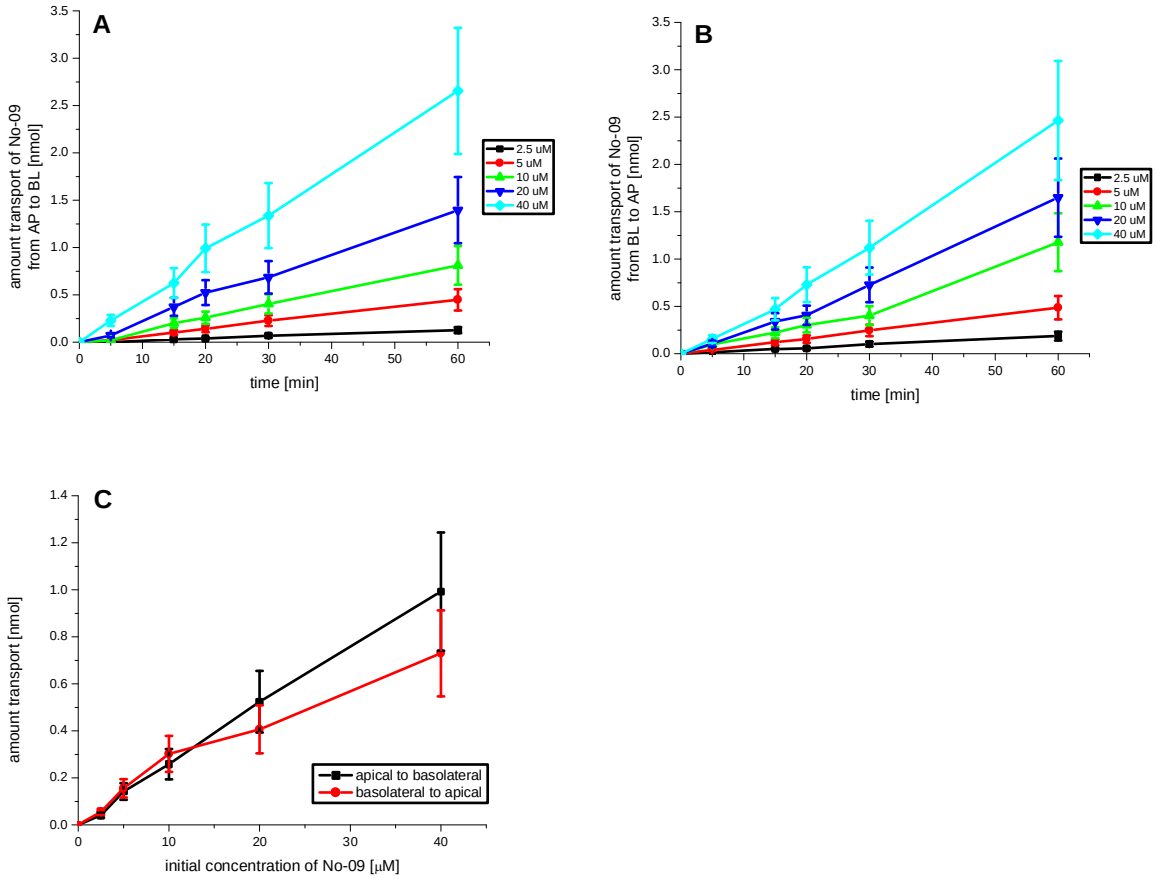

Figure 4.20 Transport of No-09 through porcine BCEC from AP to BL (**A**) and from BL to AP (**B**), and dose dependent transport after 20 min. from AP to BL and BL to AP (**C**). Values are mean ±SEM, n=3.

Time dependent transport of No-09 (Fig. 4.20) was equal in both directions at all time points and concentrations. Overall high transport (up to 2.5 nmol/60 min/cm^2, which corresponds to 250 µmol/60 min/total BCE-A) was observed in both directions. The linear dose dependent transport from AP to BL indicated passive diffusion, whereas a tendency to a saturation curve was observed from BL to AP, wherefore the involvation of a transporter may be considered. However, as this observation is rather small, simply passive diffusion may not be ruled out.

Compound	Apparent permeability (P_{app})			Approx. overall transport	
	(AP to BL) [10^{-5}cm/sec]	(BL to AP) [10^{-5}cm/sec]	P_{app} (AP to BL) / P_{app} (BL to AP)	AP to BL [µmol/60min / total BCE-A]	from BL to AP [µmol/60min / total BCE-A]
No-01	1.1±0.3	1.8±0.09	1.6	230	230
No-02	2.6±0.09	2.9±0.03	1.1	350	350
No-03	2.8±1.0	2.2±0.3	0.8	220	220
No-04	0.045±0.01	0.27±0.04	6	4	20
No-05	0.62±0.1	0.84±0.2	1.4	50	50
No-06	2.9±0.3	1.5±0.6	0.5	290	230
No-07	0.73±0.2	0.87±0.2	1.2	30	30
No-08	2.3±0.2	2.8±0.1	1.2	350	350
No-09	2.0±0.2	2.4±0.3	1.2	250	250

Table 4.3 Apparent permeability of preclinical test compounds and approx. overall transport through porcine BCEC.

Table 4.3 resumes parameters from the transport assays. The following rank order from low to high AP to BL transport was observed No-04 < No-05 < No-07 < No-01 < No-09 < No-08 < No-02 < No-03 < No-06. The influence of efflux transporters could not be assumed for any compound from the bidirectional flux, as none of the differences were statistically significant.

4.3.2 Combined study of BBB permeability and target receptor effect

Transport of the test compounds No-04 and No-05 from AP to BL in porcine BCEC was performed with the following concentrations: 2.5, 5, 10, 20, and 40 µM. Samples from the BL compartment where collected after 45 minutes. Only the initial concentration applied to the AP side, but not the concentration of the samples on the BL side was known. With these samples, the target receptor screening assay was performed in cells expressing the human target receptor (using 50 µl of sample and 100 µl of assay buffer, giving a 3-fold dilution of the sample) by the industrial collabortation partner. Standard curves comprising concentrations ranging between 100 pM and 10 µM of the investigated test compound were carried along with each experiment.

The BL samples from the transport experiment of No-04 hardly showed any effect (the estimated ED_{50} was not even reached with the BL sample of the highest used

concentration of 40 µM), assuming the transported concentrations of No-04 were to low for an adequate effect on the target receptor in the target receptor screening assay (ED_{50} of No-04=2.41µM).

Dose-response curves were gained with the BL samples from the transport experiment with No-05, used in the target receptor assay (Figure 4.21), as well as a standard curve of No-05 (Figure 4.22).

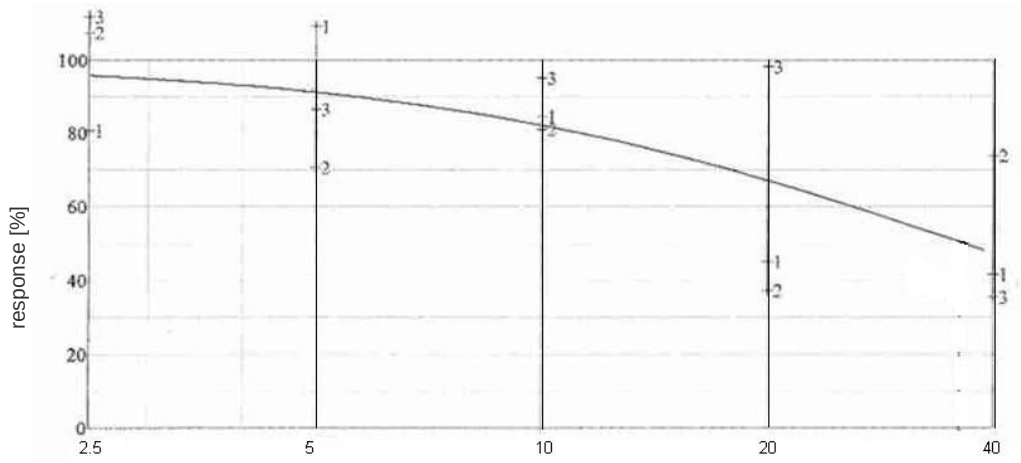

Figure 4.21 Dose-response curve of No-05 (BL samples, gained from the transport assay in porcine BCEC) in the target receptor assay. Only the initial test compound concentration applied to the transport compartment, but not the concentration of the samples applied at this assay is known. Values are mean ±SEM, n=3.

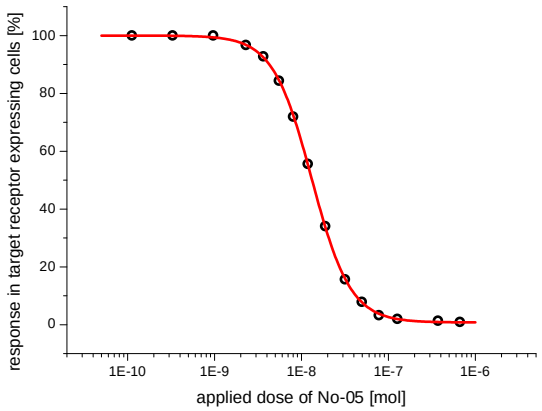

Figure 4.22 Standard curve of No-05, graphically fitted (with origin 6.1 using equation 5), from dose-response curve gained in target receptor screening assay. ED_{50} of No-05=13.4 nM.

From the extent of response gained from each of the samples applied at the target receptor screening assay, the concentrations of the samples could be estimated, knowing the relationship between the extent of response and applied dose from the standard curve.

The concentration of these samples was analyzed with LC-MS/MS by the industrial collaboration partner as well. Therefore, results of the estimated concentrations of the BL samples from the transport assay, applied in the target receptor screening assay, could be compared to the measured values. As shown in Table 4.4, the concentrations estimated with the target receptor screening assay are lower than the concentrations gained from the LC-MS/MS analysis, the difference diminishes with higher applied doses, giving a ratio of measured versus estimated concentration of 80-fold for 2.5 µM and a ratio of 2.5-fold for 40 µM initially applied concentration.

Initial AP concentration of samples [µM]	**Estimated concentration from target receptor screening assay [nM]**	**Concentrations measured by LC-MS/MS [nM]**	**Ratio measured / estimated**
2.5	0.36	29.4±9.2	81
5	15	52.9±11	3.5
10	16.5	78.9±13.4	4.8
20	36	128.3±16.8	3.5
40	48	120±8	2.5

Table 4.4 Concentrations of No-05 samples, drawn from the BL compartment after 45 minutes in a transport assay with porcine BCEC. Values gained from analysis by LC-MS/MS were compared to values gained by estimation of concentrations from the target receptor screening assay using the dose-response relationship of a standard curve. Values are mean ±SEM, n=3.

5 Discussion

5.1 Evaluation of BB19 cells as in vitro model of the BBB

The optimal *in vitro* model for the BBB accounts for active and passive transport processes, as well as non-defined drug-cell interactions. In addition, it is as little laborious as possible, and preferably is from human origin.

Paracellular transport of sucrose is a well accepted predictor to evaluate the restrictiveness of BBB cellular monolayers (Gumbleton and Audus, 2001).

On Transwell® polycarbonate filters, the BB19 cells failed to build a tight monolayer, the P_{app} is barely different to the P_{app} of empty filters, while porcine BCEC grew to optimal tightness on these filters. Tightness of BB19 cells could be improved on BD Falcon™ PETE cell culture inserts, where they exhibited a 2.4-fold higher tightness compared to empty filters, leading to a P_{app} of 1.30×10^{-5} cm/sec, which corresponds to P_{app}-values of porcine BCEC cultivated either on Transwell polycarbonate filters or on BD Falcon™ PETE cell culture inserts. The same range of P_{app}-values was reported of other cell culture models using bovine or porcine brain capillary cells (Torok et al., 2003, Dehouck et al., 1992, Abbruscato and Davis, 1999). However, Omidi and colleagues, who evaluated the immortalized mouse brain capillary endothelial cell line b.End3 found a sucrose permeability in the same range as our BB19 cells, and report that their monolayers lacked real discrimination with respect to the permeation of transcellular and paracellular probes, even though the sucrose permeability compares favorably with data in the literature for systems considered to represent a restrictive barrier (Omidi et al., 2003). It should be noted that, in opposition to P_e values, P_{app} values do not account for the blank values of empty filters, and therefore are solely expedient for the comparison of monolayers grown on the same type of cell culture inserts. Empty Transwell® polycarbonate inserts (all empty filters are precoated with rat tail collagen and are without cells) have a 2.4-fold higher sucrose permeability than the empty BD Falcon™ PETE filters, which leads to a lower sucrose permeability coefficient of $P_e = 1.45 \times 10^{-5}$ cm/sec for the porcine BCEC cultivated on Transwell® polycarbonate inserts versus $P_e = 2.25 \times 10^{-5}$cm/sec for BB19 cells cultured on BD Falcon™ PETE inserts (and $P_e = 2.66 \times 10^{-5}$cm/sec for porcine

BCEC). According to Monnaert and colleagues, P_e values higher than $1.67x10^{-5}$ cm/sec are indicative for a leaky BBB (Monnaert et al., 2004). A serum-free model with primary porcine BCECs has reached a remarkable P_e of $1.0x10^{-6}$ cm/sec, which could be even improved with hydrocortisone to a P_e of $5.0x10^{-7}$ cm/sec (Franke et al., 1999, Hoheisel et al., 1998). A permeability coefficient of $P_e=6.8x10^{-5}$cm/sec for sucrose has been reported for the well-characterized RBE4 cell line co-cultured with C6 glioma cells (Lagrange et al., 1999). Another study reported a sucrose permeability coefficient of $P_e=3.8x10^{-5}$cm/sec for RBE4 cells co-cultivated with astrocytes (Rist et al., 1997), which, according to Gumbleton and Audus, is considered to be leaky and therefore unsuitable for the study of transendothelial transport (Gumbleton and Audus, 2001).

In addition, the BB19 cell monolayers do not show any adequate discrimination between the paracellular marker sucrose and the transcellular marker propranolol (P_{app}= $1.30x10^{-5}$ vs. $2.18x10^{-5}$ cm/sec), which further confirms that the model is not suitable for transport studies yet, and still needs to be improved.

It has been shown that the microenvironment can influence the permeability properties of endothelial cells *in situ*. With respect to cellular permeability of cultured endothelial cells, astrocyte-derived factors seem to play a central role (Janzer and Raff, 1987, Stewart and Wiley, 1981). Therefore medium conditioned by C6 cells, a glioma cell line, was used. In addition, supplements were investigated, which have been shown to improve cultured BCEC monolayers. We used the cAMP analog chlorphenylthio-cAMP in combination with the cAMP specific phosphodiesterase inhibitor RO-20-1724 (Rubin et al., 1991) and the glucocorticoid dexamethasone (Grabb and Gilbert, 1995). Glucocorticoids, i.e. hydrocortisone were shown to improve the barrier properties of a porcine and a murine *in vitro* model of the BBB (Hoheisel et al., 1998, Weidenfeller et al., 2005) . 1,25-dihydroxyvitamin D_3 was shown to regulate differentiation in many cell types, including normal, immortalized, and tumor cells (Bouillon et al., 1995). The supplement concentrations we used in our experiments were in the range of the effective concentrations published in the previously cited publications.

The influence of the cell culture conditions on the differentiation of the BB19 cells and on the degree of tight junction formation was studied by the assessment of the ZO-1 pattern. Zonula occludens protein (ZO-1) is associated with the junctional complex of

high resistant tight junctions (Krause et al., 1991). A distinct morphological improvement toward a more spindle-like morphology was seen with C6-conditioned medium. The use of primary astrocytes might lead to a even better differentiation than the use of the C6 cell line (Boveri et al., 2005).

A more primary BCEC-like appearance was also seen with dexamethasone or 1,25-dihydroxyvitamin D_3. Chlorophenylthio-cAMP and RO-20-1724 failed to cause any improvement of the patterns of ZO-1, and showed no difference compared to the controls. No change upon spatial ZO-1 expression was observed. In opposition to the cell monolayers of the above cited publications, none of the cell culture conditions could improve the tightness (i.e. sucrose permeability) of the BB19 monolayers.

The expression of typical blood-brain barrier drug transporters is mandatory for the usability of potential *in vitro* cell culture systems. It has been shown that ABC transporters, such as P-gp, play a functional part in establishing a barrier between the blood and the brain (Fricker et al., 2002, Miller et al., 2000, Regina et al., 1998, Schinkel et al., 1996). Studies using mdr1a/b gene knockout mice show significantly elevated drug levels, particularly in the brain (Schinkel et al., 1997). The expression of P-gp, detected on mRNA level, Western blot and with immunostaining in BB19 cells indicates that the BB19 cell culture model exhibits important features of the BBB.

The expression of several MRP homologs in brain endothelial vessels has been reported. MRP1, MRP4, MRP5 and MRP6 have been identified in bovine brain capillaries by RT-PCR. Confocal laser scanning microscopy and Western blot analysis showed a predominant distribution of MRP1 and MRP5 in the apical plasma membrane, and an almost equal distribution of MRP4 on the apical and basolateral plasma membrane. MRP3 was detected in cultured bovine brain microvessel endothelial cells but not in capillaries (Zhang et al., 2004, Zhang et al., 2000). The presence of MRP2 in human brain, and its localization at the apical membrane of capillary endothelial cells was shown previously (Fricker et al., 2002, Miller et al., 2002, Miller et al., 2000, Potschka et al., 2003). MRP1, MRP2, MRP4, and MRP5 were detected in BB19 cells on mRNA level. MRP4 was also detected by immunostaining. However, MRP1, MRP2 and MRP5 were not detected with immunostaining. The brain multidrug resistance protein (BMDP), which had been discovered at the porcine blood-brain barrier (Eisenblatter et al., 2003), is highly homologous to the human BCRP (BCRP/ABCG2). The presence of BCRP was

demonstrated in both normal and tumor human brain tissue. Like P-gp, this transporter has been localized to the apical surface of microvessel endothelium, and both have several substrates in common (Cooray et al., 2002). The presence of BCRP in BB19 cells has been demonstrated on mRNA level, Western blot, and with immunostaining. Analysis of the total mRNA pool indicated previously that expression of BCRP in the blood-brain barrier is even higher than P-gp and MRP1, therefore it was concluded that BCRP might play an important role in the exclusion of xenobiotics from the brain (Eisenblatter et al., 2003).

Members of multispecific organic anion transport proteins (OATP2, OATs and MCTs) are present in the blood-brain barrier. Human OATP-A and the rat Oatp2 have been identified in brain capillaries by immunostaining (Gao et al., 2000, Gao et al., 1999). However, neither OATP-A nor OATP-C could be shown in BB19 cells on mRNA level.

Both OAT3, and OAT4, but no OAT1 were detected in BB19 cells by RT-PCR. Northern blot analysis previously revealed that rat OAT3 (SLC22A8) mRNA is expressed in the brain, while the role of OAT1 and OAT4 at the BBB still remains unclear.

Propranolol is a basic lipophilic drug, that has a high brain to plasma ratio and is sequestered in the brain (Pardridge et al., 1984). Therefore, it is commonly used as a transcellular marker of the blood-brain barrier. Time-dependent uptake of morphine, together with the reference substances propranolol, and sucrose into BB19 cells was performed during an incubation time of 120 minutes. Morphine penetrated to a lesser degree than propranolol, and diffusion of sucrose into the cells was minimal, which is similar to the uptake data gained from the established porcine brain capillary endothelial cell model (Huwyler et al., 1996).

Uptake of daunomycin, a substrate of P-glycoprotein (Kwon et al., 1996) was significantly increased (1.45-fold) by the P-gp inhibitor verapamil, indicating functional expression of P-gp, which indicates that, in spite of the absence of a sufficiently restrictive paracellular barrier, BB19 cells still may be suitable for drug uptake studies (Gumbleton and Audus, 2001). Preliminary investigations suggest, that monitoring the uptake kinetics into cerebral capillary endothelial cell monolayers may even be superior to transmonolayer flux measurements for predicting the passive diffusion of polar permeants across the BBB *in vivo* (Johnson and Anderson, 1999).

In conclusion, we could demonstrate that important ABC transporters, such as P-gp and BCRP that constitute the BBB, are expressed in BB19 cells. Furthermore, we were able to improve cellular morphology, tight junction protein patterns, and tightness of the monolayer towards an appearance similar to primary BCEC. Although the BB19 cells appear to be unsuitable for transendothelial assessments, it could be shown with uptake experiments, that important functional characteristics of the BBB are fulfilled. These investigations could lead to the establishment of a new *in vitro* BBB model of human origin that might be an important tool assessing BBB mechanisms.

5.2 Expression and inducibility of CYPs in BB19 cells

Besides being a physical and a transport barrier, the BBB has also been described to be a metabolic barrier, consisting of numerous enzymes, such as aminopeptidase A, aminopeptidase M, and angiotensin-converting enzyme (Allt and Lawrenson, 2000). Of the phase I metabolizing enzymes, CYPs play an important role in the biotransformation of several CNS active drugs. However, even though CYPs have been identified in the brain, their functional role still remains to be elucidated. Furthermore, data about the expression of CYPs at the BBB is very limited. Therefore we made an attempt to investigate the presence and inducibility of selected CYP isoforms (that may play a role in the metabolism of CNS active drugs) in our *in vitro* model of the BBB, the BB19 cells. On mRNA level only the presence of CYP1A1 and, to a lesser extent, CYP3A4 could be shown, whereas CYP1A2, CYP2D6, and CYP2C19 were not detected. Some agents are known to induce certain CYP isoforms, which could lead to interactions with CNS active drugs that are substrates of these CYP isoforms. Only CYP1A1 was found to be inducible by benzo[a]pyrene, whereas the treatment with rifampicin did not significantly change the expression level of CYP3A4. In general, CYP1A1, is not only induced by polycyclic aromatic hydrocarbons (PAH), CYP1A1 is also involved in the transformation of PAHs to reactive intermediates, which irreversibly bind to DNA. The main sources of these carcinogenic PAHs include tobacco smoke, urban air, and charcoal grilled food (Granberg et al., 2003). The potential role of CYP1A1 induction for the susceptibility of brain cancer requires further investigations.

The presence, of CYP1A1, but not its inducibility, could be confirmed on protein level by immunostaining and Western blot. Notably, for unknown reasons, the BB19 cells treated with benzo[a]pyrene appear to be larger than the untreated cells. To determine the causes of this finding in future investigations, a toxicity assay should be conducted, to identify a putative toxicity of the benzo[a]pyrene treatment. Several pathways have been identified, which regulate the cell size in eukaryotic cells (Bjorklund et al., 2006). Benzo[a]pyrene may be modulating these pathways, particularly by the induction of apoptosis.

The presence of CYP1A1 could not be confirmed on a functional level, as no catalytic activity could be detected in the P450-GLO™ assay. However, as a positive control is missing, the significance of this experiment is limited. Therefore, further investigations need to be carried out, to determine the role of CYP1A1 at the BBB. It may be supposable that CYP1A1 might contribute to the metabolic barrier of the BBB, protecting the brain from xenobiotics. The same might be assumed for CYP3A4, however, for definite assumptions the expression of CYP3A4 needs to be studied on protein level and functionally, as well. On the other hand, it may be assumed that CNS active drugs that are substrates of CYP1A2, CYP2D6, and CYP2C19 are mainly metabolized in the liver, as none of these enzymes could be detected in BB19 cells. However, further experiments, e.g. in freshly isolated brain capillaries, on protein level as well as functional experiments, are necessary to confirm these assumptions.

5.3 Identification of P-glycoprotein inhibitors among neuroleptic compounds

There is increasing evidence from *in vitro* assays that neuroleptic drugs may modulate P-gp function. However, so far, only little in known about the influence of newer atypical neuroleptic drugs on P-gp, and on its role in the distribution and elimination of neuroleptic compounds (El Ela et al., 2004). Different neuroleptic compounds, metabolites, and domperidone were investigated for their inhibitory properties in microtiter plate based uptake and efflux assays using mdr1 overexpressing P388/mdr1 cells, and the corresponding parental P388/par cells for the assessment of effects that are not related to P-gp. With these assays, the tested compounds could be classified into effective (clozapine, norclozapine, olanzapine,

domperidone, aripiprazole, quetiapine, risperidone, 9-OH risperidone) and noneffective P-gp inhibitors (haloperidol).

None of the tested compounds modulated the uptake or the efflux of the P-gp substrate R123 in P388/par cells, which supports the hypothesis of a selective interaction with P-gp rather than any unspecific effects or the involvement of other transport mechanisms.

The newer atypical neuroleptic drugs quetiapine and aripiprazole both showed high inhibitory properties. A previous investigation with quetiapine, were the quetiapine-mediated inhibition of [^{3}H]-talinolol transport across Caco-2 monolayers was studied, is in concordance with our findings (El Ela et al., 2004). Quetiapine has also been identified as a P-gp substrate in an ATPase assay (Boulton et al., 2002). Aripiprazole is the most recently introduced atypical neuroleptic drug, thus no P-gp investigations have been previously reported with this compound.

Clozapine and, to a lower extent, norclozapine, have been identified as P-gp inhibitors *in vitro* before as well (El Ela et al., 2004). However, in our studies, the P-gp affinity of clozapine was rather low compared to norclozapine or the other investigated compounds. A very low affinity to P-gp has also been observed previously in the ATPase assay (Boulton et al., 2002).

There are no previous investigations concerning the P-gp inhibitory properties of risperidone and its major metabolite 9-OH risperidone. Whereas it has been reported that risperidone, and to a lower extend 9-OH risperidone, are P-gp substrates *in vitro*, which was confirmed in experiments with mdr1a gene knockout mice (Ejsing et al., 2005).

Similar to the results from our efflux assay, the inhibitory potency of olanzapine to P-gp was comparatively low (El Ela et al., 2004), whereas, in contrary, an intermediate P-gp affinity and a high inhibitory capacity were detected for olanzapine in the uptake assay. The causes for these differences (e.g. unspecific effects or limitations of the assay) remain to be explored.

For haloperidol, only a very weak activity has been observed in the ATPase assay (Boulton et al., 2002), whereas, contrary to our results, a different study reported P-gp inhibitory properties *in vitro* (El Ela et al., 2004).

It has to be noted that discrepancies between the findings from our assays and literature data may be due to the different methods utilized, as observed findings depend on the experimental set-up.

Ziprasidone did not exert any influence on uptake or efflux of R123. However, the maximal applied concentration was only 10 µM. At higher concentrations, ziprasidone precipitates when the DMSO stock solution is added to the aqueous assay buffer. Due to these solubility limitations, the highest applied concentration was too low for an accurate experimental determination of the inhibitory parameters. Therefore, a possible affinity of ziprasidone to P-gp could not be determined. In general, all of the tested neuroleptic compounds are highly lipophilic, which limited the solubility of most of the investigated compounds and subsequently the application of higher concentrations. Therefore, it could not be confirmed, if a plateau was reached with the highest applied concentration. Thus, only approximate interpretations of the inhibitory properites of the applied compounds could be made.

In addition to the neuroleptic drugs and drug metabolites, we investigated the inhibitory properties of domperidone, which is a known P-gp inhibitor (Schinkel et al., 1996). Domperidone is a peripherally acting dopamine antagonist, which does not exert any CNS effects in humans or wild-type mice. Contrariwise, mdr1a gene knockout mice show extrapyramidal symptoms, which are typical neurological side effect of neuroleptic drugs. Thus, domperidone could be used as a positive control for *in vivo* experiments with mdr1a/1b gene knockout mice. Experiments with mdr1a/1b gene knockout mice could be helpful to elucidate the *in vivo* relevance of the inhibitory properties of the neuroleptic compounds, found in our *in vitro* assays.

5.4 Evaluation of BBB permeability of different CNS active compounds

5.4.1 Transport studies

The aim of this study was to investigate the BBB permeability of nine different test compounds *in vitro*. Porcine BCEC are reported to express important efflux transporters, such as P-gp, MRPs, and BCRP, and are generally accepted as *in vitro* model to study the ability of compounds to penetrate the BBB (Franke et al., 2000, Torok et al., 2003, Eisenblatter et al., 2003). The involvement of active transport was concluded by the investigation of a saturable dose-dependent transport and asymmetrical fluxes in bi-directional transendothelial transport, where a higher transport from BL to AP than from AP to BL indicates efflux by a transporter localized

on the AP (luminal) side of the BCEC. Comparing the test compounds, low transport (= 50 µmol/60min/total BCE-A) was observed from No-04, No-07, and No-05, whereas the overall transport of all the other compounds was high (220-350 µmol/60min/total BCE-A). None of the investigated compounds showed statistically significant asymmetrical fluxes. No-07 and No-05 showed clear saturation curves in both directions, whereas the transport from AP to BL was not significantly lower than in the opposite direction, which may indicate the involvement of transporters in both directions. For all other compounds, passive diffusion can be assumed, as no evidence for the involvement of active transport could be seen. No-06, showed a tendency to a saturation curve; however, the observation was small, and the standard deviation was too high for the assumption of the involvement of active transport mechanisms. Since porcine BCEC express several active transporters at the AP and BL side, further investigations would be necessary to confirm the gained results and to assign the involvement of specific transporters. Further experiments may include the inhibition of active carrier systems by the performance of the transport experiments at 4°C, or with the presence of inhibitors, such as verapamil, cyclosporine, or PSC833 for the inhibition of P-gp, or MK571 for the inhibition of MRP.

5.4.2 Combined study of BBB permeability and target receptor effect

There has been a many-fold increase of the number of compounds available for drug discovery through combinatorial chemistry (Paul, 1999, Radl, 1998), as well as the identification of new biological drug targets, which allows the identification of lead compounds in *in vitro* assays (Fernandes, 1998). However, more than 98% of candidate CNS-targeting drugs have been halted mid-development because of poor permeability across the BBB, presenting a major problem to the pharmaceutical industry (Pardridge, 2001, Terasaki et al., 2003). Until now, compounds pass through a consecutive series of screening assays, where in a first screening procedure the antagonism or inhibition of a receptor or enzyme is tested in a high-throughput *in vitro* assay, following membrane permeability properties in cell culture models in a second step (White, 2000). We have made a first attempt to develop a combined *in vitro* model, simultaneously studying BBB penetration and pharmacological effect. CNS-active compounds first have to pass the BBB (which was studied with the

transport through porcine BCEC); only this fraction will contribute to the effects on the receptor (which was obtained in the target receptor assay). This situation is incorporated in our combined approach, improving the screening-criteria for the selection of potential drug candidates, by reason that a compound with a moderate pharmacological efficacy (which is usually excluded from further screens), but with a high BBB permeability, might be a better drug candidate than a compound with a high pharmacological efficacy but poor BBB permeability properties. No-04 and No-05 (ED_{50} of 2.41 µM and 13.4 nM in the target receptor assay, respectively) were tested in the combined assay. The BBB permeability of No-04 was low, as seen in the previous transport experiment as well (approx. overall transport from AP to BL of 0.04 nmol/60min/cm^2), resulting in an insufficient response in the target receptor assay. From the dose-response curve obtained from the combined experiment with No-05, and the appropriate standard curve of No-05, the concentrations of the samples could be estimated, knowing the relationship between the extent of response and applied dose from the standard curve. These results of the estimated concentrations of the BL samples from the transport assay, which were tested in the target receptor assay, could be compared to the values measured by LC-MS/MS. If the extent of BBB penetration could be determined directly with the target receptor assay, elaborate LC-MS/MS capacity for the quantification could possibly be saved. However, the concentrations estimated with the target receptor assay were lower than the concentrations gained from the LC-MS/MS analysis. The difference diminishes with higher applied doses, giving a ratio of measured versus estimated concentration of 80-fold for 2.5 µM and a ratio of 2.5-fold for 40 µM initially applied concentration. These are preliminary experimental results from the development of this combined *in vitro* assay, with the future goal to be applied in industrial drug screening, revealing that a an extensive further optimization is necessary.

Accuracy as well as reproducibility has to be improved to obtain the right results the first time. This is required, because extensive retesting degrades the productivity of an industrially applied assay. The experimental procedure must be applicable to a wide variety of chemical structures and should therefore be validated with an appropriate number of standard compounds. The *in vitro* / *in vivo* correlation should be validated in animal models, as a high concordance with the *in vivo* situation is demanded. The experimental procedure must be optimized towards simple handling, and a minimal number of experimental steps. This procedure should be fast enough

to keep up with the input rate of new compounds from chemistry, and should allow a high degree of automatization (White, 2000).

In conclusion, the demand on this combined *in vitro* assay is to determine drug-like properties of a library of test compounds, to investigate the efficacy (which is the ability of a compound to produce a desired pharmacological effect), as well as the ability of the compound to pass through the blood-brain barrier to reach the target receptor. If the extent of BBB penetration could be determined directly out of the target receptor assay, LC-MS/MS measurements would not be necessary for the quantification anymore.

Drug-like properties are determined by further properties, such as persistence, safety, and pharmaceutical properties of the compound, such as solubility, rate of dissolution etc. Thus, for the identification of drug candidates, additional screening assays, investigating these further properties, are certainly indispensable. Our assay was designated and applicable for the discovery of CNS-active compounds. However, the ability of compounds to penetrate the blood-brain barrier is almost always of interest, not only as a property for the distribution into the brain, but also to screen for non-CNS indications, where a low BBB permeability is demanded to avoid adverse effects.

6 Conclusions and outlook

The evaluation of the immortalized human brain capillary endothelial cell line BB19 as an *in vitro* model of the BBB revealed that important ABC transporters, such as P-gp and BCRP, that constitute the BBB, are expressed in BB19 cells. Furthermore, we were able to improve the cellular morphology towards an appearance similar to primary BCEC. Although BB19 cells appear to be unsuitable for transport studies, it could be shown with uptake experiments, that important functional characteristics of the BBB are fulfilled. These investigations could lead to the establishment of a new *in vitro* model for the study of BBB uptake mechanisms.

Investigating the the presence and inducibility of CYPs in BB19 cells, only the presence of CYP1A1 and CYP3A4 could be demonstrated. Inducibility of CYP1A1 could only be shown on mRNA level, whereas no inducibility was seen for CYP3A4.
The relevance of these findings, e.g. a potential role of CYP1A1 induction at the BBB for the susceptibility of brain cancer, requires further investigatons. However, our results do not give enough evidence if CYPs, that are located at the BBB, may function to protect the brain from xenobiotics. Further studies, e.g. with freshly isolated brain capillaries and endothelial cells, could contribute to further understanding of the functional role of CYPs at the BBB.

The ability to inhibit P-gp function could be demonstrated for most of the investigated neuroleptic drugs and drug metabolites (except for haloperidol and ziprasidone). Reports from other groups are in concordance with most of our findings. Discrepancies between our results and the findings of other groups may be explained by the utilization of different methods. However, *in vivo*, additional pharmacological factors, such as metabolism by CYPs in the liver or other transport mechanisms (e.g. BCRP), may be involved. To elucidate the *in vivo* relevance of the inhibitory properties of the investigated neuroleptic compounds, there are ongoing experiments with mdr1a/1b gene knockout mice at the Psychiatric Clinic of the University of Mainz.

For the nine investigated CNS active compounds, a ranking regarding their BBB permeabilities could be determined. The involvement of active transport mechanisms was supposed for two compounds that showed clear saturation curves in both transport directions. To confirm the gained results and to assign the involvement of specific transporters, additional transport experiments should be conducted in presence of inhibitors, at 4°C to inhibit active carrier systems, or in cell lines overexpressing a specific transporter.

Our preliminary experimental results from the development of a combined *in vitro* model, simultaneously studying BBB penetration and pharmacological effect, revealed that a combined *in vitro* assay might be a promising new approach for the identification of drug candidates. Screening-criteria for the selection of potential drug candiates might be improved in a combined assay. If, in addition, the extent of BBB penetration of a test compound could be directly estimated out of this combined assay, analytical measurements could be safed. However, extensive further optimizations and validations with a wide variety of compounds are necessary to substantiate the accuracy and the reproducibility of this assay. Furthermore, the concordance to the *in vivo* situation should be evaluated in animal models. In addition, the experimental procedure will have to be optimized for industrial applications.

7 References

AASMUNDSTAD, T. A., MORLAND, J. & PAULSEN, R. E. (1995) Distribution of morphine 6-glucuronide and morphine across the blood-brain barrier in awake, freely moving rats investigated by in vivo microdialysis sampling. *J Pharmacol Exp Ther,* 275**,** 435-41.

ABBOTT, N. J. (2005) Dynamics of CNS barriers: evolution, differentiation, and modulation. *Cell Mol Neurobiol,* 25**,** 5-23.

ABBRUSCATO, T. J. & DAVIS, T. P. (1999) Combination of hypoxia/aglycemia compromises in vitro blood-brain barrier integrity. *J Pharmacol Exp Ther,* 289**,** 668-75.

AHMED-BELKACEM, A., POZZA, A., MACALOU, S., PE REZ-VICTORIA, J. M., BOUMENDJEL, A. N. & DI PIETRO, A. (2006) Inhibitors of cancer cell multidrug resistance mediated by breast cancer resistance protein (BCRP/ABCG2). *Anticancer Drugs,* 17**,** 239-243.

ALLT, G. & LAWRENSON, J. G. (2000) The blood-nerve barrier: enzymes, transporters and receptors--a comparison with the blood-brain barrier. *Brain Res Bull,* 52**,** 1-12.

ANZENBACHER, P. & ANZENBACHEROVA, E. (2001) Cytochromes P450 and metabolism of xenobiotics. *Cell Mol Life Sci,* 58**,** 737-47.

ARTHUR, F. E., SHIVERS, R. R. & BOWMAN, P. D. (1987) Astrocyte-mediated induction of tight junctions in brain capillary endothelium: an efficient in vitro model. *Brain Res,* 433**,** 155-9.

AUDUS, K. L. & BORCHARDT, R. T. (1986) Characteristics of the large neutral amino acid transport system of bovine brain microvessel endothelial cell monolayers. *J Neurochem,* 47**,** 484-8.

AURRAND-LIONS, M., JOHNSON-LEGER, C., WONG, C., DU PASQUIER, L. & IMHOF, B. A. (2001) Heterogeneity of endothelial junctions is reflected by differential expression and specific subcellular localization of the three JAM family members. *Blood,* 98**,** 3699-707.

BALABANOV, R. & DORE-DUFFY, P. (1998) Role of the CNS microvascular pericyte in the blood-brain barrier. *J Neurosci Res,* 53**,** 637-44.

BALLABH, P., BRAUN, A. & NEDERGAARD, M. (2004) The blood-brain barrier: an overview: structure, regulation, and clinical implications. *Neurobiol Dis,* 16**,** 1-13.

BEAULIEU, E., DEMEULE, M., GHITESCU, L. & BELIVEAU, R. (1997) P-glycoprotein is strongly expressed in the luminal membranes of the endothelium of blood vessels in the brain. *Biochem J,* 326 (Pt 2)**,** 539-44.

BENET, L. Z., CUMMINS, C. L. & WU, C. Y. (2004) Unmasking the dynamic interplay between efflux transporters and metabolic enzymes. *Int J Pharm,* 277**,** 3-9.

BHAMRE, S., ANANDATHEERATHAVARADA, H. K., SHANKAR, S. K., BOYD, M. R. & RAVINDRANATH, V. (1993) Purification of multiple forms of cytochrome P450 from a human brain and reconstitution of catalytic activities. *Arch Biochem Biophys,* 301**,** 251-5.

BICKEL, U. (2005) How to measure drug transport across the blood-brain barrier. *NeuroRx,* 2**,** 15-26.

BJORKLUND, M., TAIPALE, M., VARJOSALO, M., SAHARINEN, J., LAHDENPERA, J. & TAIPALE, J. (2006) Identification of pathways regulating cell size and cell-cycle progression by RNAi. *Nature,* 439**,** 1009-13.

BOADO, R. J. & PARDRIDGE, W. M. (1990) The brain-type glucose transporter mRNA is specifically expressed at the blood-brain barrier. *Biochem Biophys Res Commun,* 166**,** 174-9.

BONATE, P. L. (1995) Animal models for studying transport across the blood-brain barrier. *J Neurosci Methods,* 56**,** 1-15.

BORLAK, J. & ZWADLO, C. (2003) Expression of drug-metabolizing enzymes, nuclear transcription factors and ABC transporters in Caco-2 cells. *Xenobiotica,* 33**,** 927-43.

BORST, P., EVERS, R., KOOL, M. & WIJNHOLDS, J. (2000) A family of drug transporters: the multidrug resistance-associated proteins. *J Natl Cancer Inst,* 92**,** 1295-302.

BOUILLON, R., OKAMURA, W. H. & NORMAN, A. W. (1995) Structure-function relationships in the vitamin D endocrine system. *Endocr Rev,* 16**,** 200-57.

BOULTON, D., DEVANE, C., LISTON, H. & MARKOWITZ, J. (2002) In vitro P-glycoprotein affinity for atypical and conventional antipsychotics. *Life Sci,* 71**,** 163-9.

BOVERI, M., BEREZOWSKI, V., PRICE, A., SLUPEK, S., LENFANT, A. M., BENAUD, C., HARTUNG, T., CECCHELLI, R., PRIETO, P. & DEHOUCK, M. P. (2005) Induction of blood-brain barrier properties in cultured brain capillary endothelial cells: comparison between primary glial cells and C6 cell line. *Glia,* 51**,** 187-98.

BREEDVELD, P., BEIJNEN, J. H. & SCHELLENS, J. H. (2006) Use of P-glycoprotein and BCRP inhibitors to improve oral bioavailability and CNS penetration of anticancer drugs. *Trends Pharmacol Sci,* 27**,** 17-24.

BRIZ, O., SERRANO, M. A., MACIAS, R. I., GONZALEZ-GALLEGO, J. & MARIN, J. J. (2003) Role of organic anion-transporting polypeptides, OATP-A, OATP-C and OATP-8, in the human placenta-maternal liver tandem excretory pathway for foetal bilirubin. *Biochem J,* 371**,** 897-905.

CASNER, P. R. (2005) The effect of CYP2D6 polymorphisms on dextromethorphan metabolism in Mexican Americans. *J Clin Pharmacol,* 45**,** 1230-5.

CHIN, K. V. & LIU, B. (1994) Regulation of the multidrug resistance (MDR1) gene expression. *In Vivo,* 8**,** 835-41.

CHU, X., STRAUSS, J. R., MARIANO, M. A., LI, J., NEWTON, D. J., CAI, X., WANG, R. W., YABUT, J., HARTLEY, D. P., EVANS, D. C. & EVERS, R. (2006) Characterization of Mice Lacking the Multidrug Resistance Protein Mrp2 (Abcc2). *J Pharmacol Exp Ther*.

CISTERNINO, S., ROUSSELLE, C., LORICO, A., RAPPA, G. & SCHERRMANN, J. M. (2003) Apparent lack of Mrp1-mediated efflux at the luminal side of mouse blood-brain barrier endothelial cells. *Pharm Res,* 20**,** 904-9.

CLARK, D. E. (2003) In silico prediction of blood-brain barrier permeation. *Drug Discov Today,* 8**,** 927-33.

CONSEIL, G., DEELEY, R. G. & COLE, S. P. (2005) Polymorphisms of MRP1 (ABCC1) and related ATP-dependent drug transporters. *Pharmacogenet Genomics,* 15**,** 523-33.

COORAY, H. C., BLACKMORE, C. G., MASKELL, L. & BARRAND, M. A. (2002) Localisation of breast cancer resistance protein in microvessel endothelium of human brain. *Neuroreport,* 13**,** 2059-63.

CORDON-CARDO, C., O'BRIEN, J., CASALS, D., RITTMAN-GRAUER, L., BIEDLER, J., MELAMED, M. & JR, B. (1989) Multidrug-resistance gene (P-glycoprotein) is expressed by endothelial cells at blood-brain barrier sites. *Proc Natl Acad Sci U S A,* 86**,** 695-8.

CSERR, H. F. (1971) Physiology of the choroid plexus. *Physiol Rev,* 51**,** 273-311.

DAHL, M. L. & BERTILSSON, L. (1993) Genetically variable metabolism of antidepressants and neuroleptic drugs in man. *Pharmacogenetics,* 3**,** 61-70.

DAI, H., MARBACH, P., LEMAIRE, M., HAYES, M. & ELMQUIST, W. F. (2003) Distribution of STI-571 to the brain is limited by P-glycoprotein-mediated efflux. *J Pharmacol Exp Ther,* 304**,** 1085-92.

DAVSON, H. & OLDENDORF, W. H. (1967) Symposium on membrane transport. Transport in the central nervous system. *Proc R Soc Med,* 60**,** 326-9.

DE LANGE, E. C. (2004) Potential role of ABC transporters as a detoxification system at the blood-CSF barrier. *Adv Drug Deliv Rev,* 56**,** 1793-809.

DEAN, M. (2005) The genetics of ATP-binding cassette transporters. *Methods Enzymol,* 400**,** 409-29.

DEHOUCK, M. P., JOLLIET-RIANT, P., BREE, F., FRUCHART, J. C., CECCHELLI, R. & TILLEMENT, J. P. (1992) Drug transfer across the blood-brain barrier: correlation between in vitro and in vivo models. *J Neurochem,* 58**,** 1790-7.

DEHOUCK, M. P., MERESSE, S., DELORME, P., FRUCHART, J. C. & CECCHELLI, R. (1990) An easier, reproducible, and mass-production method to study the blood-brain barrier in vitro. *J Neurochem,* 54**,** 1798-801.

DEN OUDEN, D., VAN DEN HEUVEL, M., SCHOESTER, M., VAN RENS, G. & SONNEVELD, P. (1996) In vitro effect of GF120918, a novel reversal agent of multidrug resistance, on acute leukemia and multiple myeloma cells. *Leukemia,* 10**,** 1930-6.

DENISON, M. S. & WHITLOCK, J. P., JR. (1995) Xenobiotic-inducible transcription of cytochrome P450 genes. *J Biol Chem,* 270**,** 18175-8.

DING, X. & KAMINSKY, L. S. (2003) Human extrahepatic cytochromes P450: function in xenobiotic metabolism and tissue-selective chemical toxicity in the respiratory and gastrointestinal tracts. *Annu Rev Pharmacol Toxicol,* 43**,** 149-73.

DOYLE, L. A. & ROSS, D. D. (2003) Multidrug resistance mediated by the breast cancer resistance protein BCRP (ABCG2). *Oncogene,* 22**,** 7340-58.

DOYLE, L. A., YANG, W., ABRUZZO, L. V., KROGMANN, T., GAO, Y., RISHI, A. K. & ROSS, D. D. (1998) A multidrug resistance transporter from human MCF-7 breast cancer cells. *Proc Natl Acad Sci U S A,* 95**,** 15665-70.

DREWE, J., GUTMANN, H., FRICKER, G., TOROK, M., BEGLINGER, C. & HUWYLER, J. (1999) HIV protease inhibitor ritonavir: a more potent inhibitor of P-glycoprotein than the cyclosporine analog SDZ PSC 833. *Biochem Pharmacol,* 57**,** 1147-52.

EBNET, K., SCHULZ, C. U., MEYER ZU BRICKWEDDE, M. K., PENDL, G. G. & VESTWEBER, D. (2000) Junctional adhesion molecule interacts with the PDZ domain-containing proteins AF-6 and ZO-1. *J Biol Chem,* 275**,** 27979-88.

EHRLICH, P. (1885) Das Sauerstoff-Bedürnis des Organismus. Eine Farbanalytische Studie. *Berlin: Hirschwald*.

EISENBLATTER, T. & GALLA, H. J. (2002) A new multidrug resistance protein at the blood-brain barrier. *Biochem Biophys Res Commun,* 293**,** 1273-8.

EISENBLATTER, T., HUWEL, S. & GALLA, H. J. (2003) Characterisation of the brain multidrug resistance protein (BMDP/ABCG2/BCRP) expressed at the blood-brain barrier. *Brain Res,* 971**,** 221-31.

EJSING, T., PEDERSEN, A. & LINNET, K. (2005) P-glycoprotein interaction with risperidone and 9-OH-risperidone studied in vitro, in knock-out mice and in drug-drug interaction experiments. *Hum Psychopharmacol,* 20**,** 493-500.

EL ELA, A., HARTTER, S., SCHMITT, U., HIEMKE, C., SPAHN-LANGGUTH, H. & P, L. (2004) Identification of P-glycoprotein substrates and inhibitors among psychoactive compounds--implications for pharmacokinetics of selected substrates. *J Pharm Pharmacol,* 56**,** 967-75.

EL HAFNY, B., BOURRE, J. M. & ROUX, F. (1996) Synergistic stimulation of gamma-glutamyl transpeptidase and alkaline phosphatase activities by retinoic acid and astroglial factors in immortalized rat brain microvessel endothelial cells. *J Cell Physiol,* 167**,** 451-60.

FARIN, F. M. & OMIECINSKI, C. J. (1993) Regiospecific expression of cytochrome P-450s and microsomal epoxide hydrolase in human brain tissue. *J Toxicol Environ Health,* 40**,** 317-35.

FARKAS, E. & LUITEN, P. G. (2001) Cerebral microvascular pathology in aging and Alzheimer's disease. *Prog Neurobiol,* 64**,** 575-611.

FENSTERMACHER, J., GROSS, P., SPOSITO, N., ACUFF, V., PETTERSEN, S. & GRUBER, K. (1988) Structural and functional variations in capillary systems within the brain. *Ann N Y Acad Sci,* 529**,** 21-30.

FERNANDES, P. B. (1998) Technological advances in high-throughput screening. *Curr Opin Chem Biol,* 2**,** 597-603.

FISCHER, V., RODRIGUEZ-GASCON, A., HEITZ, F., TYNES, R., HAUCK, C., COHEN, D. & VICKERS, A. E. (1998) The multidrug resistance modulator valspodar (PSC 833) is metabolized by human cytochrome P450 3A. Implications for drug-drug interactions and pharmacological activity of the main metabolite. *Drug Metab Dispos,* 26**,** 802-11.

FRANKE, H., GALLA, H. & BEUCKMANN, C. T. (2000) Primary cultures of brain microvessel endothelial cells: a valid and flexible model to study drug transport through the blood-brain barrier in vitro. *Brain Res Brain Res Protoc,* 5**,** 248-56.

FRANKE, H., GALLA, H. J. & BEUCKMANN, C. T. (1999) An improved low-permeability in vitro-model of the blood-brain barrier: transport studies on retinoids, sucrose, haloperidol, caffeine and mannitol. *Brain Res,* 818**,** 65-71.

FRICKER, G. & MILLER, D. S. (2004) Modulation of drug transporters at the blood-brain barrier. *Pharmacology,* 70**,** 169-76.

FRICKER, G., NOBMANN, S. & MILLER, D. S. (2002) Permeability of porcine blood brain barrier to somatostatin analogues. *Br J Pharmacol,* 135**,** 1308-14.

FURUSE, M., FUJITA, K., HIIRAGI, T., FUJIMOTO, K. & TSUKITA, S. (1998) Claudin-1 and -2: novel integral membrane proteins localizing at tight junctions with no sequence similarity to occludin. *J Cell Biol,* 141**,** 1539-50.

FURUSE, M., SASAKI, H. & TSUKITA, S. (1999) Manner of interaction of heterogeneous claudin species within and between tight junction strands. *J Cell Biol,* 147**,** 891-903.

GAO, B., HAGENBUCH, B., KULLAK-UBLICK, G. A., BENKE, D., AGUZZI, A. & MEIER, P. J. (2000) Organic anion-transporting polypeptides mediate transport of opioid peptides across blood-brain barrier. *J Pharmacol Exp Ther,* 294**,** 73-9.

GAO, B., STIEGER, B., NOE, B., FRITSCHY, J. M. & MEIER, P. J. (1999) Localization of the organic anion transporting polypeptide 2 (Oatp2) in capillary endothelium and choroid plexus epithelium of rat brain. *J Histochem Cytochem,* 47**,** 1255-64.

GERVASINI, G., CARRILLO, J. A. & BENITEZ, J. (2004) Potential role of cerebral cytochrome P450 in clinical pharmacokinetics: modulation by endogenous compounds. *Clin Pharmacokinet,* 43**,** 693-706.

GOLDMANN, E. (1909) Die äussere und innere Sekretion des gesunden und kranken Organismus im Licht der vitalen Färbung. *Beitr Klin Chir,* 64**,** 192-265.

GOLDSTEIN, G. W. (1988) Endothelial cell-astrocyte interactions. A cellular model of the blood-brain barrier. *Ann N Y Acad Sci,* 529**,** 31-9.

GOODWIN, B., HODGSON, E. & LIDDLE, C. (1999) The orphan human pregnane X receptor mediates the transcriptional activation of CYP3A4 by rifampicin through a distal enhancer module. *Mol Pharmacol,* 56**,** 1329-39.

GOODWIN, J. T. & CLARK, D. E. (2005) In silico predictions of blood-brain barrier penetration: considerations to "keep in mind". *J Pharmacol Exp Ther,* 315**,** 477-83.

GRABB, P. A. & GILBERT, M. R. (1995) Neoplastic and pharmacological influence on the permeability of an in vitro blood-brain barrier. *J Neurosurg,* 82**,** 1053-8.

GRANBERG, L., OSTERGREN, A., BRANDT, I. & BRITTEBO, E. B. (2003) CYP1A1 and CYP1B1 in blood-brain interfaces: CYP1A1-dependent bioactivation of 7,12-dimethylbenz(a)anthracene in endothelial cells. *Drug Metab Dispos,* 31**,** 259-65.

GUMBLETON, M. & AUDUS, K. L. (2001) Progress and limitations in the use of in vitro cell cultures to serve as a permeability screen for the blood-brain barrier. *J Pharm Sci,* 90**,** 1681-98.

GUTMANN, H., TOROK, M., FRICKER, G., HUWYLER, J., BEGLINGER, C. & DREWE, J. (1999) Modulation of multidrug resistance protein expression in porcine brain capillary endothelial cells in vitro. *Drug Metab Dispos,* 27**,** 937-41.

HASELOFF, R. F., BLASIG, I. E., BAUER, H. C. & BAUER, H. (2005) In search of the astrocytic factor(s) modulating blood-brain barrier functions in brain capillary endothelial cells in vitro. *Cell Mol Neurobiol,* 25**,** 25-39.

HASKINS, J., GU, L., WITTCHEN, E. S., HIBBARD, J. & STEVENSON, B. R. (1998) ZO-3, a novel member of the MAGUK protein family found at the tight junction, interacts with ZO-1 and occludin. *J Cell Biol,* 141**,** 199-208.

HAWKINS, B. T. & DAVIS, T. P. (2005) The blood-brain barrier/neurovascular unit in health and disease. *Pharmacol Rev,* 57**,** 173-85.

HEDIGER, M. A., ROMERO, M. F., PENG, J. B., ROLFS, A., TAKANAGA, H. & BRUFORD, E. A. (2004) The ABCs of solute carriers: physiological, pathological and therapeutic implications of human membrane transport proteinsIntroduction. *Pflugers Arch,* 447**,** 465-8.

HELLEWELL, J. (1999) Treatment-resistant schizophrenia: reviewing the options and identifying the way forward. *J Clin Psychiatry,* 60**,** 14-9.

HIRASE, T., STADDON, J. M., SAITOU, M., ANDO-AKATSUKA, Y., ITOH, M., FURUSE, M., FUJIMOTO, K., TSUKITA, S. & RUBIN, L. L. (1997) Occludin as a possible determinant of tight junction permeability in endothelial cells. *J Cell Sci,* 110 (Pt 14)**,** 1603-13.

HOHEISEL, D., NITZ, T., FRANKE, H., WEGENER, J., HAKVOORT, A., TILLING, T. & GALLA, H. J. (1998) Hydrocortisone reinforces the blood-brain barrier properties in a serum free cell culture system. *Biochem Biophys Res Commun,* 244**,** 312-6.

HONKAKOSKI, P. & NEGISHI, M. (2000) Regulation of cytochrome P450 (CYP) genes by nuclear receptors. *Biochem J,* 347**,** 321-37.

HUWYLER, J., DREWE, J., KLUSEMANN, C. & FRICKER, G. (1996) Evidence for P-glycoprotein-modulated penetration of morphine-6-glucuronide into brain capillary endothelium. *Br J Pharmacol,* 118**,** 1879-85.

INGELMAN-SUNDBERG, M. (2005) Genetic polymorphisms of cytochrome P450 2D6 (CYP2D6): clinical consequences, evolutionary aspects and functional diversity. *Pharmacogenomics J,* 5**,** 6-13.

ITOH, M., FURUSE, M., MORITA, K., KUBOTA, K., SAITOU, M. & TSUKITA, S. (1999) Direct binding of three tight junction-associated MAGUKs, ZO-1, ZO-2, and ZO-3, with the COOH termini of claudins. *J Cell Biol,* 147**,** 1351-63.

JANZER, R. C. & RAFF, M. C. (1987) Astrocytes induce blood-brain barrier properties in endothelial cells. *Nature,* 325**,** 253-7.

JETTE, L., TETU, B. & BELIVEAU, R. (1993) High levels of P-glycoprotein detected in isolated brain capillaries. *Biochim Biophys Acta,* 1150**,** 147-54.

JOHNSON, D., FINCH, R., LIN, Z., ZEISS, C. & AC, S. (2001) The pharmacological phenotype of combined multidrug-resistance mdr1a/1b- and mrp1-deficient mice. *Cancer Res,* 61**,** 1469-76.

JOHNSON, M. D. & ANDERSON, B. D. (1999) In vitro models of the blood-brain barrier to polar permeants: comparison of transmonolayer flux measurements and cell uptake kinetics using cultured cerebral capillary endothelial cells. *J Pharm Sci,* 88**,** 620-5.

JONKER, J. W., SMIT, J. W., BRINKHUIS, R. F., MALIEPAARD, M., BEIJNEN, J. H., SCHELLENS, J. H. & SCHINKEL, A. H. (2000) Role of breast cancer resistance protein in the bioavailability and fetal penetration of topotecan. *J Natl Cancer Inst,* 92**,** 1651-6.

JULIANO, R. L. & LING, V. (1976) A surface glycoprotein modulating drug permeability in Chinese hamster ovary cell mutants. *Biochim Biophys Acta,* 455**,** 152-62.

KAKEE, A., TERASAKI, T. & SUGIYAMA, Y. (1997) Selective brain to blood efflux transport of para-aminohippuric acid across the blood-brain barrier: in vivo evidence by use of the brain efflux index method. *J Pharmacol Exp Ther,* 283**,** 1018-25.

KATHIRAMALAINATHAN, K., KAPLAN, H. L., ROMACH, M. K., BUSTO, U. E., LI, N. Y., SAWE, J., TYNDALE, R. F. & SELLERS, E. M. (2000) Inhibition of cytochrome P450 2D6 modifies codeine abuse liability. *J Clin Psychopharmacol,* 20**,** 435-44.

KATO, M., CHIBA, K., HORIKAWA, M. & SUGIYAMA, Y. (2005) The quantitative prediction of in vivo enzyme-induction caused by drug exposure from in vitro information on human hepatocytes. *Drug Metab Pharmacokinet,* 20**,** 236-43.

KEMPER, E. M., CLEYPOOL, C., BOOGERD, W., BEIJNEN, J. H. & VAN TELLINGEN, O. (2004) The influence of the P-glycoprotein inhibitor zosuquidar trihydrochloride (LY335979) on the brain penetration of paclitaxel in mice. *Cancer Chemother Pharmacol,* 53**,** 173-8.

KEMPER, E. M., VAN ZANDBERGEN, A. E., CLEYPOOL, C., MOS, H. A., BOOGERD, W., BEIJNEN, J. H. & VAN TELLINGEN, O. (2003) Increased penetration of paclitaxel into the brain by inhibition of P-Glycoprotein. *Clin Cancer Res,* 9**,** 2849-55.

KEMPER, E. M., VERHEIJ, M., BOOGERD, W., BEIJNEN, J. H. & VAN TELLINGEN, O. (2004) Improved penetration of docetaxel into the brain by co-administration of inhibitors of P-glycoprotein. *Eur J Cancer,* 40**,** 1269-74.

KERN, T. S. & ENGERMAN, R. L. (1996) Capillary lesions develop in retina rather than cerebral cortex in diabetes and experimental galactosemia. *Arch Ophthalmol,* 114**,** 306-10.

KOOL, M., DE HAAS, M., SCHEFFER, G. L., SCHEPER, R. J., VAN EIJK, M. J., JUIJN, J. A., BAAS, F. & BORST, P. (1997) Analysis of expression of cMOAT (MRP2), MRP3, MRP4, and MRP5, homologues of the multidrug resistance-associated protein gene (MRP1), in human cancer cell lines. *Cancer Res,* 57**,** 3537-47.

KRAUSE, D., MISCHECK, U., GALLA, H. J. & DERMIETZEL, R. (1991) Correlation of zonula occludens ZO-1 antigen expression and transendothelial resistance in porcine and rat cultured cerebral endothelial cells. *Neurosci Lett,* 128**,** 301-4.

KRISHNAN, R. & MARU, G. B. (2005) Inhibitory effect(s) of polymeric black tea polyphenols on the formation of B(a)P-derived DNA adducts in mouse skin. *J Environ Pathol Toxicol Oncol,* 24**,** 79-90.

KRUM, J. M. (1996) Effect of astroglial degeneration on neonatal blood-brain barrier marker expression. *Exp Neurol,* 142**,** 29-35.

KUSUHARA, H. & SUGIYAMA, Y. (2005) Active efflux across the blood-brain barrier: role of the solute carrier family. *NeuroRx,* 2**,** 73-85.

KWEI, G. Y., ALVARO, R. F., CHEN, Q., JENKINS, H. J., HOP, C. E., KEOHANE, C. A., LY, V. T., STRAUSS, J. R., WANG, R. W., WANG, Z., PIPPERT, T. R. & UMBENHAUER, D. R. (1999) Disposition of ivermectin and cyclosporin A in CF-1 mice deficient in mdr1a P-glycoprotein. *Drug Metab Dispos,* 27**,** 581-7.

KWON, Y., KAMATH, A. V. & MORRIS, M. E. (1996) Inhibitors of P-glycoprotein-mediated daunomycin transport in rat liver canalicular membrane vesicles. *J Pharm Sci,* 85**,** 935-9.

LAGRANGE, P., ROMERO, I. A., MINN, A. & REVEST, P. A. (1999) Transendothelial permeability changes induced by free radicals in an in vitro model of the blood-brain barrier. *Free Radic Biol Med,* 27**,** 667-72.

LASBENNES, F., SERCOMBE, R. & SEYLAZ, J. (1983) Monoamine oxidase activity in brain microvessels determined using natural and artificial substrates: relevance to the blood-brain barrier. *J Cereb Blood Flow Metab,* 3**,** 521-8.

LEE, S. W., KIM, W. J., CHOI, Y. K., SONG, H. S., SON, M. J., GELMAN, I. H., KIM, Y. J. & KIM, K. W. (2003) SSeCKS regulates angiogenesis and tight junction formation in blood-brain barrier. *Nat Med,* 9**,** 900-6.

LEHMANN, J. M., MCKEE, D. D., WATSON, M. A., WILLSON, T. M., MOORE, J. T. & KLIEWER, S. A. (1998) The human orphan nuclear receptor PXR is activated by compounds that regulate CYP3A4 gene expression and cause drug interactions. *J Clin Invest,* 102**,** 1016-23.

LIEBNER, S., FISCHMANN, A., RASCHER, G., DUFFNER, F., GROTE, E. H., KALBACHER, H. & WOLBURG, H. (2000) Claudin-1 and claudin-5 expression and tight junction morphology are altered in blood vessels of human glioblastoma multiforme. *Acta Neuropathol (Berl),* 100**,** 323-31.

LIMTRAKUL, P., ANUCHAPREEDA, S. & BUDDHASUKH, D. (2004) Modulation of human multidrug-resistance MDR-1 gene by natural curcuminoids. *BMC Cancer,* 4**,** 13.

LIN, J. H. (2003) Drug-drug interaction mediated by inhibition and induction of P-glycoprotein. *Adv Drug Deliv Rev,* 55**,** 53-81.

LOHMANN, C., HUWEL, S. & GALLA, H. J. (2002) Predicting blood-brain barrier permeability of drugs: evaluation of different in vitro assays. *J Drug Target,* 10**,** 263-76.

LOSCHER, W. & POTSCHKA, H. (2005) Blood-brain barrier active efflux transporters: ATP-binding cassette gene family. *NeuroRx,* 2**,** 86-98.

MARTIN-PADURA, I., LOSTAGLIO, S., SCHNEEMANN, M., WILLIAMS, L., ROMANO, M., FRUSCELLA, P., PANZERI, C., STOPPACCIARO, A., RUCO, L., VILLA, A., SIMMONS, D. & DEJANA, E. (1998) Junctional adhesion molecule, a novel member of the immunoglobulin superfamily that distributes at intercellular junctions and modulates monocyte transmigration. *J Cell Biol,* 142**,** 117-27.

MARTIN, C., BERRIDGE, G., MISTRY, P., HIGGINS, C., CHARLTON, P. & CALLAGHAN, R. (1999) The molecular interaction of the high affinity reversal agent XR9576 with P-glycoprotein. *Br J Pharmacol,* 128**,** 403-11.

MATER, S., MAICKEL, R. P. & BRODIE, B. B. (1959) Kinetics of penetration of drugs and other foreign compounds into cerebrospinal fluid and brain. *J Pharmacol Exp Ther,* 127**,** 205-11.

MATTER, K. & BALDA, M. S. (2003) Signalling to and from tight junctions. *Nat Rev Mol Cell Biol,* 4**,** 225-36.

MEYER, J., RAUH, J. & GALLA, H. J. (1991) The susceptibility of cerebral endothelial cells to astroglial induction of blood-brain barrier enzymes depends on their proliferative state. *J Neurochem,* 57**,** 1971-7.

MIKAMO, E., HARADA, S., NISHIKAWA, J. & NISHIHARA, T. (2003) Endocrine disruptors induce cytochrome P450 by affecting transcriptional regulation via pregnane X receptor. *Toxicol Appl Pharmacol,* 193**,** 66-72.

MIKSYS, S., RAO, Y., HOFFMANN, E., MASH, D. C. & TYNDALE, R. F. (2002) Regional and cellular expression of CYP2D6 in human brain: higher levels in alcoholics. *J Neurochem,* 82**,** 1376-87.

MILLER, D., GRAEFF, C., DROULLE, L., FRICKER, S. & FRICKER, G. (2002) Xenobiotic efflux pumps in isolated fish brain capillaries. *Am J Physiol Regul Integr Comp Physiol,* 282**,** R191-8.

MILLER, D. S., GRAEFF, C., DROULLE, L., FRICKER, S. & FRICKER, G. (2002) Xenobiotic efflux pumps in isolated fish brain capillaries. *Am J Physiol Regul Integr Comp Physiol,* 282**,** R191-8.

MILLER, D. S., NOBMANN, S. N., GUTMANN, H., TOEROEK, M., DREWE, J. & FRICKER, G. (2000) Xenobiotic transport across isolated brain microvessels studied by confocal microscopy. *Mol Pharmacol,* 58**,** 1357-67.

MISCHECK, U., MEYER, J. & GALLA, H. J. (1989) Characterization of gamma-glutamyl transpeptidase activity of cultured endothelial cells from porcine brain capillaries. *Cell Tissue Res,* 256**,** 221-6.

MISTRY, P., STEWART, A. J., DANGERFIELD, W., OKIJI, S., LIDDLE, C., BOOTLE, D., PLUMB, J. A., TEMPLETON, D. & CHARLTON, P. (2001) In vitro and in vivo reversal of P-glycoprotein-mediated multidrug resistance by a novel potent modulator, XR9576. *Cancer Res,* 61**,** 749-58.

MITIC, L. L., VAN ITALLIE, C. M. & ANDERSON, J. M. (2000) Molecular physiology and pathophysiology of tight junctions I. Tight junction structure and function: lessons from mutant animals and proteins. *Am J Physiol Gastrointest Liver Physiol,* 279**,** G250-4.

MONNAERT, V., TILLOY, S., BRICOUT, H., FENART, L., CECCHELLI, R. & MONFLIER, E. (2004) Behavior of alpha-, beta-, and gamma-cyclodextrins and their derivatives on an in vitro model of blood-brain barrier. *J Pharmacol Exp Ther,* 310**,** 745-51.

MORI, S., TAKANAGA, H., OHTSUKI, S., DEGUCHI, T., KANG, Y. S., HOSOYA, K. & TERASAKI, T. (2003) Rat organic anion transporter 3 (rOAT3) is responsible for brain-to-blood efflux of homovanillic acid at the abluminal membrane of brain capillary endothelial cells. *J Cereb Blood Flow Metab,* 23**,** 432-40.

MORITA, K., SASAKI, H., FURUSE, M. & TSUKITA, S. (1999) Endothelial claudin: claudin-5/TMVCF constitutes tight junction strands in endothelial cells. *J Cell Biol,* 147**,** 185-94.

MORSE, D. C., STEIN, A. P., THOMAS, P. E. & LOWNDES, H. E. (1998) Distribution and induction of cytochrome P450 1A1 and 1A2 in rat brain. *Toxicol Appl Pharmacol,* 152**,** 232-9.

OLDENDORF, W. H. (1970) Measurement of brain uptake of radiolabeled substances using a tritiated water internal standard. *Brain Res,* 24**,** 372-6.

OLDENDORF, W. H., CORNFORD, M. E. & BROWN, W. J. (1977) The large apparent work capability of the blood-brain barrier: a study of the mitochondrial content of capillary endothelial cells in brain and other tissues of the rat. *Ann Neurol,* 1**,** 409-17.

OLDENDORF, W. H., PARDRIDGE, W. M., BRAUN, L. D. & CRANE, P. D. (1982) Measurement of cerebral glucose utilization using washout after carotid injection in the rat. *J Neurochem,* 38**,** 1413-8.

OMIDI, Y., CAMPBELL, L., BARAR, J., CONNELL, D., AKHTAR, S. & GUMBLETON, M. (2003) Evaluation of the immortalised mouse brain capillary endothelial cell line, b.End3, as an in vitro blood-brain barrier model for drug uptake and transport studies. *Brain Res,* 990**,** 95-112.

ORLOWSKI, S., MIR, L., BELEHRADEK, J. J. & GARRIGOS, M. (1996) Effects of steroids and verapamil on P-glycoprotein ATPase activity: progesterone, desoxycorticosterone, corticosterone and verapamil are mutually non-exclusive modulators. *Biochem J,* 317**,** 515-22.

PAPADOPOULOS, M. C., SAADOUN, S., WOODROW, C. J., DAVIES, D. C., COSTA-MARTINS, P., MOSS, R. F., KRISHNA, S. & BELL, B. A. (2001) Occludin expression in microvessels of neoplastic and non-neoplastic human brain. *Neuropathol Appl Neurobiol,* 27**,** 384-95.

PARDRIDGE, W. M. (1998) Isolated brain capillaries: an in vitro model of blood-brain barrier research. IN PARDRIDGE, W. M. (Ed.) *Introduction to the blood-brain barrier: methodology, biology and pathology.* Cambridge, UK, Cambridge University Press.

PARDRIDGE, W. M. (1999) Blood-brain barrier biology and methodology. *J Neurovirol,* 5**,** 556-69.

PARDRIDGE, W. M. (2001) Crossing the blood-brain barrier: are we getting it right? *Drug Discov Today,* 6**,** 1-2.

PARDRIDGE, W. M., SAKIYAMA, R. & FIERER, G. (1984) Blood-brain barrier transport and brain sequestration of propranolol and lidocaine. *Am J Physiol,* 247**,** R582-8.

PAUL, S. (1999) CNS drug discovery in the 21st century. From genomics to combinatorial chemistry and back. *Br J Psychiatry Suppl***,** 23-5.

POTSCHKA, H., FEDROWITZ, M. & LOSCHER, W. (2003) Multidrug resistance protein MRP2 contributes to blood-brain barrier function and restricts antiepileptic drug activity. *J Pharmacol Exp Ther,* 306**,** 124-31.

POURTIER-MANZANEDO, A., DIDIER, A. D., MULLER, C. D. & LOOR, F. (1992) SDZ PSC 833 and SDZ 280-446 are the most active of various resistance-modifying agents in restoring rhodamine-123 retention within multidrug resistant P388 cells. *Anticancer Drugs,* 3**,** 419-25.

PRUDHOMME, J. G., SHERMAN, I. W., LAND, K. M., MOSES, A. V., STENGLEIN, S. & NELSON, J. A. (1996) Studies of Plasmodium falciparum cytoadherence using immortalized human brain capillary endothelial cells. *Int J Parasitol,* 26**,** 647-55.

RABINDRAN, S. K., ROSS, D. D., DOYLE, L. A., YANG, W. & GREENBERGER, L. M. (2000) Fumitremorgin C reverses multidrug resistance in cells transfected with the breast cancer resistance protein. *Cancer Res,* 60**,** 47-50.

RADL, S. (1998) Use of combinatorial chemistry to speed drug discovery. *Drug News Perspect,* 11**,** 507-11.

RAMSAUER, M., KRAUSE, D. & DERMIETZEL, R. (2002) Angiogenesis of the blood-brain barrier in vitro and the function of cerebral pericytes. *Faseb J,* 16**,** 1274-6.

REESE, T. S. & KARNOVSKY, M. J. (1967) Fine structural localization of a blood-brain barrier to exogenous peroxidase. *J Cell Biol,* 34**,** 207-17.

REGINA, A., KOMAN, A., PICIOTTI, M., EL HAFNY, B., CENTER, M. S., BERGMANN, R., COURAUD, P. O. & ROUX, F. (1998) Mrp1 multidrug resistance-associated protein and P-glycoprotein expression in rat brain microvessel endothelial cells. *J Neurochem,* 71**,** 705-15.

REUSS, B., DONO, R. & UNSICKER, K. (2003) Functions of fibroblast growth factor (FGF)-2 and FGF-5 in astroglial differentiation and blood-brain barrier permeability: evidence from mouse mutants. *J Neurosci,* 23**,** 6404-12.

RISAU, W., HALLMANN, R., ALBRECHT, U. & HENKE-FAHLE, S. (1986) Brain induces the expression of an early cell surface marker for blood-brain barrier-specific endothelium. *Embo J,* 5**,** 3179-83.

RIST, R. J., ROMERO, I. A., CHAN, M. W., COURAUD, P. O., ROUX, F. & ABBOTT, N. J. (1997) F-actin cytoskeleton and sucrose permeability of immortalised rat brain microvascular endothelial cell monolayers: effects of cyclic AMP and astrocytic factors. *Brain Res,* 768**,** 10-8.

ROWLAND, L. P., FINK, M. E. & RUBIN, L. L. (1991) Cerebrospinal fluid: blood-brain barrier, brain edema, and hydrocephalus. IN KANDEL, E. R., SCHWARTZ, J. H. & JESSELL, T. M. (Eds.) *Principles of neural science.* New York, Elsevier Science.

RUBIN, L. L., HALL, D. E., PORTER, S., BARBU, K., CANNON, C., HORNER, H. C., JANATPOUR, M., LIAW, C. W., MANNING, K., MORALES, J. & ET AL. (1991) A cell culture model of the blood-brain barrier. *J Cell Biol,* 115**,** 1725-35.

SCHILTER, B., ANDERSEN, M. R., ACHARYA, C. & OMIECINSKI, C. J. (2000) Activation of cytochrome P450 gene expression in the rat brain by phenobarbital-like inducers. *J Pharmacol Exp Ther,* 294**,** 916-22.

SCHINKEL, A. H. & JONKER, J. W. (2003) Mammalian drug efflux transporters of the ATP binding cassette (ABC) family: an overview. *Adv Drug Deliv Rev,* 55**,** 3-29.

SCHINKEL, A. H., MAYER, U., WAGENAAR, E., MOL, C. A., VAN DEEMTER, L., SMIT, J. J., VAN DER VALK, M. A., VOORDOUW, A. C., SPITS, H., VAN TELLINGEN, O., ZIJLMANS, J. M., FIBBE, W. E. & BORST, P. (1997) Normal viability and altered pharmacokinetics in mice lacking mdr1-type (drug-transporting) P-glycoproteins. *Proc Natl Acad Sci U S A,* 94**,** 4028-33.

SCHINKEL, A. H., SMIT, J. J., VAN TELLINGEN, O., BEIJNEN, J. H., WAGENAAR, E., VAN DEEMTER, L., MOL, C. A., VAN DER VALK, M. A., ROBANUS-MAANDAG, E. C., TE RIELE, H. P. & ET AL. (1994) Disruption of the mouse mdr1a P-glycoprotein gene leads to a deficiency in the blood-brain barrier and to increased sensitivity to drugs. *Cell,* 77**,** 491-502.

SCHINKEL, A. H., WAGENAAR, E., MOL, C. A. & VAN DEEMTER, L. (1996) P-glycoprotein in the blood-brain barrier of mice influences the brain penetration and pharmacological activity of many drugs. *J Clin Invest,* 97**,** 2517-24.

SCHWAB, D., FISCHER, H., TABATABAEI, A., POLI, S. & HUWYLER, J. (2003) Comparison of in vitro P-glycoprotein screening assays: recommendations for their use in drug discovery. *J Med Chem,* 46**,** 1716-25.

SEDLAKOVA, R., SHIVERS, R. R. & DEL MAESTRO, R. F. (1999) Ultrastructure of the blood-brain barrier in the rabbit. *J Submicrosc Cytol Pathol,* 31**,** 149-61.

SHARMA, S. & ROSE, D. (1995) Cloning, overexpression, purification, and characterization of the carboxyl-terminal nucleotide binding domain of P-glycoprotein. *J Biol Chem,* 270**,** 14085-93.

SHIVERS, R. R., ARTHUR, F. E. & BOWMAN, P. D. (1988) Induction of gap junctions and brain endothelium-like tight junctions in cultured bovine endothelial cells: local control of cell specialization. *J Submicrosc Cytol Pathol,* 20**,** 1-14.

SIEGLE, I., FRITZ, P., ECKHARDT, K., ZANGER, U. M. & EICHELBAUM, M. (2001) Cellular localization and regional distribution of CYP2D6 mRNA and protein expression in human brain. *Pharmacogenetics,* 11**,** 237-45.

SLATE, D. L., BRUNO, N. A., CASEY, S. M., ZUTSHI, N., GARVIN, L. J., WU, H. & PFISTER, J. R. (1995) RS-33295-198: a novel, potent modulator of P-glycoprotein-mediated multidrug resistance. *Anticancer Res,* 15**,** 811-4.

STANNESS, K. A., GUATTEO, E. & JANIGRO, D. (1996) A dynamic model of the blood-brain barrier "in vitro". *Neurotoxicology,* 17**,** 481-96.

STEWART, P. A. & WILEY, M. J. (1981) Developing nervous tissue induces formation of blood-brain barrier characteristics in invading endothelial cells: a study using quail--chick transplantation chimeras. *Dev Biol,* 84**,** 183-92.

SUGAWARA, I., HAMADA, H., TSURUO, T. & MORI, S. (1990) Specialized localization of P-glycoprotein recognized by MRK 16 monoclonal antibody in endothelial cells of the brain and the spinal cord. *Jpn J Cancer Res,* 81**,** 727-30.

SUGIMOTO, Y., TSUKAHARA, S., ISHIKAWA, E. & MITSUHASHI, J. (2005) Breast cancer resistance protein: molecular target for anticancer drug resistance and pharmacokinetics/pharmacodynamics. *Cancer Sci,* 96**,** 457-65.

TAKAKURA, Y., AUDUS, K. L. & BORCHARDT, R. T. (1991) Blood-brain barrier: transport studies in isolated brain capillaries and in cultured brain endothelial cells. *Adv Pharmacol,* 22**,** 137-65.

TAKASATO, Y., RAPOPORT, S. I. & SMITH, Q. R. (1984) An in situ brain perfusion technique to study cerebrovascular transport in the rat. *Am J Physiol,* 247**,** H484-93.

TERASAKI, T., OHTSUKI, S., HORI, S., TAKANAGA, H., NAKASHIMA, E. & HOSOYA, K. (2003) New approaches to in vitro models of blood-brain barrier drug transport. *Drug Discov Today,* 8**,** 944-54.

THIEBAUT, F., TSURUO, T., HAMADA, H., GOTTESMAN, M., PASTAN, I. & MC., W. (1989) Immunohistochemical localization in normal tissues of different epitopes in the multidrug transport protein P170: evidence for localization in brain capillaries and crossreactivity of one antibody with a muscle protein. *J Histochem Cytochem,* 37**,** 159-64.

THOMPSON, S., KOSZDIN, K. & BERNARDS, C. (2000) Opiate-induced analgesia is increased and prolonged in mice lacking P-glycoprotein. *Anesthesiology,* 92**,** 1392-9.

TIRONA, R. G. & KIM, R. B. (2005) Nuclear receptors and drug disposition gene regulation. *J Pharm Sci,* 94**,** 1169-86.

TONTSCH, U. & BAUER, H. C. (1991) Glial cells and neurons induce blood-brain barrier related enzymes in cultured cerebral endothelial cells. *Brain Res,* 539**,** 247-53.

TOROK, M., HUWYLER, J., GUTMANN, H., FRICKER, G. & DREWE, J. (2003) Modulation of transendothelial permeability and expression of ATP-binding cassette transporters in cultured brain capillary endothelial cells by astrocytic factors and cell-culture conditions. *Exp Brain Res,* 153**,** 356-65.

TRAN, N. D., CORREALE, J., SCHREIBER, S. S. & FISHER, M. (1999) Transforming growth factor-beta mediates astrocyte-specific regulation of brain endothelial anticoagulant factors. *Stroke,* 30**,** 1671-8.

TSURUO, T., IIDA, H., TSUKAGOSHI, S. & SAKURAI, Y. (1981) Overcoming of vincristine resistance in P388 leukemia in vivo and in vitro through enhanced cytotoxicity of vincristine and vinblastine by verapamil. *Cancer Res,* 41**,** 1967-72.

VAN DER DEEN, M., DE VRIES, E., TIMENS, W., SCHEPER, R., TIMMER-BOSSCHA, H. & DS, P. (2005) ATP-binding cassette (ABC) transporters in normal and pathological lung. *Respir Res,* 6**,** 59.

VAN HERWAARDEN, A. E. & SCHINKEL, A. H. (2006) The function of breast cancer resistance protein in epithelial barriers, stem cells and milk secretion of drugs and xenotoxins. *Trends Pharmacol Sci,* 27**,** 10-6.

VERONESI, B. (1996) Characterization of the MDCK cell line for screening neurotoxicants. *Neurotoxicology,* 17**,** 433-43.

VOIROL, P., JONZIER-PEREY, M., PORCHET, F., REYMOND, M. J., JANZER, R. C., BOURAS, C., STROBEL, H. W., KOSEL, M., EAP, C. B. & BAUMANN, P. (2000) Cytochrome P-450 activities in human and rat brain microsomes. *Brain Res,* 855**,** 235-43.

WARNER, M., KOHLER, C., HANSSON, T. & GUSTAFSSON, J. A. (1988) Regional distribution of cytochrome P-450 in the rat brain: spectral quantitation and contribution of P-450b,e, and P-450c,d. *J Neurochem,* 50**,** 1057-65.

WEBB, S., OTT, R. J. & CHERRY, S. R. (1989) Quantitation of blood-brain barrier permeability by positron emission tomography. *Phys Med Biol,* 34**,** 1767-71.

WEIDENFELLER, C., SCHROT, S., ZOZULYA, A. & GALLA, H. J. (2005) Murine brain capillary endothelial cells exhibit improved barrier properties under the influence of hydrocortisone. *Brain Res,* 1053**,** 162-74.

WESTERGREN, I., NYSTROM, B., HAMBERGER, A. & JOHANSSON, B. B. (1995) Intracerebral dialysis and the blood-brain barrier. *J Neurochem,* 64**,** 229-34.

WESTPHAL, K., WEINBRENNER, A., ZSCHIESCHE, M., FRANKE, G., KNOKE, M., OERTEL, R., FRITZ, P., VON RICHTER, O., WARZOK, R., HACHENBERG, T., KAUFFMANN, H. M., SCHRENK, D., TERHAAG, B., KROEMER, H. K. & SIEGMUND, W. (2000) Induction of P-glycoprotein by rifampin increases intestinal secretion of talinolol in human beings: a new type of drug/drug interaction. *Clin Pharmacol Ther,* 68**,** 345-55.

WHITE, R. E. (2000) High-throughput screening in drug metabolism and pharmacokinetic support of drug discovery. *Annu Rev Pharmacol Toxicol,* 40**,** 133-57.

XIAO, L., CUI, X., MADISON, V., WHITE, R. E. & CHENG, K. C. (2002) Insights from a three-dimensional model into ligand binding to constitutive active receptor. *Drug Metab Dispos,* 30**,** 951-6.

ZHANG, Y., BACHMEIER, C. & MILLER, D. W. (2003) In vitro and in vivo models for assessing drug efflux transporter activity. *Adv Drug Deliv Rev,* 55**,** 31-51.

ZHANG, Y., HAN, H., ELMQUIST, W. F. & MILLER, D. W. (2000) Expression of various multidrug resistance-associated protein (MRP) homologues in brain microvessel endothelial cells. *Brain Res,* 876**,** 148-53.

ZHANG, Y., SCHUETZ, J. D., ELMQUIST, W. F. & MILLER, D. W. (2004) Plasma membrane localization of multidrug resistance-associated protein homologs in brain capillary endothelial cells. *J Pharmacol Exp Ther,* 311**,** 449-55.

ZHOU, S., YUNG CHAN, S., CHER GOH, B., CHAN, E., DUAN, W., HUANG, M. & MCLEOD, H. L. (2005) Mechanism-based inhibition of cytochrome P450 3A4 by therapeutic drugs. *Clin Pharmacokinet,* 44**,** 279-304.

8 Appendix

8.1 Preliminary transport studies with neuroleptic drugs

The bidirectional transport assay (from AP to BL and vice versa) with porcine BCEC was applied for the identification of P-gp substrates among selected neuroleptic compounds. Therefore, in a pilot study, we studied the influence of verapamil, a P-gp inhibitor, on the BBB permeability of neuroleptic compounds, provided by the Psychiatric Clinic of the University of Mainz, Germany. The paracellular marker FITC-dextran was used to monitor the integrity of the cell monolayer. FITC-dextran permeability after 45 minutes was rather high (10-20% and 63-65% with cells or empty filters respectively from AP to BL, and 1-6% and 10-11% with cells or empty filters respectively from BL to AP) indicating an insufficient tightness of the monolayers and asymmetrical FITC-dextran transport.

The applied concentration was 200 µM for haloperidol, clozapine, norclozapine, olanzapine, quetiapine, risperidone and domperidone, 100 µM for aripiprazole and 9-OH risperidone, and 10 µM for ziprasidone. Test compounds were either applied to the apical (AP) or the basolateral (BL) side.

Figure 8.1 depicts the transport of the investigated compounds from apical to basoolateral without or in the presence of 100 µM verapamil. The transport of norclozapine from apical to basolateral was significantly increased (1.4-fold) by the P-gp inhibitor verapamil, indicating that norclozapine may be a substrate of P-gp. No significant difference was found for any of the other investgated compounds. The ziprasidone concentrations were below the limit of quantification. However, no conclusions can be made with these preliminary results.

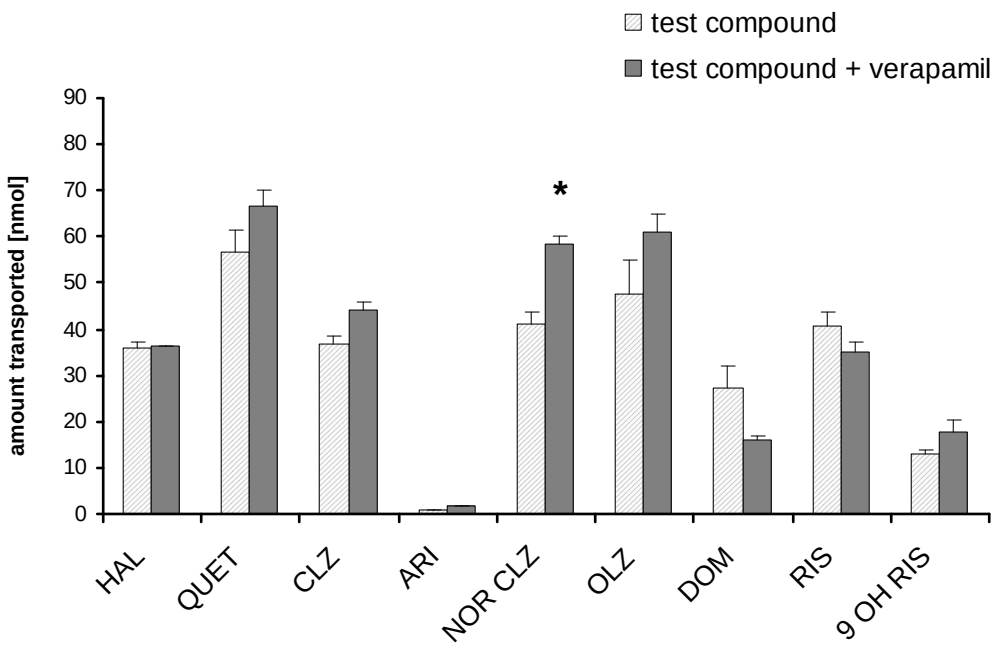

Figure 8.1 Transport of test compound from apical to basolateral with or without verapamil. Columns represent means ± SEM for 3 data points. An asterisk indicates statistical significance by Student's t-test (P<0.05)

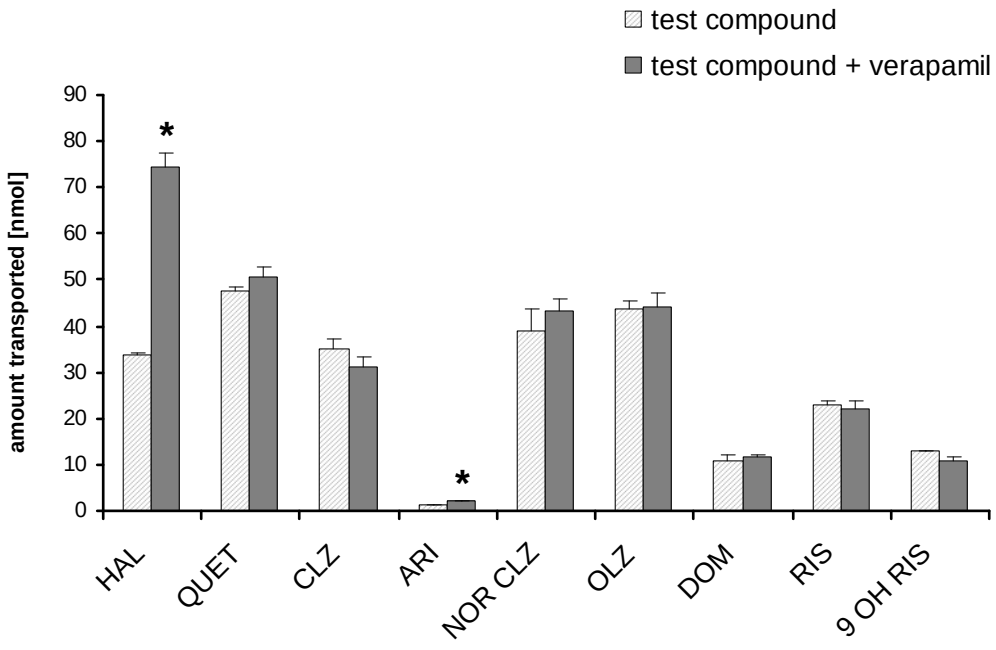

Figure 8.2 Transport of test compound from basolateral to apical with or without verapamil. Columns represent means ± SEM for 3 data points. An asterisk indicates statistical significance by Student's t-test (P<0.05).

The transport of the investigated compounds from BL to AP without or in the presence of 100 µM verapamil is shown in Figure 8.2.

Surprisingly, the transport of haloperidol and aripiprazole from BL to AP were significantly increased by the P-gp inhibitor verapamil (2.2-fold and 1.7-fold respectively). It would have been expected that the transport of a P-gp substrate from BL to AP is decreased in the presence of verapamil. No significant difference was found for any of the other investgated compounds. These results may indicate the involvement of other transport mechanisms. However, these are preliminary results, which do not allow any definite assumptions. The assay needs to be repeated with tight monolayers to reliably assess the direction of the net fluxes, and at various time points, to obtain time dependent transport data.